QUALITY CONTROL PATHWAYS IN THE PERIPHERAL NERVE WITH DISEASE AND AGING

By

SUNITHA RANGARAJU

A DISSERTATION PRESENTED TO THE GRADUATE SCHOOL
OF THE UNIVERSITY OF FLORIDA IN PARTIAL FULFILLMENT
OF THE REQUIREMENTS FOR THE DEGREE OF
DOCTOR OF PHILOSOPHY

UNIVERSITY OF FLORIDA

2010

I dedicate this work to my family, for their unconditional love and support

ACKNOWLEDGMENTS

I would like to thank my mentor Dr. Lucia Notterpek for her guidance and support and for being a tremendous influence in my development as a scientist. I am extremely grateful for the encouragement and opportunities she has provided me, to work on interesting and challenging projects. I would like to thank my committee members Drs.David Borchelt, William Dunn Jr, Susan Frost, Gerry Shaw and Matthew Sarkisian for all their critical input and intellectual contribution. I would also like to convey my thanks to our collaborators Drs. Christiaan Leeuwenburgh, Christy Carter and Adeela Kamal for their time and resources. I express my gratitude to Dr. Sue-Semple Rowland for being a student-friendly Program Director, who has always had my best interests. I am ever grateful to my parents for providing me with functional genes and unconditional love for the past 25 years. I thank my younger siblings, Vidhya and Vengada Karthik for their love, affection, and most importantly, teaching me the virtue of patience. I thank all my late grandparents, some of them whom I haven't seen and some of them who couldn't see this day. My heartfelt thanks go to my best buddies in graduate school, Karthik Bodhinathan and Mercedes Prudencio for always being there for me. I also thank my IDP and undergraduate friends who have helped me along, in this journey. I sincerely thank the past and present members of the Notterpek lab, especially Irina, Stephanie, Jonathan and Katie for all their help. I greatly appreciate the services of the administration staff –BJ, Kathy, Valerie, Teresa and Susan, who attend to me with a smiling face, whenever I knock their doors. I express my thanks to Doug Smith for assistance with confocal microscopy. Finally, I would like to acknowledge the National Institutes of Health and the Muscular Dystrophy Association for financial support.

TABLE OF CONTENTS

page

LIST OF TABLES

LIST OF FIGURES

LIST OF ABBREVIATIONS

AL	ad libitum
Atg	autophagy related homolog;
Atg12	autophagy related gene 12
CMT1A	Charcot–Marie–Tooth disease type 1A
CNS	central nervous system
CQ	chloroquine
CR	calorie restriction
di-8 ANEPPS	4-(2-(6-dibutylamino)-2-naphthalenyl)ethenyl)-1-(3-sulfopropyl) hydroxide
DIV	days *in vitro*
DMSO	dimethylsulfoxide
DRG	dorsal root ganglion
EC137	experimental compound 137
ER	endoplasmic reticulum
ERAD	ER-associated degradation
GA	Geldanamycin
GAPDH	glyceraldehyde 3-phosphate dehydrogenase
HNE	4-hydroxynonenal
HS	heat shock
HSF1	heat shock factor 1
HSP	heat shock protein
pIκB	phospho-IκB
Kv	voltage gated potassium channel

LAMP1	lysosome associated membrane protein 1;
LV	lentivirus
MAG	myelin associated glycoprotein
MAP-LC3	Microtubule associated protein light chain 3
MBP	myelin basic protein
MDA	malondialdehyde
mo	month
mUb	mono-ubiquitin
Na_v	voltage gated sodium channel
NF	neurofilament
NF-κB	nuclear factor κB
P	postnatal day
P0	protein zero
pHH3	phosphorylated histone 3
PMP22	peripheral myelin protein 22
PNS	peripheral nervous system
pS6	phosphorylated S6
pUb	poly-ubiquitin
RM	rapamycin
ROS	reactive oxygen species
SC	Schwann cell
Stv	starvation
TNF-α	tumor necrosis factor α

UPS	ubiquitin-proteasome system
Wt	wild type

Abstract of Dissertation Presented to the Graduate School
of the University of Florida in Partial Fulfillment of the
Requirements for the Degree of Doctor of Philosophy

QUALITY CONTROL PATHWAYS IN THE PERIPHERAL NERVE WITH DISEASE AND AGING

By

Sunitha Rangaraju

May 2010

Chair: Lucia Notterpek
Major: Medical Sciences–Neuroscience

Peripheral myelin protein 22 (PMP22) is a hydrophobic membrane glycoprotein expressed predominantly by myelinating Schwann cells (SCs). A heterozygous gene duplication of, or point mutations in *PMP22* in humans lead to the most common demyelinating peripheral neuropathies, namely Charcot-Marie-Tooth disease Type 1A (CMT1A). PMP22 overproducer C22 transgenic mice, and spontaneous point mutation (L16P) mouse Trembler J (TrJ), model the disease and display the clinical phenotypes. Affected nerves from these mouse models contain abnormally localized intracellular PMP22 inclusions associated with severe demyelination, similar to the human disease. Previous studies from our lab demonstrate that activation of protein homeostasis pathways, namely, chaperones and autophagy are able to reduce PMP22 aggregates in a toxin-induced cellular model. Furthermore, intermittent fasting, a dietary approach to activate chaperone and autophagy pathways substantially improves myelination and locomotor functions in neuropathic mice. In this study, we have assessed whether pharmacological stimulation of chaperone and autophagy pathways can aid the processing of PMP22 and alleviate the related myelin defects in neuropathic mice. For activation of chaperones and autophagy pathways, small molecules EC137 (from

Biogen Idec, Cambridge, MA) and rapamycin (RM), respectively, were employed. Exposure of myelinating dorsal root ganglion (DRG) explants from neuropathic mice to EC137 (50nM) or RM (25nM) results in the correct processing and trafficking of PMP22 as well as an overall improvement in myelination. The onset of this disease is ~35 years in humans and is progressive with age. Hence, we determined the contribution of normal aging to disease progression in a longitudinal study with rats. First, we confirmed previous findings that there is an age-related decline in myelin and axonal proteins in rats. Concomitantly, we found that there are abnormal age-related changes in key proteins that are part of the chaperone and autophagy pathways, along with increase in proteasomal substrates, oxidatively damaged proteins, pro-inflammatory mediators and immune cells. Interestingly, our studies show that a life-long calorie restriction (CR) diet dramatically minimizes adverse age-related changes in the chaperone and autophagy pathways and maintains myelination with age. Furthermore, diet restriction diminishes age-related oxidative damage to the peripheral nerve, as well as the hostile immunological and inflammatory components, to improve peripheral nerve health. Together, these results demonstrate that quality control mechanisms such as chaperones and autophagy, activated by pharmacological as well as dietary means, are pathways with therapeutic potential, to tackle the age- and disease-related abnormalities in PMP22- associated neuropathies.

CHAPTER 1
INTRODUCTION

Myelination in the Peripheral Nervous System

Myelin sheath is a multi-lamellar, lipid-rich structure deposited in segments along the axons of the central and peripheral nervous systems (CNS and PNS). The principal role of the myelin sheath is the insulation of axons which allows faster transmission of the nervous impulse. In the PNS, myelin sheath is formed by the differentiation of the plasma membrane of Schwann cells (SCs). During the development program in the PNS, SC precursors migrate from the neural crest and come in close contact with the peripheral axons (Kamholz et al., 1999). A large bundle of naked axons become ensheathed by a single layer of SCs. The establishment of axonal contact triggers SC proliferation (Salzer, 1997). As the SCs undergo rapid proliferation, the axons are segregated by “radial sorting”, sending their processes deeper into the bundle of axons. A 1:1 relationship is established between a SC and an isolated axonal segment to be myelinated (Bunge et al., 1989). The SCs that do not form 1:1 relationships with the axons mature into a non-myelinating type that embed multiple axons within them (Jessen and Mirsky, 2005). After the formation of a 1:1 relationship with the axon, the promyelinating SC subsequently undergoes a pronounced lateral elongation along the axon, and simultaneously secretes a continuous mucopolysaccharide basal lamina at the abaxonal (external) surface of the SC/axon unit. The basal lamina establishes connections with the extracellular matrix. This enables the SC to begin wrapping around the axon inwardly (Bunge et al., 1989). The ability of SCs to elaborate a basal lamina correlates with their capacity to proceed to myelination (Bunge et al., 1989) and is one of the key events that drives SC differentiation towards myelination (Carey et al., 1986;

Eldridge et al., 1987). As the SC membrane wraps around the axon, the many layers compress and the majority of the cytoplasm is extruded. This results in the formation of compact (myelin lamellae) and non-compact (cytoplasmic regions including the Schmidt-Lantermann incisures, paranodal loops and the outer and inner mesaxons) compartments of mature PNS myelin. Each segment of the axon myelinated by a single SC is termed ‘internode’ and the uncovered axonal portions in between the internodes are the ‘nodes of Ranvier’. These are higly specialized regions enriched with ion channels that facilitate nervous impulse (Garbay et al., 2000). The presence of axons is not only required for the expression of the myelin genes during development, but also for the maintenance of a myelinating phenotype (Wood and Bunge, 1975; Uyemura and Kitamura, 1991).

Myelin Constituents

In both mammalian and non-mammalian species, lipids account for 72–78% of the dry mass of PNS myelin (Garbay et al., 2000). Proteins represent between 20 and 30% of the dry mass of myelin. The major PNS myelin proteins are myelin protein zero (P0, 50-70%), myelin basic protein (MBP, 5-15%), myelin associated glycoprotein (MAG, 1%), periaxin (5%) and peripheral myelin protein 22 (PMP22, 2-5%). The myelin proteins that constitute <0.5% are E-cadherin and connexin (Cx32). In addition to these well known proteins, recently, a novel myelin protein, MP11 (myelin protein of 11 kDa) has been identified that is preferentially expressed in the PNS compared to CNS (Ryu et al., 2008).

P0 is a 28-kDa integral membrane glycoprotein, which is specific to PNS myelin. The putative role for the P0 protein is to function as a membrane adhesion molecule and to promote and maintain tight compaction of the myelin structure by homophilic

interactions via the L2/HNK-1 adhesion epitope (Filbin et al., 1990). In contrast to P0, MBP is present in both the PNS and the CNS myelin, which contains a high percentage (about 25%) of basic residues distributed throughout its polypeptide chain. In the PNS, P0, together with the MBP, is thought to be involved in the compaction of the myelin sheath via electrostatic interactions with acidic lipids in the membrane (Omlin et al., 1982; Martini et al., 1995).

MAG and Cx32 are located in the non-compact myelin. MAG is localized in the periaxonal SC membrane, the external and internal mesaxons, the paranodal loops of the nodes of Ranvier and the Schmidt-Lanterman incisures (Martini and Schachner, 1986; Trapp, 1990). MAG is believed to participate in axonal recognition and adhesion, intermembrane spacing, signal transduction during glial cell differentiation, regulation of neurite outgrowth, and in the maintenance of axon-myelin integrity (Trapp, 1990; McKerracher et al., 1994; Mukhopadhyay et al., 1994; Fruttiger et al., 1995). The extracellular domain of MAG possesses the L2/HNK-1 epitope similar to P0 (McGarry et al., 1983; Inuzuka et al., 1984; Kruse et al., 1985; Snipes et al., 1993). Cx32 is a gap junction protein that allows the movement of ions and small molecules to move through the multilamellar myelin membrane (Scherer et al., 1999). MP11 is a glycoprotein specifically localized to the Schmidt-Lanterman incisures and paranodal loops of the peripheral nerve (Ryu et al., 2008).

PMP22 is a 22 kDa, tetraspan, hydrophobic, integral membrane glycoprotein, expressed mainly by myelinating SCs (Snipes et al., 1993). PMP22 also contains the L2-HNK-1 adhesion epitope in its first putative extracellular loop, to which a carbohydrate moiety linked to asparagine 41 is present (Snipes et al., 1993). The

carbohydrate residue in PMP22 may be involved in conferring adhesive properties (Snipes et al., 1993) suggesting that the role of PMP22 in myelin may be similar to that of the P0 glycoprotein (Pareek et al., 1993). Furthermore, *PMP22*, *P0* and *MBP* genes are coexpressed (Kuhn et al., 1993) and their protein expression is coregulated (Hagedorn et al., 1999; Notterpek et al., 1999a) in myelinating SCs. Also, there is evidence for direct physical interaction between PMP22 and P0 proteins (D'Urso et al., 1999; Hasse et al., 2004). Although, it has been almost two decades since its discovery (Snipes et al., 1992), the exact function of PMP22 has not been elucidated, yet.

The Proposed Functions for Peripheral Myelin Protein 22

The human *PMP22* gene, located on chromosome 17, spans a 40 kbp region and contains six exons (Patel et al., 1992). In mouse and rat genomes, *PMP22* gene is located on chromosome 11. In both humans and rodents, PMP22 expression is regulated by two alternatively used promoters, producing two mRNAs (1A and 1B) (Suter et al., 1994) which encode the same protein but differ only by their 5′ untranslated region (Bosse et al., 1994; Bosse et al., 1999). The expression of the 1A mRNA predominates in peripheral myelin, while the 1B mRNA is the major species expressed in non-neural tissues. In addition to myelinating SCs in the PNS, PMP22 mRNA transcripts have been found in the embryonic and adult stages in both neuronal and nonneuronal tissues (Baechner et al., 1995; Parmantier et al., 1995; Notterpek et al., 2001; Roux et al., 2004). The post-transcriptional regulation of PMP22 in SCs during myelination, by microRNAs, has been recently demonstrated (Verrier et al., 2009).

In the PNS, PMP22 is largely confined to the compact portion of myelin (Snipes et al., 1992; Haney et al., 1996). PMP22 has been proposed to have an important role in PNS myelin synthesis and assembly based upon the observations that point mutations

in the *PMP22* gene, leads to a PNS-specific dysmyelination (defects in the formation of myelination) (Garbay et al., 2000). As a step towards understanding the function of PMP22, extensive studies have been carried out in PMP22 knock-out mice (PMP22-/-). PMP22-deficient mice display a delay in the onset of myelination (Adlkofer et al., 1995; Adlkofer et al., 1997b; Amici et al., 2006). PMP22-/- animals have few myelinated axons in which the myelin is too thick with respect to the axonal diameter. These structures, called tomacula, result from a focal hypermyelination, and consist of redundant myelin loops with normal spacing (Adlkofer et al., 1995; Amici et al., 2006). Thus, point mutations of PMP22 lead to dysmyelination while the complete disruption of the *PMP22* gene leads to focal hypermyelination and demyelination (loss of myelin sheaths). Based upon these results, it has been proposed that PMP22 is involved in the initiation of myelination, determination of myelin thickness and stabilization of the myelin sheath (Naef and Suter, 1998). In addition to its structural role in compact myelin, PMP22 is a binding partner in the integrin/laminin complex (Amici et al., 2006). This finding correlates with numerous SC-axon profiles showing loose basal lamina in PMP22 deficient (Amici et al., 2006) and overexpressing (Magyar et al., 1996) phenotypes. In the PMP22-/- mice, loose basal lamina might correspond to the missing PMP22-integrin connection, suggesting the involvement of PMP22 in mediating interactions of Schwann cells with the extracellular matrix. The PMP22-integrin interaction has proposed functions in the regulation of cellular growth (Zoidl et al., 1995; Zoidl et al., 1997), cell spreading, differentiation and migration of SCs (Niemann et al., 2000; Nobbio et al., 2004), cellular adhesion (Suter and Snipes, 1995; Hasse et al., 2004) and apoptosis (Fabbretti et al., 1995; Brancolini et al., 1999; Brancolini et al., 2000; Sancho et al.,

2001; Roux et al., 2005). Overall, it appears that *PMP22* is a dosage-sensitive gene, with two functional alleles being required for proper myelin formation and maintenance in the PNS (Adlkofer et al., 1995; Huxley et al., 1996; Adlkofer et al., 1997b; Adlkofer et al., 1997a; Perea et al., 2001). Additionally, PMP22 has been identified as an early component of the developing blood-nerve and blood-brain barrier at intercellular junctions (Notterpek et al., 2001; Roux et al., 2004). PMP22 also modulates epithelial morphology and monolayer permeability in cell culture (Roux et al., 2005). This property of PMP22 can be attributed to some similarities in its primary amino acid sequence with the claudin family of tight junction proteins (Van Itallie and Anderson, 2006). Finally, the fact that SCs expressing a truncated version of PMP22 protein proliferates at a significantly higher rate than those expressing the Wt (Johnson et al., 2005) suggests a possible role for PMP22 in cell cycle regulation and SC differentiation.

PMP22-Associated Neuropathies

Hereditary peripheral neuropathies comprise a heterogeneous group of disorders termed Charcot-Marie-Tooth diseases (CMT), among which, Charcot–Marie–Tooth disease type 1A (CMT1A) is the most prevalent form. It affects approximately one in 5,000 people which constitutes about 50% of all CMT cases, however, there is currently no cure for this disease (Shy et al., 2008). CMT1A is a demyelinating neuropathy mainly associated with a 1.5-megabase duplication in human chromosome 17 that includes the *PMP22* locus (Lupski et al., 1991). The main hallmark of CMT1A is demyelination and, consequently, a marked reduction in nerve conduction velocity together with slowly progressive distal muscular atrophy and weakness (Gabreels-Festen and Wetering, 1999). On the other hand, the deletion of the 1.5-megabase region in human chromosome 17 or truncation of the protein results in a milder variant known as

Hereditary Neuropathy with liability to Pressure Palsies (HNPP) (Chance et al., 1993). Patients diagnosed with HNPP exhibit a clinically heterogeneous recurrent focal neuropathy following minor nerve trauma that is characterized mainly by segmental demyelination and focal myelin thickening (tomacula) (Pareyson et al., 1996; Chance, 1999). Compared to CMT1A, the reduction in nerve conduction velocity in HNPP is lesser, and in general, the symptoms exhibited are not as severe (Gabreels-Festen and Wetering, 1999).

In addition to deletion and duplication, a variety of single point mutations in the *PMP22* gene have been identified in a small percentage of CMT1A cases, and in another type of related neuropathy, known as Dejerine-Sottas Syndrome (DSS) (Roa et al., 1993). Most mutations are dominantly inherited, affecting hydrophobic regions of the protein and are generally associated with severe phenotypes. DSS is chronic motor and sensory neuropathy with early-onset, marked reduction in nerve conduction velocity and more severe clinical pathology than CMT1A (Gabreels-Festen and Wetering, 1999). Not only mutations in PMP22, but, mutations in other essential constituents of peripheral myelin proteins such as P0 and Cx32 lead to other types of CMT diseases, namely CMT1B and CMTX, respectively (Scherer and Wrabetz, 2008). Furthermore, P0 physically interacts with PMP22 and the gene-dosage sensitivity of both proteins is consistent with the hypothesis that the two proteins are required in correct stoichiometric amounts in myelin.

Overall, the phenotypes resulting from most point mutations are more critical than the duplication or the deletion paradigms (Gabreels-Festen et al., 1995; Tyson et al., 1997; Boerkoel et al., 2002). In this context, independent mouse studies of the disease

have suggested that secondary to the SC damage, the phenotype severity is influenced by impaired SC-neuronal interaction, aberrant expression and reorganization of axonal ion channels, pronounced damage to axonal cytoskeleton and transport as well as recruitment of macrophages (Kohl et al., ; Kohl et al., ; Maier et al., 2002; Misko et al., 2002; Devaux and Scherer, 2005; Martini et al., 2008).

Mouse Models of PMP22-Associated Peripheral Neuropathies

Animal models display similar behavioral and morphological abnormalities found in human patients (Notterpek and Tolwani, 1999). Extensive studies in genetically engineered PMP22 overexpressor rats (Sereda et al., 1996; Niemann et al., 1999) and mice (Huxley et al., 1996; Perea et al., 2001; Robertson et al., 2002a), as well as PMP22-deficient mice (Adlkofer et al., 1995; Maycox et al., 1997; Fortun et al., 2006), have underscored the importance of adequate levels of PMP22 for myelin formation and stability (Huxley et al., 1996; Huxley et al., 1998; Niemann et al., 1999; Perea et al., 2001). Out of the several transgenic rodent CMT1A models that are based on the overexpression of the wild type (Wt) PMP22, the transgenic mouse termed C22, which has seven copies of the human PMP22 integrated in its genome and expresses ~1.7 times more PMP22 than Wt serves as an accurate model for heterozygous *PMP22* gene duplication (Huxley et al., 1996). The C22 mice mimics some of the morphological and behavioral phenotypes of the human disease (Huxley et al., 1996; Huxley et al., 1998; Fortun et al., 2006). Similar to the disease manifestation in humans diagnosed with CMT1A, C22 mice display slowed nerve conduction velocity, a reduction in the percentage of myelinated fibers and demyelinating axonal profiles in the adult (Huxley et al., 1996; Huxley et al., 1998; Robertson et al., 2002b). Phenotypically, heterozygous C22 mice show unsteady gait, muscle weakness and progressive paralyses of the hind

limbs (Huxley et al., 1996). In a conditional mouse model with regulatable PMP22 overexpression, the disease phenotype was corrected when the expression of the exogenous pmp22 was shut down (Perea et al., 2001). This demonstration opened an avenue for therapeutic intervention to reverse CMT1A linked with PMP22 duplication. This fact is further supported by independent studies with progesterone antagonists or ascorbic acid treatment where the neuropathy associated with PMP22 overexpression in CMT1A models is ameliorated by a mechanism likely involving a reduction in PMP22 expression (Sereda et al., 2003; Passage et al., 2004; Meyer zu Horste et al., 2007)**.**

Mouse models that accurately mimic CMT1A arising from point mutations in PMP22 include, the Trembler (Tr) and Trembler J (TrJ) mice, which are spontaneous mutations identified (Suter et al., 1992). The fact that the exact same point mutations have been identified in patients diagnosed with CMT1A validates these mouse models (Valentijn et al., 1992). In the Tr mouse, Glycine-150 is substituted by Aspartic acid (G150D), resulting in a new negatively charged amino acid in the fourth transmembrane domain of PMP22 (Snipes et al., 1993). Similarly, the TrJ mouse carries a point mutation that substitutes Leucine for Proline at position 16 (L16P), an α-helix breaking amino acid (Snipes et al., 1993), that leads to a transition from α-helix to β-sheet (Yamada et al., 2003). These mutations give rise to similar, but not identical neuropathies that have been used to model CMT1A, as well as DSS (Suter et al., 1992; Notterpek and Tolwani, 1999).

Based on the observation that both single gene deletion (HNPP) and duplication of *PMP22* are associated with demyelinating peripheral neuropathies, it has been proposed that these disorders are caused by a gene-dosage effect (Gabriel et al.,

1997). Furthermore, the demonstration that disease is more severe in the duplication and point mutation than the deletion paradigms (Gabreels-Festen et al., 1995; Adlkofer et al., 1997a; Boerkoel et al., 2002) strongly indicates a toxic gain-of-function of the point mutated or duplicated PMP22. The nature of the toxic gain-of-function has not been elucidated; however, impaired intracellular trafficking of mutant PMP22 in cellular quality control compartments and failure of PMP22 to incorporate into myelin have been proposed (Sanders et al., 2001).

Quality Control Mechanisms for PMP22 in TrJ and C22 Mouse Models

Extensive studies on the trafficking of Wt PMP22 reveals two checkpoints in the synthesis and processing of the protein- the endoplasmic reticulum (ER) and the Golgi compartments (Snipes et al., 1993). In normal SCs, ~20% of the newly-synthesized PMP22 is properly folded, glycosylated and trafficked via the ER and Golgi to the cell membrane. The other 80% of the protein is rapidly degraded within 30 minutes (min) via ER-associated degradation (ERAD) by the proteasome machinery (Pareek et al., 1997; Notterpek et al., 1999a; Ryan et al., 2002). Unlike other membrane proteins, PMP22 has a very short half-life, which may result from the inability of such a highly hydrophobic protein to fold correctly in the ER compartment. Alternatively, it is also possible that an intracellular function of PMP22 requires this rapid turnover (Naef and Suter, 1998). Ultimately, only a small fraction of the newly synthesized PMP22 trafficks through the Golgi and acquires its correct N-glycosylation modification. Once it has trafficked past the medial Golgi, upon an unidentified signal derived from SC-axonal contact, PMP22 translocates to the plasma membrane and incorporates into myelin membrane (Pareek et al., 1997). In SCs from PMP22 neuropathic mice, the ratio of PMP22 degradation and proper folding is greatly altered, resulting in the retention of

PMP22 in cytosolic aggregates (Fortun et al., 2003; Fortun et al., 2006). Infact, this phenomenon is also observed in nerve biopsies from CMT1A patients with *PMP22* gene duplication or point mutations. Patient tissues show PMP22-like immunoreactivity within the SC cytoplasm, representing the accumulation of PMP22, in addition to thin-myelin like staining (Nishimura et al., 1996; Hanemann et al., 2000).

Mammalian cells are endowed with three levels of defense mechanisms against the potentially toxic effects of protein aggregates. They are the quality control pathways namely, molecular chaperones (also known as heat shock protein (HSPs)), which suppress protein misfolding and aggregation (Broadley and Hartl, 2009), the ubiquitin-proteasome system (UPS), which degrades misfolded proteins that are unable to fold (Tai and Schuman, 2008) and macroautophagy, which is involved in eliminating proteins that have escaped the surveillance of the other two systems (Jaeger and Wyss-Coray, 2009). While the proteasomal degradation is a selective process, which recognizes and degrades protein substrates conjugated to a poly-ubiquitin (pUb) chain (Tai and Schuman, 2008), autophagy is a less selective clearance mechanism (Jaeger and Wyss-Coray, 2009). Lysosomes could be involved in the degradation of the aggregated proteins, most likely through the the autophagy-lysosomal pathway (Tai and Schuman, 2008).

In response to PMP22 overexpression, these quality control systems appear to be overwhelmed and protein aggregates are formed, *in vitro* (Chies et al., 2003; Fortun et al., 2006), in animal models as well as in CMT1A human patients (Nishimura et al., 1996; Hanemann et al., 2000). In the C22 overexpression mouse model, a reduced PMP22 turnover and presence of PMP22 aggregates is associated with impaired

proteasome activity (Fortun et al., 2005; Fortun et al., 2006). Also the presence of spontaneous protein aggregates in C22 mice is concomitant with the activation and recruitment of components of the autophagy-lysosomal pathway to the site of protein aggregation (Fortun et al., 2003; Fortun et al., 2006; Fortun et al., 2007). In addition, PMP22 aggregates recruit molecular chaperones and components of proteasome machinery, which further alter the homeostatic balance of the cell (Fortun et al., 2006). In terms of membrane protein trafficking, overexpression of PMP22, but not a point mutation in PMP22, in cell culture induces the formation of actin/phosphatidylinositol (4,5)-biphosphate (PI-4,5-P_2)-positive vacuoles and PMP22 accumulates in these vacuoles (Chies et al., 2003). Whether, these PMP22-containing actin/PI-4,5-P_2-positive pool of vacuoles cross talk with the late endosomal and autophagy-lysosomal pathways, is not clear.

With regards to the L16P point mutation in TrJ mice, mutant PMP22 and Wt PMP22 form homo- and hetero-dimers and multimers (Tobler et al., 1999; Tobler et al., 2002). The L16P mutant PMP22 proteins are retained in the intermediate compartment and ER (Tobler et al., 1999). In addition, the TrJ mutant interacts with the ER chaperone, calnexin for a longer time than the normal protein (Dickson et al., 2002) in a glycan-independent manner and this correlates with a reduced diffusion rate within the ER membrane (Fontanini et al., 2005). The retained mutant PMP22 protein traps the Wt PMP22 in the intermediate compartment between the ER and Golgi and thus may block part of its transport to the cell membrane by a dominant-negative mechanism. The mutant PMP22 protein causes a deleterious effect even in the absence of Wt PMP22 indicating a toxic gain-of-function (Adlkofer et al., 1997a). Different *in vitro* studies have

suggested that TrJ and other point-mutated PMP22s are not incorporated into plasma membrane (D'Urso et al., 1998; Naef and Suter, 1999; Tobler et al., 1999; Colby et al., 2000; Sanders et al., 2001). Studies in our lab show that, in SCs from TrJ mice, the turnover rate of PMP22 and the activity of the proteasome are reduced, concomitant with the assembly of protein aggregates (Fortun et al., 2003; Fortun et al., 2005). The endosomal-lysosomal pathway (Notterpek et al., 1997) and ubiquitination (Ryan et al., 2002; Fortun et al., 2005) are also upregulated in SCs from TrJ mice. PMP22 aggregates (Notterpek et al., 1999b; Ryan et al., 2002) and myelin-like figures (Dickson et al., 2002), reminiscent of autophagic vacuoles (Dunn, 1990) have been found in TrJ SCs. In addition, the cytosolic PMP22 aggregates recruit molecular chaperones, components of proteasome machinery and autophagy-lysosomal pathway, which further alter the homeostatic balance of the cell (Fortun et al., 2003; Fortun et al., 2005; Fortun et al., 2006; Fortun et al., 2007).

Implications of Protein Aggregation in PMP22-Associated Neuropathy Models

In response to pharmacological inhibition of the proteasome, cells in culture accumulate misfolded poly-ubiquitinated (pUb) substrates in aggregates, which are transported along the microtubules towards the centrosome to form an inclusion, termed the aggresome (Kopito, 2000). It has been proposed that these inclusions form when the cell’s capacity to degrade misfolded protein is exceeded (Kopito, 2000). Inclusion formation is associated with the pathogenesis of many neurodegenerative diseases (Kopito, 2000; Goldberg, 2003). The characteristic features of aggresomes include, perinuclear assembly at the centrosome in a microtubule-dependent fashion, devoid of membrane structures, encaged by vimentin and exclusion from ER and Golgi (Johnston et al., 1998).

In SC cultured from Wt mice, after a 16h treatment with a proteasome inhibitor, PMP22 accumulates in aggresomes and displays all the characteristic features of aggresomes (Notterpek et al., 1999b). These aggresomes have been shown to colocalize with ubiquitin and the HSPs and recruit lysosomes and autophagosomes (Fortun et al., 2007). Similar to the Wt-, the Tr- and TrJ- PMP22s also form aggresomes in response to proteasome inhibition, *in vitro*, although they do so with a higher propensity to spontaneously form high molecular weight oligomers (Ryan et al., 2002; Tobler et al., 2002). In SCs from C22 and TrJ mice, PMP22 aggregates associate with chaperones, autophagosomes and lysosomes, suggesting an endogenous activation of these pathways in response to the presence of misfolded proteins (Notterpek et al., 1997; Ryan et al., 2002; Fortun et al., 2003; Fortun et al., 2006). Based on these results, it is likely that the formation of protein aggregates in both paradigms represents a common protective response of the cell to cope with the excess or mutated PMP22 (Ryan et al., 2002; Fortun et al., 2003; Fortun et al., 2007).

The formation of large PMP22 aggregates may be a protective response of SCs to eliminate misfolded protein under conditions of compromised proteasome activity (Isaacs et al., 2002; Fortun et al., 2003). However, the implications of inclusion body formation within the cytoplasm are still controversial. It has been proposed that the inclusion bodies in neurodegenerative conditions are protective, whereas the intermediate aggregates trigger neuronal toxicity by an unknown sequence of events (Muchowski and Wacker, 2005). However, the incidence of cell death is not a prominent feature in cell and mouse models of CMT1A neuropathies (Fortun et al., 2003; Fortun et al., 2006). One possible mechanism by which aggregates could affect cellular biology is

by compromised proteasome activity (Bence et al., 2001). The excess of (C22) or missense mutation (TrJ) in PMP22 overload the proteasome pathway, leading to a reduction in the turnover rate of the protein (Fortun et al., 2003; Fortun et al., 2006). This leads to accumulation of PMP22, together with other unrelated ubiquitinated substrates, like MBP (Akaishi et al., 1996), to form aggregates (Fortun et al., 2005). Another possible mechanism of putative toxicity associated with aggresomes is by the recruitment of components of protein quality control machinery to the site of aggregation and their entrapment in non-functional complexes (Corboy et al., 2005). Indeed, in cultured SCs from TrJ and C22 mice, PMP22 aggregates are immunoreactive for components of the UPS machinery (Fortun et al., 2003; Fortun et al., 2005; Fortun et al., 2006), which if trapped within, could contribute to an additional loss of proteasomal activity (Tai and Schuman, 2008). In agreement to both the possibilities, the presence of PMP22 aggregates in overexpression (C22) and point mutation (TrJ) models correlate with reduced proteasome activity (Fortun et al., 2005; Fortun et al., 2006).

Hence, protein aggregation represents an “autocatalytic loop” by which, the presence of aggregates further triggers their formation by means of an impaired proteasomal activity (Kopito, 2000). Despite the initial protective nature of aggregates, they could contribute to cellular dysfunction if they are not cleared eventually.

Chaperones in the processing of PMP22 aggregates

Cytosolic chaperones play an important role in the disassembly of molecular aggregates and accelerate the refolding of insoluble molecules (Sherman and Goldberg, 2001). The heat shock response (HSR) and HSPs have been shown to have therapeutic potential and has been implicated in many neurodegenerative diseases based on their protective role against intracellular aggregates (Westerheide and

Morimoto, 2005). HSPs (molecular chaperones) might prevent toxicity by at least three ways including blocking inappropriate protein interactions, facilitating disease protein degradation or sequestration, and blocking downstream signaling events that lead to cellular dysfunction and death (Muchowski and Wacker, 2005).

The heat shock protein family includes the HSP90, HSP70, HSP40, and small heat shock protein (sHSP) families consisting of HSP27 and αB-crystallin. The HSR is regulated at the transcriptional level by the heat shock transcription factor 1 (HSF1) (Pirkkala et al., 2001). HSF1 exists normally in a negatively regulated state as an inert monomer in complex with HSP90 and upon exposure to a variety of stresses, including HS and HSP90 inhibitors, HSF1 is derepressed. This is followed by hyperphosphorylation, nuclear translocation and trimerization of HSF1, leading to the transcription and translation of HSPs (Westerheide and Morimoto, 2005). Geldanamycin, a HSP90 inhibitor, binds to the ATP site on HSP90 and blocks its interaction with HSF1, promoting HSF1 activation and the synthesis of HSPs (Prodromou et al., 1997; Zou et al., 1998).

The formation of protein aggregates is common among the “protein conformational diseases such as Alzheimer’s (AD), Parkinson’s (PD), Huntington’s (HD) amyotrophic lateral sclerosis (ALS) and prion diseases. The aggregation and the associated toxicity of the disease-related proteins, tau and Aβ in AD and α-synuclein in PD, huntingtin in HD, superoxide dismutase 1 in ALS and the prion protein (PrP) are suppressed by overexpression of HSP70 *in vitro* as well as *in vivo* in some diseases (Broadley and Hartl, 2009). Pharmacological molecules such as geldanamycin and its derivatives that can induce a family of HSPs as opposed to overexpression of only HSP70, offer a

viable and translational approach to suppress aggregation and cytotoxicity in these diseases (Kalmar and Greensmith, 2009)

The reason for the endogenous recruitment of HSPs to PMP22 aggregates in neuropathic nerves of C22 and TrJ mice (Fortun et al., 2003; Fortun et al., 2006) is uncertain, but it might represent an attempt of refolding and/or the targeting of the misfolded proteins for degradation (Broadley and Hartl, 2009). Infact, live cell imaging experiments show that HSP70 associates transiently with huntingtin aggregates, with association-dissociation kinetics identical to chaperone interactions with unfolded polypeptides likely reflecting the efforts of this chaperone to direct the unfolding and dissociation of substrates from the aggregate (Kim et al., 2002b).On the contrary, the protection observed in drosophila models of Parkinson's and polyglutamine expansion diseases due to the elevation of HSPs is not associated with a reduction in the number of inclusions and suppresses aggregate formation and/or cellular toxicity (Auluck and Bonini, 2002; Kazemi-Esfarjani and Benzer, 2002). In the PMP22 aggregation model, a protective role for chaperones in preventing the accumulation of misfolded proteins is supported by our previous study where HS-preconditioning or GA treatment hinders the formation of PMP22 aggresomes (Fortun et al., 2007). Similarly, in culture models, induction of HSPs, results in the suppression of the intracellular aggregation of several unrelated proteins (Broadley and Hartl, 2009). Collectively, these observations have lead to the hypothesis that the elevated levels of HSPs reduce or dampen aggregate formation and cellular degeneration.

When chaperones cannot repair misfolded proteins, chaperone-mediated targeting to the UPS or to lysosomes results in their degradation (Muchowski and Wacker, 2005).

CHIP (carboxy terminus of HSC70-interacting protein) is a protein that binds heat shock cognate 70 (HSC70) or HSP70 in the mammalian cytosol (Ballinger et al., 1999) and acts similar to the E3 ligase enzyme in the UPS to facilitate the transfer of a pUb chain to the misfolded substrate to carry out the chaperone-assisted proteasomal degradation (Jiang et al., 2001). Thus, CHIP mediates crosstalk between molecular chaperones and the UPS and aids the degradation of specific chaperone substrates (Luders et al., 2000).

The importance of HSPs in regulating ubiquitinated substrates is further emphasized by a HSF1 knock-out mouse model (hsf1-/-) which shows accumulation of ubiquitinated substrates in brain and primary astrocytes in response to the absence of HSF1 (Homma et al., 2007). The accumulation of ubiquitinated substrates in the embryonic fibroblasts from the hsf1-/- mice is associated with impaired proteasome activity. More strikingly, the hsf1-/- mice exhibit demyelination in the spinal cord and reduced steady-state levels of myelin proteins in different regions of the brain (Homma et al., 2007). These results imply that myelination is a highly demanding process in terms of quality control pathway requirements such as HSPs (Homma et al., 2007). Together, these studies support the idea that HS pathway has a therapeutic potential for PMP22-associated neuropathies.

Role of autophagy in PMP22 protein processing

Macroautophagy, from hereon referred to as autophagy, is a constitutive event involved in the bulk degradation of long-lived cytosolic proteins and organelles. In this mechanism of degradation, cytosolic cargo is engulfed in double membrane structures called autophagosomes. After maturation, autophagosomes fuse with the lysosomes to enable degradation of the cargo by the lysosomal enzymes (Klionsky and Emr, 2000).

Autophagy is induced under conditions of physiological stress, such as starvation and the process requires the coordinated function of proteins encoded by *Atg* (autophagy-related) genes (Klionsky and Emr, 2000). Work from our lab and others have shown that autophagosomes associate within or adjacent to the surface of cytoplasmic protein aggregates formed upon proteasome inhibition (Wojcik et al., 1996; Fortun et al., 2003; Rideout et al., 2004; Fortun et al., 2005; Komatsu et al., 2005; Fortun et al., 2006; Fortun et al., 2007). Furthermore, in the TrJ and C22 neuropathic models,concomitant to impairment of proteasome activity, autophagy proteins are recruited to the PMP22 aggregates (Fortun et al., 2003; Fortun et al., 2006). These results suggest that, when proteasome activity is compromised, to maintain subcellular homeostasis and prevent the accumulation of potentially harmful protein aggregates, proteasome substrates are re-routed to an alternative pathway, namely autophagy-lysosomal degradation. Studies have shown that, in response to experimental proteasome inhibition, autophagosomes are formed indicative of enhanced macroautophagy, thus establishing a relationship between these two major protein degradation pathways (Iwata et al., 2005; Ding et al., 2007; Fortun et al., 2007).

Our studies show that, experimental enhancement of autophagy hampers the formation of PMP22 aggresomes and prevents the accumulation of unrelated substrates of ubiquitin proteasome system, when the proteasome is inhibited (Fortun et al., 2003; Fortun et al., 2007). This underscores the therapeutic potential of this pathway in PMP22-associated neuropathies. The development of pharmacologic agents to stimulate autophagy therefore could provide a therapeutic approach for PMP22 neuropathies as well as other protein misfolding diseases associated with aggregate

formation. Aggresome assembly is a multi-step process, by which small aggregates throughout the cell are transported along microtubules towards the centrosome, where they form the final inclusion (Johnston et al., 1998; Notterpek et al., 1999b). Thus, it is likely that upon activation of autophagy under experimental conditions, small aggregates are engulfed within autophagosomes, reducing the load of proteins being transported towards the centrosome. In the protein conformational diseases, autophagy is endogenously activated, but appears to be impaired in conjunction with protein aggregation (Jaeger and Wyss-Coray, 2009). Pharmacological activation of autophagy by rapamycin (RM) or other small molecule enhancers of autophagy promotes the clearance of misfolded proteins and suppresses toxicity in cell culture and animal models of AD, PD, HD, ALS and spinocerebellar ataxia (Jaeger and Wyss-Coray, 2009).

Autophagy is activated as a compensatory mechanism in response to proteasome inhibition in protein misfolding disorders. The converse of this theory has been demonstrated in autophagy gene knock-out models. The role of autophagy in the degradation of ubiquitinated substrates is supported by the accumulation of ubiquitinated aggregates in the liver of conditional *Atg7*-deficient mice, which have defective autophagy, but intact UPS activity (Komatsu et al., 2005). Two independent studies provide striking findings that, mice deficient in *Atg5* (*Atg5*-/-) or *Atg7* (*Atg7*-/-) genes specifically in CNS form pUb intracellular inclusions in the brain and develop neurodegenerative symptoms, even without the expression of any disease-causing, aggregate-prone proteins (Hara et al., 2006; Komatsu et al., 2006). In *Atg7*-/- mice, pUb proteins accumulated and aggregated into inclusions despite apparently normal

proteasome function, which suggests that basal autophagy may be essential in clearing some misfolded proteins that are beyond the degradative capability of the proteasome (Hara et al., 2006; Komatsu et al., 2006; Mizushima and Hara, 2006). Similar conclusions have been made in cell culture models, where chemical inhibition of autophagy at the autophagosome formation or autophagosome– lysosome fusion stages is associated with enhanced protein aggregation and cell death (Ravikumar et al., 2002). In agreement to these findings, the simultaneous inhibition of the proteasomal degradation and autophagy in our SC model is associated with more pronounced accumulation of PMP22, as compared to proteasome inhibition alone (Fortun et al., 2007). Together, these studies suggest that, in the case of proteasomal impairment, activating autophagy is beneficial and serves as an alternative route through which misfolded proteins caould be removed.

Contribution of Aging in Peripheral Neuropathies

It is well-established that protein aggregation diseases such as AD, PD, HD, ALS etc. are age-related neurodegenerative disorders. The contribution of the events of normal aging in these brain disorders is thought to trigger as well as further exacerbate the disease condition (Keller et al., 2004). Similar to these CNS disorders, CMT1A is progressive with age (Shy et al., 2008). The onset of CMT1A in humans is ~35 years, although the patient possesses the defective *PMP22* gene since their birth (Shy et al., 2008). The rate of progression of CMT1A in patients is measured using neurological and electrophysiological parameters such as nerve conduction velocity, sensory nerve action potential (SNAP) and compound muscle action potential (CMAP) to assess the defects in the nerve and muscle function (Shy et al., 2008). These measurements show a significant yearly decline with disease succession (Shy et al., 2008). The disease

progression appears to be faster in older patients; however, the exact reason for the age-related progression has not yet been determined (Shy et al., 2008). There are very few longitudinal studies that have been performed in humans. Such long-term aging studies are relatively easier to perform in rodents. Similar to the human diseases, the mouse models of CMT1A also show progressive degenerative changes in pathological processes as well as locomotor functions (Madorsky et al., 2009). Unpublished results from our lab indicate that there is an age-related impairment in protein homeostatic pathways such as chaperones, autophagy, proteasome and increase in PMP22 aggregation in neuropathic mice (Narvaez et al, in preparation). In order to dissect and differentiate the molecular events in quality control pathways that take place due to disease and those that take place due to normal aging, we performed a longitudinal study with Wt rats (Chapter 4 and 5).

The Effect of Normal Aging on Peripheral Nerve Health

Aging is associated with structural, functional and biochemical alterations in the nervous system. Neurons with long processes, such as the ones in the PNS, are particularly vulnerable to degeneration (Mattson and Magnus, 2006), and are at risk to age-related modifications. The pathways/machineries that are susceptible to age-related alterations are metabolic pathways including glycolysis and energy metabolism, cellular cytoskeleton and transport as well as cellular stress responses such as chaperones, autophagy and UPS (Martinez et al., 2009). These pathways are known to regulate important functions in the neurons and glia. Since myelination is a highly-metabolically active pathway maintained by intricate signaling events between neurons and glia (Garbay et al., 2000), disease- or age-related degenerative changes in either cell type have global influences on overall nerve structure and function. Furthermore,

similar to CMT1A disease, aging of the PNS, could lead to aberrant alterations in the quality control pathways due to build-up of damaged proteins. Myelinated peripheral nerves from animals that undergo normal aging, show fiber loss and morphological irregularities (Verdu et al., 2000), as well as a notable reduction in the expression of myelin and neurofilament genes and proteins (Parhad et al., 1995; Melcangi et al., 1999; Melcangi et al., 2000; Uchida et al., 2004). There is evidence for demyelination and occasional remyelination in aged rat sciatic nerves, associated with nerve fiber degeneration (Sharma et al., 1980; Grover-Johnson and Spencer, 1981; Adinolfi et al., 1991). In response to the demyelination, SCs respond by hyperproliferating and increasing in number (Gregson and Hall, 1973) which leads to their and dedifferentiation (Zanazzi et al., 2001). Similar to the disease phenotype in CMT1A (Huxley et al., 1996; Huxley et al., 1998), normal aging is also associated with changes in functional measures such as decline in nerve conduction velocity and muscle strength, and decreases in sensory discrimination, autonomic responses and endoneurial blood flow (Verdu et al., 2000). Together, these alterations contribute to decline in neuromuscular function and affect physical strength.

Similar to the cases of diseases, reduction in the expression of functional proteins and the accumulation of damaged and misfolded proteins have been observed in a variety of organisms with aging (Sitte et al., 2000; Squier, 2001; Calabrese et al., 2004; Keller et al., 2004; Grune et al., 2005). The extent to which damaged proteins accumulate with disease as well as aging is highly dependent upon the cell's capacity to repair or remove them by subcellular homeostatic mechanisms (Stadtman, 2001), namely chaperones, autophagy and proteasomal degradation. With an age-related

decline in the activity of these quality control mechanisms, damaged proteins such as undegraded pUb substrates and organelles can accumulate and lead to cellular dysfunction and cell death (Macario and Conway de Macario, 2002; Bergamini et al., 2004). Particularly, metabolically active cells such as myelinating SCs and postmitotic cells such as neurons (Boulton et al., 2004; Weissman et al., 2007) are sensitive to the accumulation of damaged proteins.

In addition to impaired protein homeostatic pathways, aging of organ systems is associated with the accumulation of oxidatively damaged polynucleotides, proteins, carbohydrates and lipids, which leads to protein aggregation and cytotoxicity (Keller et al., 2004). This concept is called the “Oxidative Stress Theory of Aging” whereby age-related loss of proper physiological function is due to the accumulation of oxidative damage (Bokov et al., 2004). Particularly, oxidation of proteins promotes protein aggregation due to the increase in rate of misfolding and higher hydrophobicity acquired by the modification (Keller et al., 2004). The specialized form of intracellular aggregates seen with aging is termed “lipofuscin”. Lipofuscin is a dynamic assembly of protein, lipids and carbohydrates (Keller et al., 2004). Again, long-lived postmitotic cells such as neurons and energy-demanding SCs, whose functions rely on proper intracellular protein trafficking, are at greater risk and amass greater amounts of oxidative damage (Agarwal and Sohal, 1994; Sohal et al., 1994; Keller et al., 2004). In addition, SCs are rich in polyunsaturated fatty acids (Garbay et al., 2000) which serve as substrates for reactive oxygen species (ROS)-mediated lipid peroxidation (Smith et al., 1999; Blair, 2001). The accumulation of waste material is not only harmful due to its interference with biological functions, but also for imparting toxicity via lipid peroxidation products

(Levine and Stadtman, 2001; Grune and Davies, 2003).Together, the buildup of age-related damaged material along with their inefficient removal by homeostatic mechanisms become a concern in the vulnerable neurons and SCs of peripheral nerves.

Calorie Restriction Prevents Age-Related Alterations and Neurodegeneration

A well-accepted approach to slow the aging process and prolong lifespan is through dietary modulation, such as calorie restriction (CR) and intermittent fasting (Johnson et al., 2006; Martin et al., 2006). Dietary restriction can induce HSPs (Heydari et al., 1996; Selsby et al., 2005) and autophagy (Bergamini et al., 2003; Wohlgemuth et al., 2007) and therefore support the maintenance of healthy cells and organs. While much work concerning dietary modulation has focused on the central nervous system (CNS), peripheral organs and lifespan (Feuers et al., 1989; Mattson et al., 2001; Jolly, 2004), little is known about the effects of such approach on peripheral nerves. In the CNS, life-long reduction in calorie intake has been shown to preserve long-term potentiation (Hori et al., 1992) and ameliorate age-related cognitive decline (Pitsikas and Algeri, 1992). In the periphery, the decline in muscle mass and strength with age is ameliorated with a life-long CR diet (Marzetti et al., 2008; Xu et al., 2008), which in part might be underlined by improved neural function. Furthermore, a 5-month-long intermittent fasting diet, which is another dietary modulation, improves myelination and locomotor behavior in neuropathic mice (Madorsky et al., 2009).

Restriction of calorie-intake is an effective method to lower levels of oxidative stress and slow age-associated changes, as well as to extend lifespan in mammals (Sohal and Weindruch, 1996; Martin et al., 2006). Previous studies have shown that calorie restriction (CR) decreases mitochondrial ROS generation and oxidative damage

to DNA, protein and lipids (Lambert et al., 2004). CR has been found to reduce markers of age-related chronic inflammation (Martin et al., 2006; Chung et al., 2009) likely by sustained activation of chaperones (Keller et al., 2004). Although there have been extensive studies on the ability of CR to reduce age-related oxidative damage in protein homeostatic and oxidative stress pathways in the CNS (Martin et al., 2006), little is known about the beneficial effects of CR on age-associated changes in the PNS and its influence on myelination and peripheral nerve health.

The overall hypothesis tested in the studies described in this dissertation is that activation of quality control pathways such as HSR and autophagy by pharmacological or dietary means will be beneficial for the processing of PMP22 and maintenance of myelin with disease and age. In Chapter 2 of this study, we have tested whether HSP90 inhibitor-mediated induction of HSPs restore the subcellular homeostasis and improve the myelination in a neuropathic mouse model. In Chapter 3, we have determined whether increasing the robustness of autophagy, by pharmacological activation of this pathway by RM is beneficial for minimizing protein aggregation and correcting the associated myelin defects in C22 and TrJ neuropathic mouse models. In Chapters 4 and 5 of this study, we have assessed the age-related alterations in the protein homeostatic mechanisms and oxidative stress pathway to investigate their possible contribution to myelin and neuronal defects with age. We have also examined the potential of the dietary intervention method, CR, to maintain the quality control pathways and peripheral nerve health.

CHAPTER 2
PHARMACOLOGICAL INDUCTION OF THE HEAT SHOCK RESPONSE IMPROVES MYELINATION IN A NEUROPATHIC MODEL

Introduction

Hereditary peripheral neuropathies comprise a heterogeneous group of disorders, among which Charcot–Marie–Tooth disease type 1A (CMT1A) is the most prevalent form (Shy et al., 2001). CMT1A is a demyelinating neuropathy mainly associated with a 1.5-megabase duplication on human chromosome 17 that includes the *PMP22* locus (Lupski et al., 1991). Transgenic rodent models based on the overexpression of the Wt PMP22 reproduce features of the human condition and provide experimental models to study disease pathogenesis (Huxley et al., 1996; Magyar et al., 1996; Sereda et al., 1996; Perea et al., 2001; Robertson et al., 2002b). One of these transgenic lines termed C22, express approximately 1.7-fold higher levels of the PMP22 mRNA and display slowed nerve conduction velocity and a reduction in the percentage of myelinated fibers (Huxley et al., 1996; Huxley et al., 1998; Robertson et al., 1999; Robertson et al., 2002b).

Eukaryotic cells maintain protein homeostasis by using a collection of quality control pathways known as the unfolded protein response (UPR). Induction of UPR leads to the attenuated protein translation in the ER, ER-assisted folding and ER-associated degradation (ERAD) via the proteasome (Kincaid and Cooper, 2007). PMP22 folds with only a modest efficiency even under normal conditions (Sanders et al., 2001), as approximately eighty percent of the newly-synthesized protein is degraded by the proteasome (Pareek et al., 1997; Notterpek et al., 1999a). In response to PMP22 overexpression, the quality control system appears to be overwhelmed and protein aggregates form. In the C22 mouse model, a reduced turnover of the newly-synthesized

PMP22 is associated with the presence of cytosolic protein aggregates within SCs and impaired proteasome activity (Fortun et al., 2006). In myelinating DRG explant cultures, the retention of PMP22 within the SC cytosol decreases the amount of protein at the plasma membrane (Fortun et al., 2006), which could contribute to the observed myelin defects in affected mice.

A promising therapeutic approach for protein misfolding disorders, such as PMP22-associated neuropathies, involves the enhancement of chaperone expression (Muchowski and Wacker, 2005). Inhibitors of HSP90, including geldanamycin (GA) and its pharmacologically improved derivatives, 17-DMAG and 17-AAG, have been shown to suppress aggregation of mutant huntingtin and α-synuclein in cultured cells (Sittler et al., 2001; Hay et al., 2004; McLean et al., 2004; Herbst and Wanker, 2007). A family of small molecule HSP90 inhibitors significantly reduce tau protein levels and selectively clear specific phospho-tau aggregates in association with an increase in the levels of HSP27, HSP40 and HSP70 (Dickey et al., 2005; Dickey et al., 2006). These studies underscore the importance of HSPs in the elimination of misfolded proteins in neurodegenerative diseases; however their potential application for hereditary peripheral neuropathies has not been tested. Here we show that out of fifteen small molecule inhibitors of HSP90, EC137 effectively enhances chaperone levels and improves myelination, along with the trafficking of PMP22, in DRG explant cultures from neuropathic mice.

Materials and Methods

Mouse Colonies

The PMP22 overexpressor (C22) (Huxley et al., 1996) mouse breeding colony is housed under SPF conditions at the University of Florida, McKnight Brain Institute

animal facility. The use of animals for these studies has been approved by an Institutional Animal Care and Use Committee (IACUC). Genomic DNA was isolated from tail biopsies of mouse pups (less than 10 days old) and litters were genotyped by PCR (Huxley et al., 1996).

Non-Myelinating SC Cultures

Primary SC cultures from genotyped postnatal day 6 (P6) Wt and C22 mouse pups, or neonatal rat pups, were prepared and maintained as described (Ryan et al., 2002). Cells were grown to ~80% confluency in Dulbecco's modified Eagle's medium containing 10% fetal calf serum (Hyclone, Logan, UT, USA), 2.5 (mouse) or 5 µM (rat) forskolin (Calbiochem, La Jolla, CA, USA) and 10 µg/mL bovine pituitary extract (Biomedical Technologies Inc, Stoughton, MA, USA).

Cellular Toxicity Assay

Non-myelinating rat SC cultures were treated with small-molecule, synthetic HSP90 inhibitors at 50 nM and 500 nM (Dickey et al., 2005; Dickey et al., 2006; Dickey et al., 2007) concentrations for 16 h and then incubated in the MTT (3-[4,5-dimethylthiazol-2-yl]-2,5-diphenyl tetrazolium bromide) solution (0.5 mg/ml) for 5 h at 37 °C, producing the formazan product as a result of the cleavage of the tetrazolium salt MTT by the mitochondrial enzyme succinate-dehydrogenase (Mosmann, 1983). The amount of blue formazan product is directly proportional to the number of viable cells present. The optical density (OD) of each well was measured using an automated plate reader (550 nm) (Heaton et al., 2004). The toxicity of each test compound with respect to dimethylsulphoxide (DMSO) treated control cells from three independent experiments was determined and graphed as the percentage of cell death. Statistical significance was determined by using Student’s t-test.

DRG Explant Cultures and Compound Treatment Paradigms

Mouse DRG explant cultures were established as described (Cosgaya et al., 2002). Pregnant Wt and heterozygous C22 mice were sacrificed according to guidelines of University of Florida Institutional Animal Care and Use Committee. DRGs were collected from embryonic day 12-14 mice, digested with 0.25% trypsin (Gibco, Rockville, MD), dissociated and plated on rat tail collagen-coated (Biomedical Technologies, Inc.) glass coverslips. DNA was isolated from each embryo for genotyping by PCR, as described above. Explants were maintained in minimum essential medium (MEM; Gibco) supplemented with 10% fetal calf serum (Hyclone, Logan, UT), 0.3% glucose (Sigma-Aldrich, St. Louis, MO), 10 mM HEPES (Cellgro; Mediatech, Inc., Herndon, VA), and 100 ng/ml nerve growth factor (Harlan Bioproducts for Science, Madison, WI) for 7 days. In the case of the GA paradigm, myelination was initiated for 10 days by the addition of ascorbic acid (50 µg/ml; Sigma-Aldrich) which was followed by GA exposure for 72 h. For exposure with EC137, cultures were maintained under myelination-promoting conditions for 14 days and treated with compound for two 48 h periods, with a 48 h washout, in between. After the second 48 h treatment and a 16 h washout, the cultures were processed for immunostaining and Western blot analyses (Fig, 2-5A). For SC depleted neuronal cultures (Einheber et al., 1993), the explants were treated for 24 or 48 h with HSP90 inhibitors.

Primary Antibodies

Antibodies for protein chaperones included anti-HSP70, -HSP40, -αB-crystallin and -calnexin (all polyclonal rabbit antibodies, from Stressgen, Victoria British Columbia,

Canada), rat anti-HSP90 (Stressgen) and goat anti-HSP27 (Santa Cruz, CA). To monitor the HS transcriptional response, a polyclonal rabbit anti-HSF1 antibody (Stressgen) was employed. Antibodies for myelin proteins included monoclonal mouse-anti myelin associated glycoprotein (MAG), rat anti-myelin basic protein (MBP) (both from Chemicon, Temencula, CA, USA), mouse anti-P0 (Archelos et al., 1993a). To detect PMP22, a 1:1 mixture of two rabbit polyclonal antibodies, developed against a peptide corresponding to the second extracellular loop of the human or the rat PMP22, was used (Pareek et al., 1997; Fortun et al., 2006). Monoclonal anti-actin, -tubulin (both from Sigma), or glyceraldehyde-3-phosphate dehydrogenase (GAPDH) (clone 1D4, EnCor Biotechnology Inc., Alachua, FL, USA) served as protein loading controls. Polyclonal rabbit anti-ubiquitin (Dako, Carpinteria, CA) was purchased from the indicated supplier.

Immunolabeling Studies

Non-myelinating SCs and myelinating DRG explant cultures on glass coverslips were fixed with 4% paraformaldehyde for 10 min and permeabilized with 100% methanol for 5 min at -20 °C. After blocking with 10% normal goat serum, the samples were incubated with the indicated primary antibodies overnight at 4°C, followed by the appropriate secondary antibodies, including Alexa Fluor 594 goat anti-rabbit IgG, Alexa Fluor 488 goat anti-rat IgG and Alexa Fluor 488 goat anti-mouse IgG (all from Molecular Probes, Eugene, OR). Hoechst dye (Molecular Probes) was included in the secondary antibody solution at 10 µg/ml to visualize nuclei. Coverslips were mounted using the ProLong Antifade kit (Molecular Probes). Samples were imaged with a Spot camera

attached to a Nikon Eclipse E800 microscope, or a Leica TCS SP2 AOBS Spectral confocal microscope and were formatted for printing by using Adobe Photoshop 5.5.

Biochemical Studies

Untreated control and compound treated cultures were lysed in sodium dodecyl sulfate (SDS) gel sample buffer (62.5 nM Tris, pH 6.8, 10% glycerol, 3% SDS) and protein concentrations were determined using BCA assay (Pierce, Rockford, IL, USA). Samples were analyzed on polyacrylamide gels under reducing conditions (except for the determination of MAG), and transferred to nitrocellulose membranes (Bio-Rad Laboratories, Hercules, CA, USA). Membranes were blocked in 5% non-fat milk in PBS and incubated overnight with primary antibodies. After washing, anti-mouse, anti-rabbit or anti-rat HRP-linked secondary antibodies were added for 2 h. Bound antibodies were visualized using an enhanced chemiluminescence detection kit (PerkinElmer Life Sciences, Boston, MA, USA). Films were digitally imaged using a GS-710 densitometer (Bio-Rad Laboratories) and were formatted for printing by using Adobe Photoshop 5.5. Densitometric analysis of Western blots was performed using Scion image software.

Quantification of Myelin Internode Lengths

DRG explant cultures were subjected to the treatment paradigms described above and immunostained with an anti-MBP antibody to label internodal myelin segments (Amici et al., 2007). Internode lengths from Wt and C22 cultures from three independent experiments were measured with Spot RT software (Diagnostic Instruments, Inc., Sterling Heights, MI). Measurements were collected from three coverslips per genotype per treatment paradigm. Statistical significance was determined by using Student's t-test using GraphPad Prism software.

Results

Myelin Production in C22 Neuropathic Samples is Enhanced by Geldanamycin

In the DRG explant model, sensory neurons and SCs from normal mouse embryos produce many myelinated segments, while samples from neuropathic mice only form a few shortened segments (Fortun et al., 2006; Amici et al., 2007). SCs cultured with DRG neurons from C22 neuropathic mice accumulate PMP22 within their cytosol (Fig. 2-1A, upper left, arrows) (Fortun et al., 2006). To test, whether enhancement of protein chaperone expression might be beneficial for myelination in these samples, DRG explants from C22 mice were treated with GA for 72 h and processed for immunolabeling and Western blots (Fig. 2-1). GA is a naturally occurring ansamycin antibiotic which inhibits HSP90, thereby activating HSF1 and the expression of chaperones, including HSP70, HSP40 and HSP27 (McDonough and Patterson, 2003). Exposure of explant cultures from neuropathic mice to 50 nM GA for 72 h reduced the presence of cytosolic PMP22 aggregates (Fig. 2-1A, upper right), as compared to DMSO-treated control samples (Fig. 2-1A, upper left, arrows). Treatment with GA also increased myelin production, as judged from immunolabeling with an anti-MBP antibody (Fig. 2-1A, lower right). As shown in previous studies with GA (Nixon et al., 1994; Kim et al., 1999; Petrucelli et al., 2004), in total protein lysates we detected a prominent induction of HSP70 and HSP27, as compared to DMSO-treated controls (Fig. 2-1B). In agreement with the enhanced myelination (Fig. 2-1A), we also detected an increase in the steady-state level of PMP22 (Fig. 2-1B), which is known to correlate with compact myelin formation (Snipes et al., 1992). While additional studies of GA-treated cultures indicate a consistent improvement of myelination in explants from neuropathic mice, prolonged exposure to this compound is known to be toxic (Miyata, 2005). Therefore,

we decided to test a class of synthetic HSP90 inhibitors, which cause less toxicity in cultured neuroglioma cells and have the potential for *in vivo* application (Dickey et al., 2005; Dickey et al., 2007).

Small-Molecule HSP90 Inhibitors Enhance Chaperone Expression in SCs

To begin our studies with the synthetic HSP90 inhibitors (EC compounds), non-myelinating primary rat SC cultures were treated for 16 h at 50 and 500 nM concentrations, followed by MTT cellular toxicity assay (Fig. 2-2A). We used rat SCs for the initial screening of the compounds due to the relative ease of obtaining a large number of homogeneous cell populations from neonatal rat nerves, as compared to mouse. In comparison to GA, which led to a significant 20-25% glial cell death ($p<0.001$), several EC compounds were less toxic to SCs. For example, EC137 at 50 nM has significantly less cellular toxicity as compared to GA at 50 nM ($p<0.001$) (Fig. 2-2A). In parallel with the cellular toxicity studies, we have tested the ability of these compounds to induce HSP70 expression (Fig. 2-2B). Eight out of fifteen tested compounds induced HSP70 at 50 nM, while thirteen out of fifteen were effective at 500 nM (Fig. 2-2B). Furthermore, two negative controls, EC116 and EC117 that are structurally-related inactive HSP90 inhibitors, failed to induce HSP70. The levels of calnexin, which is an ER chaperone rather than a HSP, are unaltered by exposure of the cells to the HSP90 inhibitors (Fig. 2-2B). From these results, we chose EC137, EC119, EC127 and EC139 for further studies at 50 nM concentrations. While all four of these compounds at 50 nM concentrations enhanced HSP70 expression in rat SCs, pilot studies with neuropathic samples identified EC137 as the most effective compound in reducing the levels of poly-ubiquitinated proteins (Fig. 2-3A). In agreement with our previous studies (Ryan et al., 2002; Fortun et al., 2003), the basal levels of HSP70 are

elevated in SCs from neuropathic mice, which is further enhanced upon treatment with HSP90 inhibitors.

To characterize the effect of EC137 on glial gene expression, the dose-dependent induction of a panel of chaperones was determined at five different concentrations, including 10, 50, 100, 250 and 500 nM (Fig. 2-3B). Compared to control levels, after a 16 h treatment with 10 nM EC137 the expression of HSP70, HSP27 and αB-crystallin are enhanced. However, the levels of these HSPs are elevated ~3-fold higher at the 50 nM dosage and are comparable to HS (45 °C for 20 min) preconditioning, followed by an 8 h chase (Fig. 2-3B). In agreement with known molecular targets of EC137, this concentration also enhanced the levels of HSP90 and HSP40 in the SCs. As treatment of the cells with higher dosages of EC137 did not appear to further stimulate chaperone expression, we chose the 50 nM concentration for subsequent studies. To optimize potential treatment paradigms for the myelinating samples, the induction of HSPs was analyzed after 4, 8, 16, 24 and 48 h incubation with 50 nM EC137 (Fig. 2-3C). As judged from the Western blot, the peak expression of HSPs is observed at 16 h. As seen previously (Fig. 2-2B), the levels of the ER chaperone calnexin are unaffected by EC137 (Fig. 2-3C). To further characterize the kinetics of HSP induction by EC137, SC cultures were treated for 4 h, followed by wash out and chase time points at 4, 24 and 36 h (Fig. 2-3D). As shown in the Western blot, a 4 h treatment with EC137 is associated with a sustained expression of HSP70 up to 36 h (Fig. 2-3D). In comparison, the influence on the levels of HSP27 is short-lived. The effects of EC137 on HSP70 in non-myelinating rat SCs were confirmed by immunostaining (Fig. 2-3E). As compared to DMSO controls, HSP70-like immunoreactivity is prominent and detected within the cell soma after EC137 treatment.

Inhibitors of HSP90, such as EC137 enhance the expression of chaperones by promoting the nuclear localization and phosphorylation of HSF1 (Westerheide and Morimoto, 2005). To investigate the activation of HSF1 in our SC model, cells were exposed to a brief HS (45 °C for 20 min) (Fortun et al., 2007), or 50 nM EC137 for 2, 4, 8 or 16 h, followed by analysis with an HSF1 antibody (Fig. 2-4A). HS preconditioning leads to rapid phosphorylation of HSF1, as detected by a shift in the mobility of the protein on SDS gels (Fig. 2-4A, arrow). The activation of HSF1 by HS is transient, as the non-phosphorylated form (Fig. 2-4A, arrowhead) becomes the prominent protein after a 0.5 h chase. In comparison, EC137 exposure promotes HSF1 phosphorylation starting from 2 h post-treatment and the active phosphorylated form remains for up to 8 h. The protein returns to baseline by 16 h (Fig. 2-4A). To corroborate the activation of HSF1 by EC137, we determined protein localization in cells post HS or after a 2 h compound exposure (Fig. 2-4B). In DMSO treated control cells, HSF1 is detected both in and around the nucleus (Fig. 2-4B, top panel, arrows). HS preconditioning of the cells promotes the translocation of HSF1 to the nucleus within 20 minutes (Fig. 2-4B, middle panel, arrows). Similarly, exposure of the cultures to EC137 for 2 h leads to prominent nuclear HSF1-like immunoreactivity (Fig. 2-4B, bottom panel, arrows). Together, these studies indicate that synthetic inhibitors of HSF1 are well tolerated by primary peripheral glial cells and EC137 is an effective inducer of the HS response, as judged from the enhanced and sustained expression of HSPs post-treatment. The results of the cellular toxicity and protein expression studies with EC137 from rat SCs (Figs. 2-2 to 2-4), were confirmed in mouse SC isolated from Wt pups, prior to the beginning of the studies with the explant cultures from transgenic mice.

Enhancement of HSPs Promotes Myelination in Explant Cultures from Neuropathic Mice

Next, we asked whether induction of HSPs could assist in the processing of glial proteins and improve myelination in samples from neuropathic mice. To test the influence of EC137 on myelination, DRGs from Wt and C22 embryos were incubated with DMSO as a control, or EC137 (50 nM), according to the paradigm shown (Fig. 2-5A). The treatment with EC137 was initiated after a 14-day period under myelination-promoting conditions (Fig. 2-5A). The explants were exposed to EC137 (50 nM) for a total of 96 h according to the schedule shown. This treatment paradigm is based on the data obtained from our dosage and time course experiments (Fig. 2-3 panels B-D). In order to maximize the chaperone response, we chose 48 h exposure, during which time HSP levels are elevated in both SC and DRG explant cultures (Fig. 2-3C, 2-6D). The 48 h washout was selected based on the maintenance of chaperone expression for over 36 h (Fig. 2-3D). For the detection of compact myelin, samples were immunostained with antibodies to MBP (Fig. 2-5B). As previously shown (Fortun et al., 2006; Amici et al., 2007), SCs in explant cultures from Wt embryos deposit numerous anti-MBP antibody reactive myelin segments, with or without compound treatment (Fig. 2-5B, top panels). At higher magnification, MBP-like immunoreactivity appears as the characteristic "rail-road tracks" of compact myelin (Fig. 2-5B, top panel, insets on bottom right). In comparison, in DRGs from C22 embryos, the DMSO control samples contain few, short MBP-positive myelin segments. Significantly, treatment of the neuropathic cultures with EC137 is associated with a pronounced improvement in the abundance of myelin internodes (Fig. 2-5B, bottom right). As indicated in the inset, myelin formed in response to EC137 exposure appears similar to those formed in cultures from Wt mice. To

quantify the improvement in myelination in explant cultures from neuropathic mice, we measured MBP-reactive internode lengths (Fig. 2-5C). The average internode length of Wt DRGs treated with DMSO is 161.1 ± 4.818 μm (mean ± SEM). In Wt DRGs treated with EC137 there is a small, but statistically significant increase in internode lengths (178.8 ± 4.797 μm; $p<0.05$) (Fig. 2-5C). Strikingly, in DRGs from neuropathic mice, we found a 5-fold increase in internode lengths after treatment with EC137 (increase from 22.60 ± 1.384 μm to 90.26 ± 8.410 μm; $p<0.001$) (Fig. 2-5C). These results indicate that activation of HSPs has a positive influence on myelination by peripheral glial cells, particularly those from neuropathic mice.

To corroborate the positive influence of EC137 on myelin protein expression, total protein lysates of DRGs from Wt and C22 embryos at the end of the treatment paradigms were analyzed by Western blots (Fig. 2-5D). In agreement with the improvement in myelin internode formation in EC137-treated samples (Fig. 2-5B and C), we found an increase in the steady-state level of myelin proteins, including MAG, P0 and MBP (Fig. 2-5D). In samples from Wt mice, there was a ~1.3-1.7-fold increase in the above mentioned myelin proteins, as determined by densitometric analysis, an effect that is statistically significant ($p<0.05$ for all the myelin proteins in Wt samples, n=3). In comparison, in samples from neuropathic mice, we detected a pronounced ~14-fold increase in the levels of MBP ($p<0.01$, n=3), ~4-fold increase in P0 ($p<0.01$, n=3) and ~3-fold increase in MAG ($p<0.05$, n=3) (Fig. 2-5D), subsequent to EC137 treatment. As expected, EC137 exposure is associated with a pronounced induction in HSP70 in both Wt and neuropathic samples. The blots shown are representative of at least three independent experiments for each condition and were reprobed with an antibody to GAPDH to monitor protein loading.

In nerves of C22 neuropathic mice, by ^{35}S pulse-chase analysis we detected an accumulation of endo H-sensitive PMP22 and an increase in PMP22 levels, when we used a combination of antibodies against the mouse and the human protein (Fortun et al., 2006). Therefore, rather than comparing the overall levels of PMP22 between our Wt and neuropathic samples, we asked whether the subcellular trafficking of PMP22 is influenced by EC137 treatment (Fig. 2-6A). Accumulation of endo H-resistant PMP22 within SCs correlates with myelination and represents the long-lived membrane form of the protein (Pareek et al., 1997). The fraction of endo H-resistant PMP22 in DMSO-treated DRGs from Wt and C22 embryos is comparable to that seen in sciatic nerve lysates from 6-month old Wt and C22 mice, respectively (Fig. 2-6A) (also see Fortun et al., 2006), thus mimicking the *in vivo* situation closely. With EC137 treatment, the endo H-resistant fraction in Wt DRGs is slightly increased from 84 to 86% ($p=0.12$; $n=3$). In comparison, in DRGs from neuropathic mice the endo H-resistant pool of PMP22 is significantly improved from 56.03 ± 1.23% to 73.97 ± 0.92% (mean ± SEM, $p<0.001$; $n=3$). Compare the levels of endo H-resistant ~22 kDa (arrow) and endo H-sensitive 18 kDa forms (arrowhead)] (Fig. 2-6A). The slowed mobility of the endo H-resistant PMP22 in EC137-treated samples, as compared to DMSO controls, is consistent among independent samples and may reflect altered glycosylation and/or folding of the protein.

The intracellular retention of PMP22 in samples from C22 mice is associated with an accumulation of poly-ubiquitinated proteins and an impairment of proteasome activity (Fortun et al., 2006). To test if EC137 (50 nM) treatment impacts the accumulation of such slow-migrating poly-ubiquitinated proteins in SCs from C22 mice, cell lysates with or without compound treatment were analyzed with an ubiquitin antibody (Fig. 2-6B). In agreement with our initial studies (Fig. 2-3A), a 16 h treatment with EC137 is associated

with a reduction in high molecular weight poly-ubiquitinated substrates in SCs from C22 mice, as well as Wt mice. This reduction in poly-ubiquitinated substrates is statistically significant in SCs from C22 mice ($p<0.01$; $n=3$) but not in SCs from Wt mice ($p=0.29$; $n=3$) (Fig. 2-6B). GAPDH is shown as a protein loading control.

Improvement in myelination by neuropathic samples could be mediated by an influence of EC137 on glial, as well as neuronal genes. Therefore, we tested purified Wt and C22 mouse SCs (Fig. 2-6C), and DRG neurons with or without glia (Fig. 2-6D), for their response to EC137 treatment. As shown on the Western blots for treatment of DRGs from Wt and C22 mice (Fig. 2-5D), EC137 enhances the steady-state levels of HSP70 and αB-crystallin in SCs from Wt and C22 mice, alike (Fig. 2-6C). In agreement with our previous studies (Ryan et al., 2002; Fortun et al., 2003) and also seen previously (Fig. 2-3A), the basal levels of HSP70 and αB-crystallin are elevated in neuropathic mouse SCs as compared to Wt (compare DMSO controls in Fig. 2-6C), likely as a response to accumulated poly-ubiquitinated substrates. The basal levels of HSP27 and HSP40 in DMSO-treated SCs from C22 mice are comparable to that of SCs from Wt mice and are enhanced in response to EC137 treatment. The steady-state expression of HSP90 (Fig. 2-6C), calnexin and Bip/Grp78 (data not shown) are largely unaffected by EC137. DRG explants from Wt mice containing SCs respond to EC137 by induction of HSP70, HSP27 and αB-crystallin after a 48 h treatment (50 nM), while DRG neurons without SCs show an attenuated reaction (Fig. 2-6D). The same experiment was also done for 24 h treatment with EC137 (50 nM) and essentially showed a similar pattern of induction (data not shown). This result indicates that EC137 primarily influences chaperone synthesis in peripheral glial cells, as compared to sensory neurons.

Discussion

Enhancement of the HS response by natural or synthetic compounds is of therapeutic interest for protein misfolding disorders (Westerheide and Morimoto, 2005). Hereditary neuropathies linked to the misexpression of PMP22 share characteristics with such disorders including the formation of cytosolic protein aggregates (Fortun et al., 2003; Fortun et al., 2006). Here we tested if enhancement of the chaperone pathway through inhibition of HSP90 would be beneficial for myelin formation by SCs from neuropathic mice with PMP22 misexpression. The chosen synthetic, small molecule HSP90 inhibitors offer a favorable approach as they exhibit low cellular toxicity, and induce sustained expression of HSPs (Dickey et al., 2005; Dickey et al., 2007). Our results indicate that non-myelinating and myelinating glial cells respond to EC137 by increased expression of chaperones, including HSP70, HSP27 and αB-crystallin. Significantly, the enhancement of chaperones is associated with a pronounced improvement in myelination in neuron-glia explant cultures from neuropathic mice, as compared to untreated controls. These results suggest that peripheral glial cells are amenable to pharmacologic modulation of the HS response and recommend further studies with these compounds.

While the precise molecular mechanism by which inhibition of HSP90 aids myelin formation by SCs from neuropathic mice is unclear, it likely involves the assistance of chaperones in the folding and processing of myelin proteins, including PMP22 (Fig. 2-7). Studies in cultured cells and neuropathic nerves indicate that PMP22 is prone to aggregation and accumulates in the cytoplasm of SCs when the proteasome is inhibited or the protein is misexpressed (Fig. 2-7A) (Notterpek et al., 1999b; Fortun et al., 2003; Fortun et al., 2007). These intracellular PMP22 aggregates retain cytosolic chaperones

and MBP, which alters protein homeostasis within SCs. The sustained enhancement of the available pool of chaperones by EC137 likely aids the correct folding of newly-synthesized PMP22 and other glial proteins, and promotes their trafficking to the plasma membrane (Fig. 2-7B). The observed increase in the endo H-resistant fraction of PMP22 in EC137 treated cultures (Fig. 2-6A) indeed supports a primary influence of this compound on protein folding. The treatment with EC137 also decreased the levels of poly-ubiquitinated proteins within SCs from C22 neuropathic mice (Fig. 2-6B), which may suggest an effect on protein degradation. Based on our current results, a potential role for chaperones in aiding the removal of misfolded PMP22 cannot be ruled out.

A protective role for chaperones in preventing the misfolding and subsequent aggregation of PMP22 is supported by our previous *in vitro* studies (Notterpek et al., 1999a; Fortun et al., 2007). In normal non-myelinating rat SCs, under conditions of proteasome inhibition, over ninety percent of the cells form PMP22 aggregates. When these studies were performed in conjunction with HS preconditioning or GA treatment, the misfolding of PMP22 was significantly reduced (Fortun et al., 2007). The decrease in protein aggregate formation in this pharmacologic model was likely due to the enhancement of cytosolic molecular chaperones, which aid the processing of newly-synthesized PMP22 and/or refolding of small aggregates before the assembly of large inclusions. In the same assay, GA was more effective in preventing protein aggregate formation, as compared to HS (Fortun et al., 2007). GA binds to the ATP site on HSP90 and blocks its interaction with HSF1, and thus promotes HSF1 activation and the synthesis of HSPs (Prodromou et al., 1997; Zou et al., 1998). However, extended or high dose treatment with GA is associated with cellular toxicity which limits the potential therapeutic use of this compound (Miyata, 2005). EC137 a synthetic small molecule

inhibitor of HSP90 used in this study has suitable pharmacokinetic profile (Figs. 2-2 to 2-4) for potential therapeutic use and enhances the levels of HSP70 for over 36 h in SCs, as compared to vehicle control (Fig. 2-3D). Intraperitoneal injection of EC102, a small synthetic HSP90 inhibitor, and EC72, a derivative of GA, in mouse models of tauopathy and experimental autoimmune encephalomyelitis, respectively, induced high levels of HSP70 with low toxicity and was associated with an amelioration of disease (Dello Russo et al., 2006; Dickey et al., 2007). It is yet to be determined if EC137 identified in this study could be administered intraperitoneally to neuropathic mice.

The modulation of the HSR in preventing the aggregation of cytosolic and nuclear disease-linked proteins has been studied extensively (Westerheide and Morimoto, 2005). For example, live cell imaging experiments show that HSP70 associates transiently with huntingtin aggregates, with association-dissociation kinetics identical to chaperone interactions with unfolded polypeptides (Kim et al., 2002b). On the contrary, the protection observed in Drosophila models of Parkinson's and polyglutamine expansion in response to overexpression of HSP70 is not accompanied by a reduction in the number of inclusions (Warrick et al., 1999; Auluck et al., 2002; Kazemi-Esfarjani and Benzer, 2002). A multidomain glycoprotein whose misfolding is associated with disease is cystic fibrosis transmembrane regulator (CFTR) (Amaral and Kunzelmann, 2007). CFTR and PMP22 share similarities in their high propensity for aggregation and they are both substrates for proteasomal degradation (Johnston et al., 1998; Notterpek et al., 1999b). In cells stably transfected with Wt CFTR, the overexpression of HSP70 and its co-chaperone HSP40 was associated with an increased stability of the immature CFTR, but had no influence on the maturation of the protein (Farinha et al., 2002). Currently it is unknown if the beneficial effects of elevated HSPs on PMP22 processing

are mediated by direct or indirect interactions between these proteins. The only chaperone so far identified to interact with PMP22 is calnexin (Dickson et al., 2002).

In general, a critical role for chaperones in myelination is supported by multiple studies, in distinct model systems. The association of HSP70 with MBP in an ATP-dependent manner in the normal human brain (Lund et al., 2006) implies that HSP70 is involved in the proper folding and trafficking (Hartl, 1996) of this cytosolic myelin protein. Indeed, constitutive expression of HSC70 appears to be essential for the correct expression of MBP during the differentiation of oligodendrocytes (Aquino et al., 1998). When HSC70 expression was shut-down the steady-state levels of MBP dramatically decreased (Aquino et al., 1998). In agreement, we observed elevated expression of MBP and significant increase in MBP-positive myelin internodes in response to EC137 treatment, as compared to control samples (Fig. 2-5). This functional improvement correlates with induction of HSP70 and HSP27 within SCs (Figs. 2-5D, 2-6C). In an independent study using the transgenic approach, the deletion of *hsf1* resulted in a demyelinating phenotype, possibly due to defects in oligodendrocyte differentiation, or myelin synthesis and assembly (Homma et al., 2007). These results support our working model (Fig. 2-7), in which induction of HSPs via HSF1 activation in myelinating neuropathic SCs enhances the cytosolic chaperone pool, reduces the accumulation of poly-ubiquitinated substrates, and aids the trafficking of PMP22.

Studies in CMT1A pedigrees and genetically engineered neuropathic models underscore the importance of adequate levels of correctly-folded PMP22 for myelin formation and stability (Kuhlenbaumer et al., 2002; Robertson et al., 2002b). In C22 mice, the secretory pathway appears to be overwhelmed as we detected an accumulation of newly-synthesized PMP22 within the cytosol and a decrease in the

endo H-resistant PMP22 at the plasma membrane (Fortun et al., 2006). In agreement, studies of sural nerve biopsies from CMT1A patients with PMP22 gene duplication or point mutations show PMP22-like immunoreactivity in the myelin sheath, as well as within the SC cytoplasm (Nishimura et al., 1996; Hanemann et al., 2000). However, the PMP22-like myelin staining is thin (Nishimura et al., 1996) and there is a reduction in the number of PMP22-positive myelinated fibres (Hanemann et al., 1994), implying that only a small fraction of PMP22 is incorporated into myelin. Previously published therapeutic approaches to correct the myelin defects in PMP22-associated neuropathies include the use of progesterone antagonists and ascorbic acid (Sereda et al., 2003; Passage et al., 2004). In both of these studies, the neuropathic phenotype was substantially ameliorated by the interventions, and ascorbic acid is now in clinical trial for CMT 1A (Pareyson et al., 2006). Our current findings, while posing to be promising in culture, await further testing in neuropathic mice where optimal bioavailability of these compounds in peripheral nerves can be established. Based on data presented here, the tested small molecule inhibitors of HSP90, particularly EC137, could potentially offer a new approach for the treatment of demyelinating neuropathies.

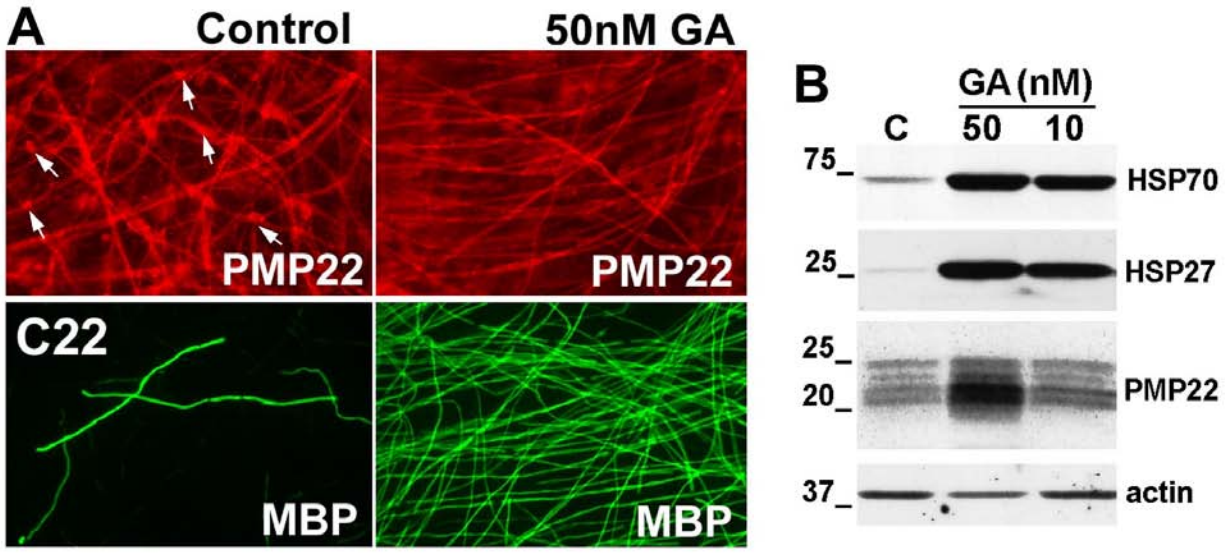

Figure 2-1. Myelin production is stimulated by geldanamycin. (A) DRG explant cultures from C22 mice under myelinating conditions, were treated with DMSO or GA (50 nM) for 72 h, and stained with polyclonal anti-PMP22 (red) or anti-MBP (green) antibodies. Enhanced PMP22-like immunoreactivity is associated with the SC bodies (arrows) in the DMSO-treated samples. Magnification, X40. (B) The steady-state levels of HSP70, HSP27 and PMP22 were determined in total lysates of DRG explant cultures (20 µg/lane) from C22 neuropathic mice after 72 h of GA-treatment (10 and 50 nM), as compared to DMSO control (C). Actin serves as a protein loading control. Molecular mass in kDa.

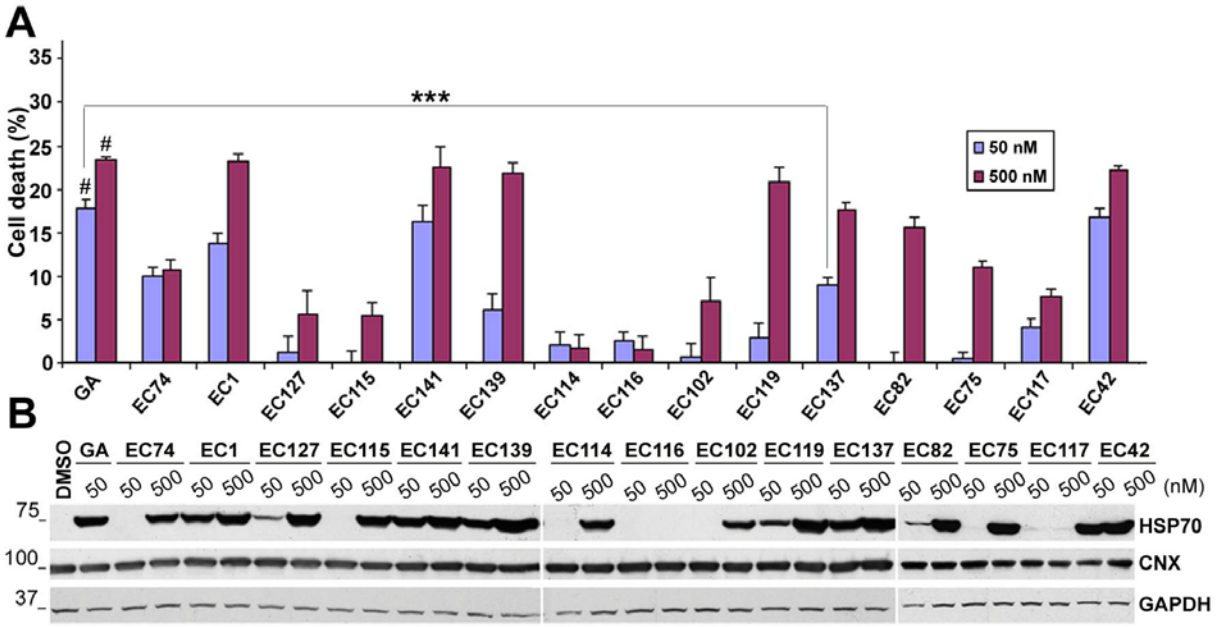

Figure 2-2. Cellular toxicity and chaperone expression for the HSP90 inhibitors. (A) Non-myelinating rat SCs were treated with DMSO (control) or HSP90 inhibitors at 50 and 500 nM concentrations for 16 h and then incubated in MTT (0.5 mg/ml) for 5 h at 37 °C. The toxicity of the test compounds was determined from three independent experiments with respect to DMSO treated control cells, which was set at 0% cell death (***$p<0.001$ and #$p<0.001$ with respect to DMSO control). Error bars indicate SEM. (B) The levels of HSP70 and calnexin (CNX) were determined by Western blot analyses in total cell lysates (20 µg/lane) after 16 h treatment. GAPDH is shown as a protein loading control. Molecular mass in kDa.

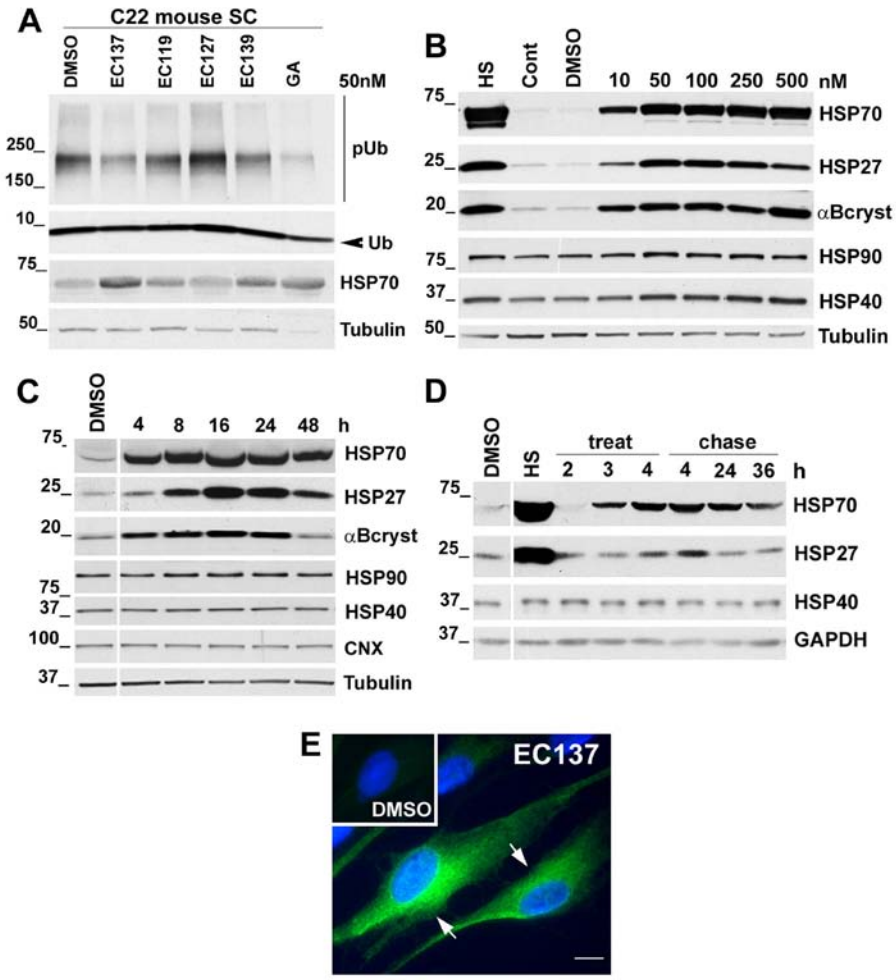

Figure 2-3. EC137 stimulates chaperone production in non-myelinating SCs in dose and time-dependent manner. (A) SCs from C22 neuropathic mice were treated with low toxicity HSP90 inhibitors (EC137, EC119, EC127, EC139; all at 50 nM) and GA (50 nM) for 16 h and the levels of poly-ubiquitinated (pUb) substrates and HSP70 were analyzed by Western blots (20 µg/lane). Arrowhead indicates mono-ubiquitin (Ub). (B) For the dosage response, the levels of HSPs after EC137 treatment of rat SCs (10, 50, 100, 250 or 500 nM) were analyzed in total cell lysates (20 µg/lane). HS followed by 8 h chase at 37 °C is included as positive control. (C) For time-course studies, the levels of HSPs were analyzed after treatment with EC137 (50 nM) for 4, 8, 16, 24 or 48 h. (D) To assess the maintenance of chaperone expression, cells were treated with EC137 (50 nM) for 2, 3 and 4 h. After the 4 h treatment, EC137 was washed out and chaperone expression assayed at 4, 24 and 36 h chase time points. Molecular mass in kDa. Tubulin (A-C) or GAPDH (D) is shown as a protein loading control. (E) In cells treated with EC137 (50 nM, 16 h) the localization of HSP70 is detected with an anti-HSP70 (green) antibody. SCs treated with DMSO (control) exhibit low levels of HSP70-like immunoreactivity (upper left, inset). Hoechst dye was used to stain the nuclei. Scale bar, 10 µm.

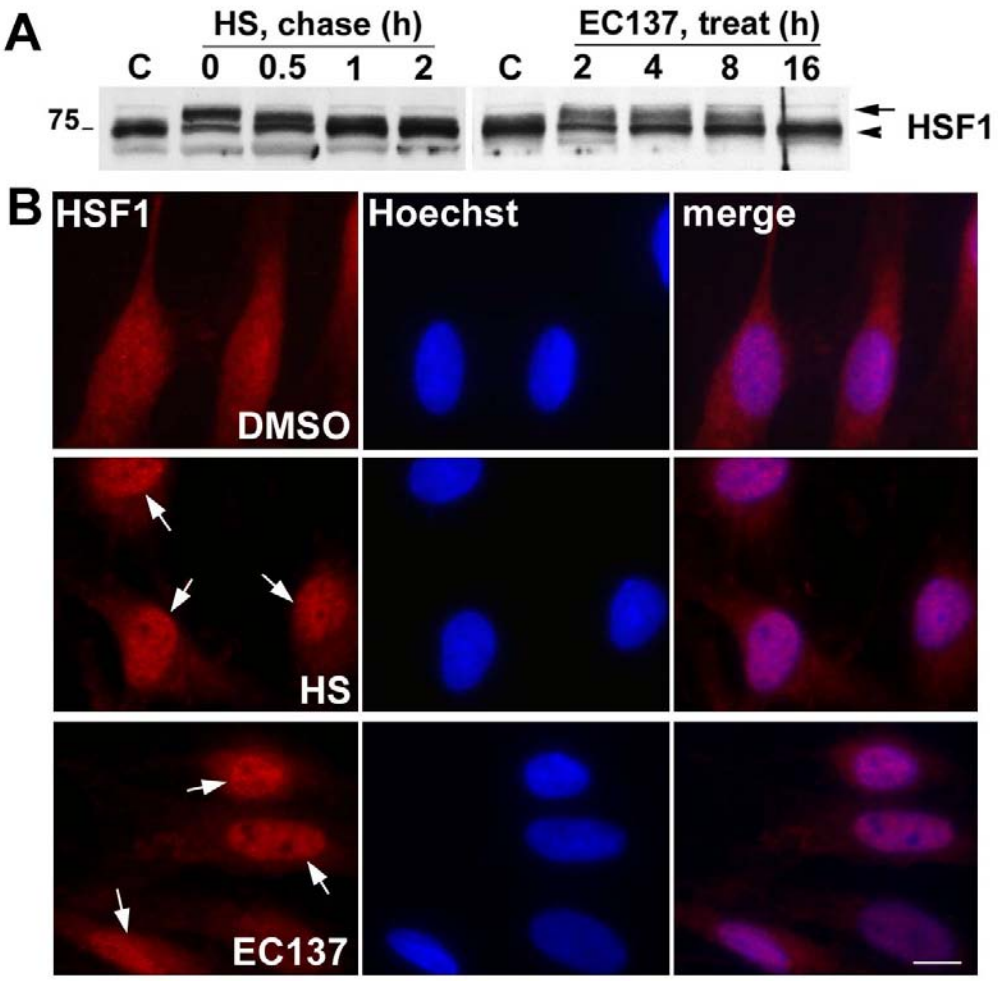

Figure 2-4. Treatment with EC137 activates HSF1. (A) The phosphorylation state of HSF1 after HS and EC137 (50 nM) treatment was assayed by Western blot (20 µg/lane). Phosphorylated HSF1 is indicated by the arrow and the arrowhead marks the migration position of the non-phosphorylated form. Molecular mass in kDa. (B) Cultured rat SCs were treated with HSP90 inhibitor, EC137 and the translocation of HSF1 from cytosol to the nucleus was monitored by staining with an anti-HSF1 (red) antibody. In untreated cells, HSF1 is predominantly cytosolic (upper panel). HS pre-conditioning (45 °C for 20 min) leads to rapid (0 h) nuclear localization of HSF1 (middle panel, arrows). The localization of HSF1 within the nucleus is detected at 2 h after treatment with EC137 (50 nM) (lower panel, arrows). Hoechst dye was used to stain the nuclei. Scale bar, 10µm.

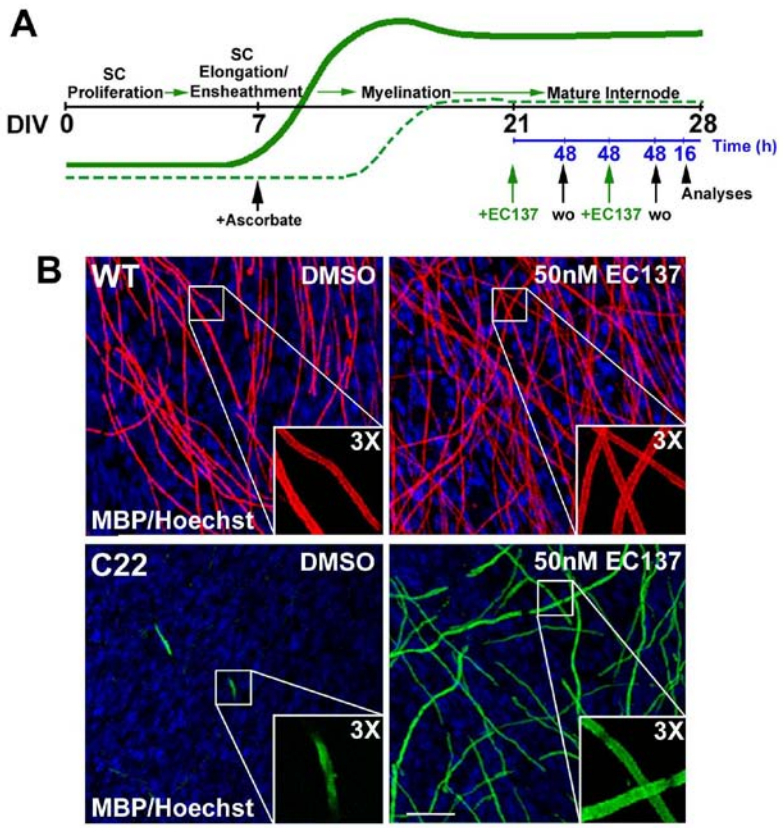

Figure 2-5. Myelin production by neuropathic explant cultures is enhanced by EC137. (A) Schematic of the treatment paradigm for DRGs from Wt and C22 mice with EC137. The black line indicates the time-scale for days *in vitro* (DIV). The lines in green, bold and dashed, represent the expression profiles of myelin proteins in DRGs from Wt and C22 mice respectively. The blue line indicates the time-scale (h) for EC137 treatment. Starting on DIV21, a pulse treatment of EC137 (50 nM) (green arrows) was added for 48 h, followed by 48 h washout (wo, black arrows). This sequence was repeated and a second wash out (16 h) was followed by analyses of the samples (arrow head). (B) DRG explant cultures from Wt (top panel) and C22 neuropathic (bottom panel) mice, under myelinating conditions, were treated with DMSO (control) or EC137 (50 nM) for a total of 96 h as described (A), and stained with an anti-MBP antibody. Insets show the outlined regions at 3X magnification. Hoechst dye was used to stain the nuclei. Scale bar, 40 µm. (C) The lengths of the myelin internodes (n is at least 100 for each condition) were measured in explant cultures from Wt and C22 mice treated with DMSO or EC137 (50nM), using Spot Advanced software. *$p<0.05$, ***$p< 0.001$. Error bars show SEM. (D) DRG explants from Wt and C22 mice were treated as described (A) and whole protein lysates (40 µg/lane) were analyzed for the levels of myelin proteins MAG, P0 and MBP, and of HSP70 from at least three independent experiments. Arrows on the MBP blots indicate the 21.5, 18.5, 17 and 14 kDa isoforms. GAPDH serves as a loading control. Molecular mass in kDa.

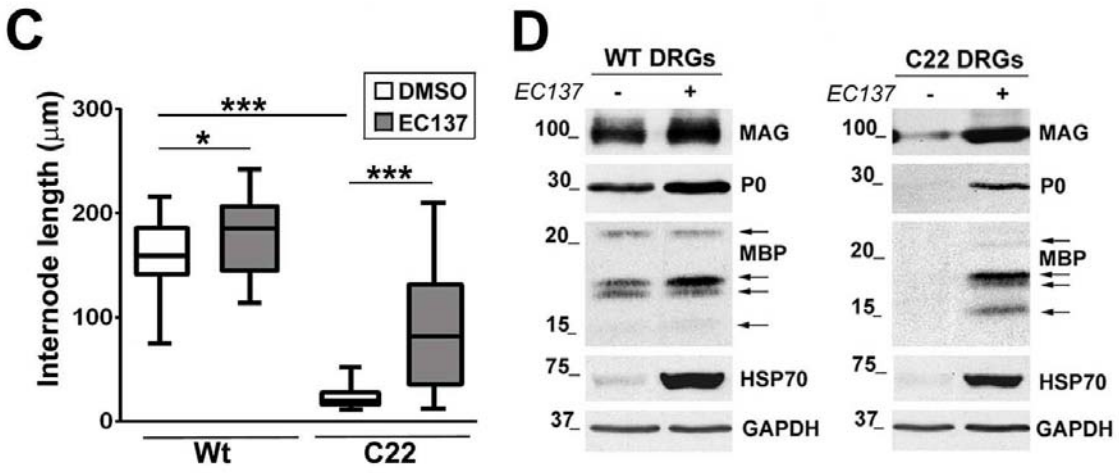

Figure 2-5. Continued

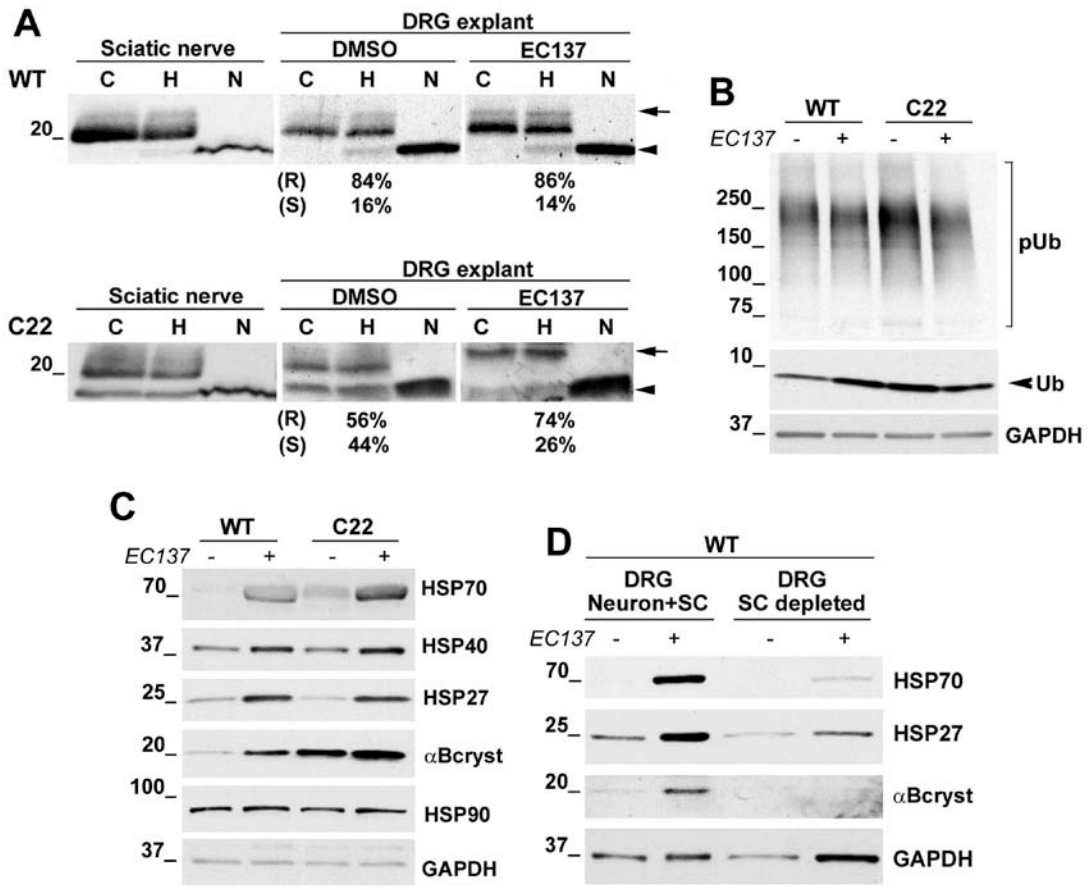

Figure 2-6. Induction of chaperones aids the processing and trafficking of PMP22. (A) Sciatic nerve lysates (10µg/lane) from 6-month-old Wt and C22 mouse (n=3) were treated with endo H (H) or PNGase F (N) and blotted with anti-PMP22 antibody. Total lysates (20µg/lane) from Wt (top) and neuropathic (bottom) DRG explants treated with DMSO or EC137 (50nM) were incubated with endo H (H) or PNGase F (N) and PMP22 was detected. R denotes endo H-resistant and S denotes endo H-sensitive fractions (%) of PMP22. (B) A representative blot for the levels of poly-ubiquitinated proteins in lysates (20µg/lane) of SCs from Wt and C22 mice treated with DMSO and EC137 (50 nM). (C) The levels of HSP70, HSP40, HSP27, αB-crystallin and HSP90 in SC lysates (20µg/lane) from Wt and C22 mice (n=3) treated with DMSO and EC137 (50nM) were assayed. (D) The levels of HSP70, HSP27 and αB-crystallin in DRG explants, and SC-depleted DRG neurons from Wt mice, after treatment with DMSO or EC137 (50nM, 48 h) are shown. GAPDH serves as a constitutive marker for the blots. Molecular mass in kDa.

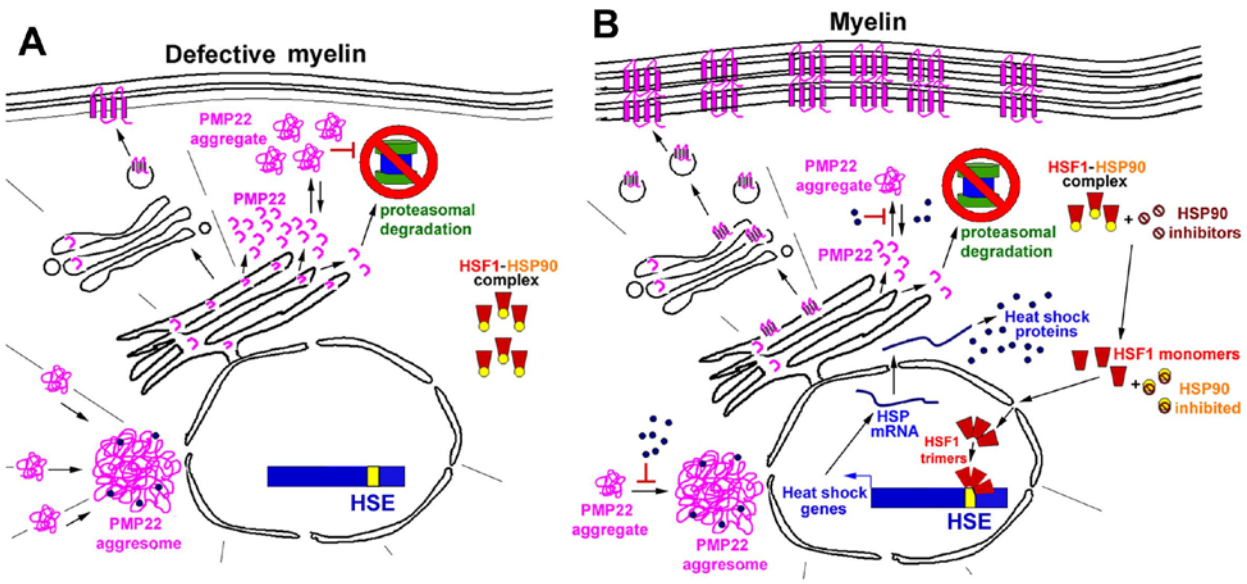

Figure 2-7. Working model: HSP90 inhibitor aids PMP22 processing and improves myelination in neuropathic samples. (A) In SCs from neuropathic mice, there is an accumulation of PMP22 in cytosolic aggregates, which is associated with an impairment of protein degradation by the proteasome. Only a small fraction of PMP22 is transported to the plasma membrane, which leads to defects in myelination. (B) Exposure of SCs to HSP90 inhibitors promotes the activation and nuclear translocation of HSF1. The induction of HS genes and the expression of HSPs prevent the aggregation and promote the correct folding and processing of PMP22, as well as other myelin proteins. Restoration of subcellular protein homeostasis improves myelin formation.

CHAPTER 3
ENHANCEMENT OF AUTOPHAGY BY RAPAMYCIN IMPROVES MYELINATION IN SCHWANN CELLS FROM NEUROPATHIC MICE

Introduction

Aggregation of misfolded proteins and their sequestration into intracellular inclusions is a problem common to diseases of the CNS and PNS (Stefani and Dobson, 2003). CMT1A is a prevalent protein misfolding disease in humans characterized by progressive demyelination of peripheral nerves and associated neuromuscular deficits. During the last ten years there have been many advances with the molecular diagnosis of CMT neuropathies, however effective drug therapy is still not available (Pareyson and Marchesi, 2009). Duplications of, or point mutations within, the *PMP22* gene are known to cause CMT1A (Shy et al., 2001) and other related neuropathies. PMP22 is a hydrophobic integral membrane glycoprotein that is mostly expressed by myelinating SCs (Pareek et al., 1997). Transgenic mice based on the overexpression of the human Wt PMP22 termed C22, and spontaneous mutant (L16P) Trembler J (TrJ), reproduce features of the human neuropathy and provide valuable experimental models to study disease pathogenesis (Suter et al., 1992; Huxley et al., 1996).

PMP22 folds with only a modest efficiency under normal conditions (Sanders et al., 2001) and nearly eighty percent of the newly-synthesized protein is rapidly turned over by the proteasome (Pareek et al., 1997; Notterpek et al., 1999a). In response to PMP22 overproduction and the L16P mutation, excessive or defective PMP22 polypeptides are targeted for degradation by the ubiquitin-proteasome system and accumulate in cytosolic aggregates (Fortun et al., 2003; Fortun et al., 2005; Fortun et al., 2006). Autophagic and lysosomal components as well as HSPs are recruited to ubiquitin-positive PMP22 aggregates in nerves of C22 and TrJ mice, likely reflecting an

attempt by the cells to clear them through alternate pathways. This sequence of events decreases the amount of PMP22 protein within the SC plasma membrane, and likely contributes to the pronounced demyelinating phenotype (Huxley et al., 1996; Notterpek et al., 1997; Fortun et al., 2003; Fortun et al., 2006).

Promising therapeutic approaches for protein misfolding disorders, such as PMP22-associated-neuropathies, include increasing the synthesis of HSPs (Muchowski and Wacker, 2005) and stimulating autophagic protein degradation (Sarkar et al., 2009). In previous studies, we demonstrated that the activation of autophagy by amino acid and serum deprivation (Fortun et al., 2003; Fortun et al., 2007), or intermittent-fasting, suppressed the accumulation of misfolded proteins within neuropathic SCs and improved myelination in TrJ mice (Madorsky et al., 2009). Since such dramatic dietary restriction is not suitable for therapy in humans, here we asked whether pharmacological activation of autophagy within myelinating SCs could offer similar benefits. Rapamycin (RM), a macrolide antibiotic, is a widely used inhibitor of the mammalian target of rapamycin (mTOR) and induces autophagy in a variety of cell types (Sabers et al., 1995; Sarkar and Rubinsztein, 2008). In this study, we show that autophagy is a critical pathway for RM-mediated myelin improvement in neuropathic SCs.

Materials and Methods

Mouse Colonies

PMP22 overexpressor (C22) (Huxley et al., 1996) and spontaneous mutant TrJ (Suter et al., 1992) neuropathic mouse breeding colonies are housed under SPF conditions at the University of Florida, McKnight Brain Institute animal facility. The use of animals for these studies has been approved by an Institutional Animal Care and Use

Committee (IACUC). Genomic DNA was isolated from tail biopsies of mouse pups (less than 10-days old) and litters were genotyped by PCR (Huxley et al., 1996; Notterpek et al., 1997).

Primary Mouse SC Cultures

SC cultures from genotyped postnatal day 6 Wt, C22 and TrJ mouse pups were prepared and maintained as described with slight modifications (Nicholson et al., 2001). Nerves were dissected and enzymatically digested over a period of 2 h. The digestion medium consisted of Dulbecco's Modification of Eagle's Medium/F12 (DMEM/F12) with GlutaMAX-I (Gibco, Grand Island, NY), 15% Fetal Bovine Serum (FBS) (Hyclone, Logan, UT), penicillin streptomycin (Gibco) and an enzyme cocktail of 0.03% collagenase type III (Worthington, Lakewood, NJ), 0.1% hyaluronidase (Sigma-Aldrich, St.Louis, MI) and 1.25 units/mL dispase (Worthington). Next, the cell suspensions were washed once and resuspended in culture medium (DMEM/F12 containing 15% FBS). Cells were then plated in drops on poly-L-lysine (Sigma-Aldrich) coated plastic petri-dishes and allowed to adhere overnight. The next day, cells were washed with DMEM/F12 followed by addition of DMEM/F12 containing 15% FBS, 10 μM of antimitotic agent cytosine β-D-arabinofuranoside (Sigma-Aldrich), to eradicate contaminating fibroblasts. After two 48 h periods of antimitotic treatments, given on alternate days, standard growth medium (DMEM/F12 containing 10% FBS, 10 μg/mL bovine pituitary extract [Biomedical Technologies, Inc., Stroughton, MA] and 2.5 μM forskolin [Calbiochem, La Jolla, CA]) was added and the cells were allowed to proliferate for 2 days to reach 80% confluency.

Autophagic Flux Measurement

Rapamycin (RM) (Calbiochem, San Diego, CA) was dissolved in ethanol vehicle and 0.5 mM stocks were stored at -80 °C. Chloroquine (CQ) (Sigma-Aldrich) was dissolved in water to a stock of 50 mM and aliquots were stored at -80 °C. SCs were treated with vehicle control (Ct) or RM at a final concentration of 25 nM, either in the presence or absence of CQ for 48 h. Following this, the cultures were lysed and analyzed for microtubule-associated protein light chain 3 (MAP-LC3, from here onwards referred to as LC3) by Western blots. A statistically significant increase in LC3 II band intensity in RM+CQ compared to Ct+CQ samples indicates an enhanced autophagic flux and signifies that the pathway attains completion (Mizushima and Yoshimori, 2007).

Metabolic Labeling and ^{35}S-Pulse Studies

SCs were treated with vehicle control (Ct), RM (25 nM) for 48 h or positive control cyclohexamide (Tocris, Bristol, UK) (Chx, 100 µg/ml) for 12 h. During the last 1.5 h of incubation, the cells were starved in methionine- and cysteine-free media with or without RM for 1 h. Following this, a 30 min pulse of medium containing 0.25 mCi/ml *trans* ^{35}S (ICN Biochemicals, Costa Mesa, CA) was added. After lysis in RIPA buffer (Pareek et al., 1997), proteins were precipitated with 5% trichloroacetate and bound ^{35}S-radioactivity was counted in a scintillation counter (LS6500, Beckman Coulter, Fullerton, CA). The counts per minute per µg of protein (cpm/µg protein) were quantified from triplicate experiments. Simultaneously, equal amounts of proteins were separated by SDS-PAGE and the gels were dried and treated with AMPLIFY (Amersham Biosciences, Arlington Heights, IL). Dried gels were exposed to Classic autoradiography film (Molecular Technologies, St.Louis, MO) at -80ºC. Densitometry was performed on the *trans* ^{35}S-labeled protein bands using Scion Image software (Scion, Frederick, MD).

Quantification was performed from triplicate experiments and statistical analysis was performed by Student's t-test using GraphPad Prism.

DRG Explant Cultures and RM Treatment Paradigms

DRG explant cultures were established from Wt, C22 and TrJ mouse embryos as described (Fortun et al., 2006). Cultures were exposed to RM (25 nM) for the indicated time points (Fig. 3-3A), including the last 8 h prior to analysis by immunostaining and Western blots. SC-depleted neuronal cultures (Einheber et al., 1993) were treated for 48 h with RM (25 nM) or vehicle.

Lentiviral Transduction of Mouse DRG Explants

Pre-packaged lentiviral particles were purchased from a commercial provider (Santa Cruz Biotechnology, Santa Cruz, CA), which either encoded a non-targeting shRNA (negative shRNA) (cat# sc-108080), or a sequence specifically targeting mouse Atg12 (cat# sc-72579-V). For the Atg12 knock-down experiments, negative (Neg.) or Atg12 shRNA lentiviral particles were combined with the DRGs from Wt or TrJ mouse embryos at the time of plating. Each individual culture was transduced with approximately 7.5 x 10^4 infectious units of virus. Following transduction, cultures expressing either Neg. or Atg12 shRNA were subjected to the late treatment paradigm (Fig. 3-3A) with RM. Each shRNA transduction experiment was performed at least three times from independent DRG isolations.

To monitor the lentiviral transduction efficiency and transgene expression for the duration of the experiments, we incubated additional subsets of DRG explants with lentiviral particles encoding GFP (cat# sc-108084). Transduction efficiency was obtained as the ratio of the number of GFP+ to total number of cells, from eight random visual fields from three independent culture experiments.

Biochemical Studies

Control and RM treated samples were lysed and processed for Western analyses. The processing of PMP22 was assessed by treatment of the protein lysates with PNGaseF (N) or endo H (H) (New England Biolabs, Ipswich, MA) (Pareek et al., 1997). For the detection of PMP22 and protein zero (P0) we used previously characterized rabbit polyclonal and mouse monoclonal antibodies, respectively (Archelos et al., 1993b; Pareek et al., 1997). All other commercially available primary antibodies are listed in Suppl. Table 1. For the Western blots, bound primary antibodies were detected with appropriate HRP-linked secondary antibodies and visualized using the enhanced chemiluminescence detection kit (PerkinElmer Life Sciences, Boston, MA). Films were digitally imaged using a GS-710 densitometer (Bio-Rad Laboratories) and densitometric analysis of scans from three independent experiments was performed using Scion image. Statistical significance was determined by Student's t-test using GraphPad Prism.

Immunolabeling Studies

Myelinating DRG explant cultures on glass coverslips were fixed, permeabilized and processed for immunostaining with anti-MBP antibodies (Amici et al., 2007). Bound primary antibodies were detected with Alexa Fluor 594 goat anti-rat IgGs (Molecular Probes, Eugene, OR). Hoechst dye (Molecular Probes) was included in the secondary antibody solution to visualize nuclei. Coverslips were mounted using the ProLong Antifade kit (Molecular Probes). Samples were imaged with an Olympus 1X81-DSU spinning disk confocal microscope and were formatted for printing by using Adobe Photoshop 5.5.

Quantification of Myelin Internode Abundance and Lengths

DRG explant cultures were subjected to the treatment paradigms described above and immunostained with an anti-MBP antibody to label internodal myelin segments (Amici et al., 2007). The abundance of myelin internodes was counted as the number of MBP+ internodal segments per 0.1 mm^2 area from three independent experiments, and eight random visual fields per condition (Fig. 3-3A). Internode lengths from the same experiments were measured with Spot RT software (Diagnostic Instruments, Inc., Sterling Heights, MI). Measurements were collected from three coverslips per genotype per treatment paradigm (n=130-260). Statistical significance was determined by Student's t-test using GraphPad Prism software.

Results

Rapamycin Activates Autophagy in Primary Mouse SCs

The activation of autophagy by dietary restriction is able to suppress the formation of PMP22 aggregates and stimulate myelin formation in TrJ mice (Madorsky et al., 2009). To enhance autophagy by pharmacologic means, we exposed mouse SCs to varying doses (10-500 nM) of RM (Sarkar and Rubinsztein, 2008). After six hour (h) incubation, mTOR complex 1 (mTORC1) activity was monitored by the dephosphorylation of phospho-S6 (pS6) ribosomal protein and the activation of autophagy via the lipidation of LC3 (Fig. 3-1A). Based on the observed response, we chose the 25 nM concentration for all subsequent studies as it was the lowest dosage that consistently activated autophagy within Wt cells (Fig. 3-1A to 3-1C). To optimize the frequency of the treatment, the dephosphorylation of pS6 and the conversion of LC3 I to LC3 II (lipidated form) were analyzed over 2-48 h period (Fig. 3-1B). As shown on the Western blot, RM exposure activates autophagy within SCs for at least 48 h, leading to a pronounced

increase in the ratio of lipidated LC3 II/LC3 I (Fig. 3-1C, **p<0.01, n=3). As exposure of certain cell lines to RM at 100 nM concentration can lead to dephosphorylation of Akt through the mTOR complex 2 (mTORC2) pathway (Sarbassov et al., 2006), we analyzed the same cell lysates for phosphorylated Akt (pAkt) (Ser473) (Fig. 3-2A). While over the 48 h treatment period there was a slight decline in the levels of pAkt, when we analyzed samples from three independent experiments this change was not statistically significant (Fig. 3-2B). This data suggest that under the described conditions RM acts primarily via the mTORC1 complex within primary mouse SCs.

To assess autophagic flux, a subset of samples were co-treated with RM and CQ, which inhibits the degradation of LC3 II by lysosomal hydrolases (Maiuri et al., 2007; Mizushima and Yoshimori, 2007). As shown on the blot (Fig. 3-3A) and supported by semi-quantitative analyses (Fig. 3-3B), the simultaneous exposure of SCs to RM and CQ leads to a significant increase in LC3 II, as compared to CQ treatment alone (**p<0.01, n=4). In agreement with the elevated basal lysosomal activity in neuropathic samples (Notterpek et al., 1997; Fortun et al., 2006), the response of C22 SCs to CQ alone is more robust than of Wt. Still, we detected an increase in LC3 II levels upon co-treatment (Fig. 3-3C), which is significant in three independent experiments (Fig. 3-3D, *p<0.05, n=3). These data indicate that while the basal level of autophagy is distinct between Wt and neuropathic samples, RM enhances the response in both cell types.

The intracellular retention of PMP22 in samples from C22 mice is associated with an accumulation of poly-ubiquitinated proteins and an impairment of proteasome activity (Fortun et al., 2006). Hence, we asked whether RM-activated autophagy could suppress the accumulation of pUb substrates within these cells. While we detected a slight

reduction in slow-migrating pUb proteins in Wt samples, this change was more pronounced in cells from neuropathic mice (Fig. 3-3E). As reported previously (Fortun et al., 2006), semi-quantitative analyses confirmed the accumulation of pUb proteins in C22 SCs, as compared to Wt (Fig. 3-3F, *$p<0.05$, n=3), and its reduction by RM (Fig. 3-3F, **$p<0.01$, n=3). To evaluate the effect of extended (48 h) RM treatment on protein synthesis in general within primary SCs, we performed ^{35}S-pulse labeling followed by autoradiography (Pareek et al., 1997) and scintillation counting. Analyses of autoradiographs (Fig. 3-4A), and quantification of protein bound ^{35}S (Fig. 3-4B), reveal that 48 h exposure of the cells to RM does not significantly alter protein synthesis, as compared to vehicle control. These results support the notion that RM promotes the clearance of pUb proteins from neuropathic SCs by activating autophagy, rather than by blocking protein synthesis.

Myelin Production in C22 Neuropathic Samples is Enhanced by Rapamycin

DRG explant cultures from C22 neuropathic mice are impaired in their ability to make myelin (Fortun et al., 2006; Rangaraju et al., 2008), therefore serve as an ideal model to test potential therapeutic compounds for enhancing myelination. Control samples Ct* and Ct** were obtained on days *in vitro* (DIV) 9 and 15, respectively, either two or eight days post-ascorbate, which time points coincided with the initiation of early and late RM exposures (Fig. 3-5A). Ascorbate is necessary for the initiation of myelination (Eldridge et al., 1987) and was included in all of our experiments. As expected from previous *in vivo* and *in vitro* studies (Huxley et al., 1996; Fortun et al., 2006), whole protein lysates of vehicle treated neuropathic cultures harvested on DIV24 contain low levels of myelin proteins, as compared to Wt (Fig. 3-5B, C). However, in

response to RM they show an increase in the steady-state expression of both MBP and P0 (Fig. 3-5B, C). The effect is more pronounced when the cultures were analyzed after the late treatment paradigm, as seen from the quantification of three independent experiments (Fig. 3-6). This data also show that RM exposure enhanced myelin protein synthesis by Wt SCs, which is nearly significant in the late treatment paradigm.

We confirmed the positive effect of RM on myelination by immunostaining DRG explant cultures with an anti-MBP antibody (Fig. 3-7). Cultures from Wt mice contain numerous MBP-positive myelin internodes, while C22 explants form only a few shortened internodes (Fortun et al., 2006). Significantly, RM treatment of affected cultures is associated with a dramatic improvement in the number and length of myelin internodes, as shown on the confocal images (Fig. 3-7A). The characteristic, railroad-like appearance of myelin tracks is displayed in the enlargements in each of the panels (Fig. 3-7A, insets, 3X magnification). Quantifications of the number (Fig. 3-7B) and length (Fig. 3-7C) of myelin internodes reveal highly significant improvements in samples from neuropathic mice, after both early and late RM treatments (***$p<0.001$, $n=3$). Wt DRGs show a slight, but not significant increase in the number of myelin internodes with the intervention (Fig. 3-7B, n.s, $n=3$); however a lengthening of internodal myelin is significant for both early and late treatment paradigms (Fig. 3-7C, $p<0.05$, $n=3$). As the myelinating cultures contain DRG neurons, we tested the response of SC-depleted Wt and C22 cultures (Einheber et al., 1993) to RM. While RM is active in neurons, as judged from the pronounced dephosphorylation of pS6, induction of autophagy is less apparent (Fig. 3-8A). Quantification of the LC3 II and LC3 I ratios

indicate that peripheral neurons are less responsive to RM as compared to SCs (Fig. 3-8B, C). Together, these results demonstrate that the exposure of myelinating SCs to RM is beneficial for myelin synthesis, particularly for cells from neuropathic mice.

Activation of Autophagy Improves PMP22 Trafficking

The accumulation of endo H-resistant PMP22 at the SC membrane correlates with myelin synthesis (Pareek et al., 1997; Notterpek et al., 1999a). Therefore, besides measuring the overall levels of PMP22 in our samples, we determined the subcellular trafficking of the protein (Fig. 3-9A). Consistent with the improvements in myelination (Figs. 3-3 and 3-4), the overall levels of PMP22 are increased in neuropathic samples after early and late RM exposure (Fig. 3-9A). Significantly, we detected an increase in the fraction of endoH-resistant PMP22 in RM treated cultures, as compared to vehicle. Since PMP22 exists in various glycosylated forms, we used N-glycosidase (PNGase F) to confirm that the identified protein bands are indeed PMP22 (Pareek et al., 1997). Semi-quantitative analyses of three independent experiments confirmed the reduced levels of endo H-resistant PMP22 in C22 neuropathic samples, as compared to Wt (Fig. 3-9B, ***$p<0.001$, n=3-4) (Fortun et al., 2006), and its improvement after RM exposure at both early and late RM treatments (Fig. 3-9B, **$p<0.01$, n=3). There is a slight increase in the endo H-resistant fraction of PMP22 in the Wt samples after early and late RM treatment, however, it is not significant ($p=0.0576$, $p=0.0855$, n=4). These results indicate that enhancement of autophagy within C22 neuropathic SCs is associated with an improvement in myelin formation and the subcellular processing of PMP22 (Figs. 3-5, 3-6, 3-7 and 3-9).

The Positive Effect of RM is not Genotype Specific

A suitable therapeutic agent for hereditary neuropathies would not be genotype-specific, but rather show efficacy in multiple models. To assess whether RM could be beneficial for PMP22 point mutant neuropathies, we carried out studies with SCs and myelinating explant cultures from TrJ mice (Fig. 3-10). Similar to the C22 model, DRGs from TrJ mice were incubated with RM at early or late stages of myelination and analyzed for MBP and P0 (Fig. 3-10). Myelinating explants from TrJ mice respond positively to RM and show an increase in the steady-state levels of MBP and P0 (Fig. 3-10A, B). In agreement, DRG cultures immunolabeled with an MBP antibody reveal a pronounced increase in MBP-positive myelin segments in response to treatment (Fig. 3-10C). Quantification from three independent experiments shows a significant improvement in the number (Fig. 3-10D, ***$p<0.001$, $n=3$) and length (Fig. 3-10E, **$p<0.01$, $n=3$) of myelin internodes, as compared to vehicle. We confirmed the autophagic response in TrJ SCs, by analyzing protein lysates for pUb and LC3 after 48 h treatment with RM (Fig. 3-11A). As seen with the C22 sample (Fig. 3-3E, F), treatment with RM promotes a significant reduction in slow-migrating pUb substrates (Fig. 3-11B) and an approximately two-fold increase in LC3-II/LC3 I ratios (Fig. 3-11C). Therefore, RM is an effective enhancer of autophagy in SCs from TrJ mice and improves their myelination capacity when in neuronal contact.

Autophagy is a Critical Pathway for the Myelin-Promoting Effect of Rapamycin

While RM is an effective enhancer of autophagy in SCs (Figs. 3-1, 3-3 and 3-11), to confirm the contribution of this pathway to the observed positive effects, we utilized lentiviral-mediated shRNA gene ablation (Bolis et al., 2009). We transduced DRG

explants with lentivirus carrying GFP and visualized the efficiency of transduction by direct GFP fluorescence (Fig. 3-12). We obtained high transduction efficiency which was nearly 65% (64.66±9.04) on DIV11 (Fig. 3-12A) and around 62% (62.23±11.88) on DIV26 (Fig. 3-12B). We performed shRNA-mediated inhibition of the vital autophagy gene, autophagy related gene 12 (*Atg12*) that is required for the elongation of the autophagosome (Dreux et al., 2009). Scramble negative (Neg.) and Atg12 shRNA transduced Wt and TrJ explants were treated with vehicle control (Ct) or RM as described in Fig. 3-5A. Upon analysis of the protein lysates at the end of the treatment, the steady-state levels of Atg12 protein is reduced in samples transduced with Atg12 shRNA, both in the absence and presence of RM (Fig. 3-13A). We analyzed the levels of MBP and P0 within the same samples (Fig. 3-13A). Quantification from three independent experiments reveals that Atg12 protein levels are reduced by ~50% in cultures expressing Atg12 shRNA, as compared to those transduced with Neg. shRNA. (Fig. 3-13B, *$p<0.05$). Analyses of MBP levels normalized to glyceraldehyde 3-phosphate dehydrogenase (GAPDH) reveal that downregulation of Atg12 did not significantly decrease MBP in Ct and RM treated Wt samples (Fig. 3-13C, n.s, n=3). However, the effect of RM to slightly improve MBP levels in Wt DRGs (see Fig. 3-6), in this case transduced with Neg. shRNA, is reproducible (Fig. 3-13A, $p=0.0569$). The reduction in Atg12 did not lead to a significant decrease in MBP in Ct samples from TrJ mice (Fig. 3-13C, n=3). As seen previously (Fig. 3-10B), we detected improvement in MBP levels with RM treatment in Neg. shRNA transduced neuropathic samples (Fig. 3-13C, **$p<0.01$), which was then largely abolished by the inhibition of Atg12 (Fig. 3-13C, *$p<0.05$, n=3). Similarly, the RM-mediated improvements in P0 levels are attenuated by

the knock-down of Atg-12 (Fig. 3-13D). Together, these results indicate that an intact autophagy pathway is necessary for the myelination-promoting activity of RM.

Discussion

Hereditary neuropathies are common among the population, yet treatment options for affected individuals are limited. Currently, there is no effective drug therapy for CMT1A neuropathies and supportive care is limited to rehabilitation and surgical treatments (Pareyson and Marchesi, 2009). A recent twelve-month clinical trial with ascorbic acid did not produce positive results, as efficacy of this antioxidant was not shown (Micallef et al., 2009). Here we tested RM, a widely used therapeutic compound for its ability to enhance autophagic response within neuropathic SCs, and improve their capacity to myelinate. We show that RM effectively activated autophagy in mouse SCs and lead to a significant reduction in pUb substrates. SCs from neuropathic mice responded to low concentrations (25 nM) of RM and produced more myelin, as compared to vehicle controls. Significantly, RM improved myelination in two genetically distinct neuropathic models, including the gene duplication (C22) and the point mutation (TrJ) genotypes. Knockdown of a key autophagy gene Atg12 in myelinating SCs abolished the improvements in myelination by RM, suggesting a crucial role for autophagy in this beneficial effect.

CMT1A neuropathies associated with PMP22 gene duplication or mutations share characteristics with protein misfolding disorders, including the accumulation of ubiquitin-reactive protein aggregates and alterations in chaperone levels (Winklhofer et al., 2008). Once protein aggregates form they can interfere with essential cellular functions, such as myelination in the case of SCs. In this study, the reduction in pUb substrates with RM treatment is evident in SCs from both neuropathic models. The decline in the

accumulation of pUb substrates by autophagy may help in alleviating the burden on the proteasomal pathway (Fortun et al., 2005), which is the main degradative mechanism for the removal of newly-synthesized PMP22 (Pareek et al., 1997). Restoration of protein homeostasis, including the improvement in the processing of PMP22, would likely provide a more permissive environment for myelination by SCs from neuropathic mice. Since P0 and MBP genes are coexpressed with PMP22 in myelinating SCs (Kuhn et al., 1993) and at the protein level PMP22 and P0 interact (Hasse et al., 2004), the improvement in PMP22 processing by RM most likely contributed to the concomitant increase in the expression of P0 and MBP (Figs. 3-5, 3-7 and 3-10).

Compounds that enhance the activity of intracellular quality control mechanisms are possible treatment approaches for protein aggregation disorders. The roles of the chaperone and autophagy pathways in peripheral nerve biology have been less studied as compared to neurons and glia of the CNS, nonetheless a decline in the activity and/or efficiency of protein folding and/or degradation mechanisms likely contribute to age-associated degenerative changes in myelinated peripheral nerves. In a previous study, we chose the intermittent fasting regimen as proof-of-principle intervention to activate chaperones and autophagy in neuropathic mice (Madorsky et al., 2009). After a five month long intervention, diet restricted mice showed an improvement in locomotor performance and myelination, as compared to ad libitum (AL) fed littermates. Since such drastic dietary restriction is not suitable for humans, compounds that enhance chaperone production and/or autophagy will be more attractive for future therapies.

Autophagy is a particularly appealing target for therapeutic development for neurodegenerative diseases which are progressive with age, as activation of autophagy

in normal aged mice appears to extend lifespan without negative side effects (Harrison et al., 2009). Upregulating autophagy by RM and other small molecules has been shown to suppress aggregation of disease-linked proteins, including huntingtin, alpha-synuclein, and to reduce cellular toxicity (Jaeger and Wyss-Coray, 2009). More recently, RM and its analog have been shown to confer neuroprotection and ameliorate disease symptoms in mouse models of Parkinson's disease (Malagelada et al.) and spinocerebellar ataxia type 3 (Menzies et al.), respectively. Independent studies using the transgenic approach confirm the involvement of autophagy in the removal of misfolded proteins, as mice deficient in autophagy genes within the CNS form intracellular inclusions and develop neurodegenerative symptoms (Hara et al., 2006; Komatsu et al., 2006; Mizushima and Hara, 2006). Consistent with these findings, the presence of misfolded aggregated PMP22 within peripheral nerves is associated with the neuropathic phenotype and demyelination (Fortun et al., 2003; Fortun et al., 2006). In comparison, aggregates are reduced and myelin is improved in response to activation of autophagy and chaperones by long-term dietary restriction (Madorsky et al., 2009; Rangaraju et al., 2009), or by RM treatment as shown here. The results presented here are comparable to the increase in myelination in neuropathic samples by pharmacological activation of the HS pathway (Rangaraju et al., 2008), and suggest that combined pharmacological activation of the two protein quality control mechanisms, HS and autophagy pathways, might provide additive benefits.

RM is a widely used therapeutic compound that can elicit unique responses in different model systems and at given doses (Sarkar and Rubinsztein, 2008). With regards to the neural biology, besides its influence on autophagy in protein aggregation-

linked neurodegenerative disorders (Jaeger and Wyss-Coray, 2009), RM has been tested in models of brain tumors and neuronal cell death. For example, in a mouse model of tuberous sclerosis the exposure of young mice to RM was associated with improved phenotype, including enhanced myelination (Meikle et al., 2008). In our PNS models, RM has a pronounced positive effect on SC function, specifically on myelination. We detected an increase in both the abundance and the lengths of myelin internodes indicating that RM supported the differentiation of myelinating SCs and their capacity to expand myelin sheaths (Figs. 3-7 and 3-10). The Atg12 knockdown experiments indicate that an intact autophagy pathway is necessary for the myelin improvements in RM-treated cultures (Fig. 3-13). This result supports our hypothesis that restoration of protein homeostasis within SCs improves the cells ability to myelinate axons. Nonetheless, contribution from other mechanisms such as the Akt pathway cannot be ruled out at this time. Akt is involved in neuregulin-mediated SC survival (Li et al., 2001) and in regulating myelination by oligodendrocytes (Narayanan et al., 2009). Additionally, RM is known to affect the endocytic pathway which appears to be important for myelination and membrane wrapping (Saito et al., 2005; Winterstein et al., 2008). Therefore, while the rationale for our studies with RM as a therapeutic agent for PMP22-associated neuropathies stem from our investigations of PMP22 trafficking and protein aggregation, it is possible that besides autophagy, RM will benefit neuropathic nerves through other mechanisms. The observed improvement in samples from Wt mice supports such hypothesis. In addition, in mice, RM may suppress the immune component of the neuropathy, which could offer an additional benefit to affected nerves (Hartung et al., 1992).

Based on the positive results presented here, we propose that RM is a suitable compound for further testing in neuropathic mice. As shown by our cellular studies, this drug is well-tolerated by myelinating SCs as well as peripheral neurons and is effective at the low nM range. A recent study in aged mice showed that RM fed late in life extends lifespan, without toxic side effects (Harrison et al., 2009). RM is an FDA-approved drug that is widely used in immunosuppression following organ transplantation, however chronic use of RM can lead to adverse side-effects (Kahan, 2008). As SCs respond robustly to RM and the PNS is outside of the blood brain barrier, it is possible that peripheral nerves will respond to this compound more robustly than the CNS. In addition, small molecule enhancers of autophagy are being developed and identified and could offer alternatives for RM in the future (Sarkar and Rubinsztein, 2008). In summary, our results provide further support for the involvement of autophagy as a protective pathway in PMP22-associated neuropathies and provide a positive step toward identifying pharmacologic agents for these disorders.

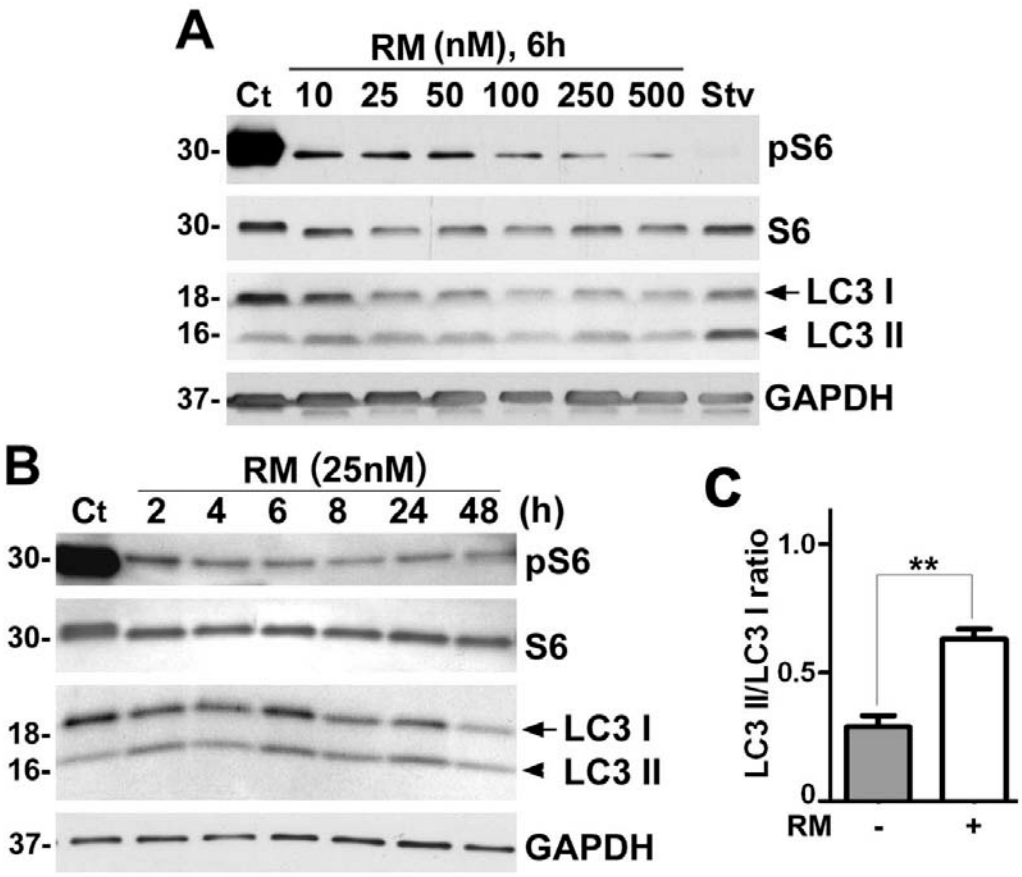

Figure 3-1. Rapamycin effectively induces autophagy in cultured mouse SCs. (A) For the RM dose response, the expression levels of the indicated proteins were monitored via Western blot. Lysates of vehicle control (Ct) and 4 h starvation (Stv) medium treated cells were included as negative and positive controls, respectively. (B) For the time-course studies, the levels of the same proteins were analyzed after treatment with Ct or RM (25 nM) for the indicated times. (A, B) GAPDH is the protein loading control. Molecular mass, in kDa. (C) The ratios of LC3 II to LC3 I band intensities measured from Western blots of cell lysates treated with vehicle (-) or 25 nM RM (+) for 48 h are shown. (**$p<0.01$, t-test, mean±SEM, n=3).

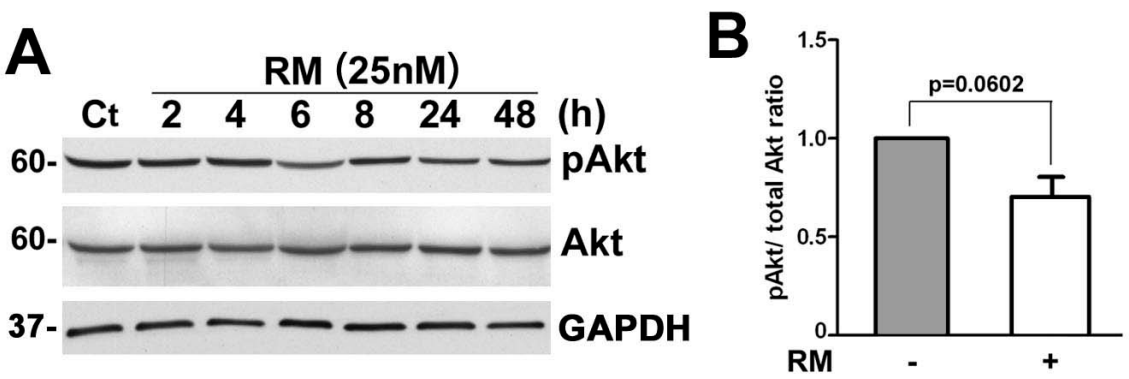

Figure 3-2. Rapamycin treatment has minimal effect on the Akt pathway in mouse SCs. (A) The levels of phosphorylated Akt (pAkt) and total Akt were analyzed after treatment with Ct or RM at 25 nM for the indicated times. GAPDH is the protein loading control. Molecular mass, in kDa. (B) Quantification of the ratio of pAkt/total Akt without (-) or with (+) RM (25 nM, 48 h) is shown (p=0.0602, t-test, mean±SEM, n=4).

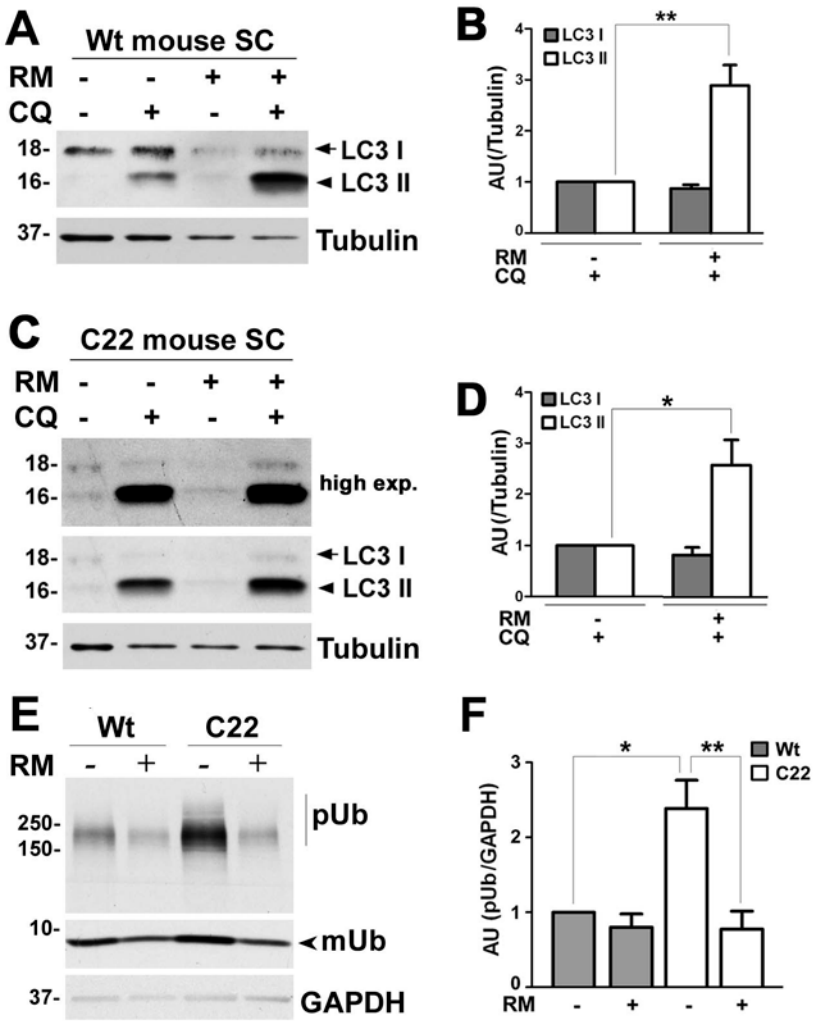

Figure 3-3. Enhancement of autophagy reduces the levels of ubiquitinated substrates. (A) Wt mouse SCs were treated with vehicle control (-) or RM (+), without (-) or with (+) the lysosomotropic alkaline CQ. The level of autophagy markers LC3 I (arrow) and LC3 II (arrowhead) were determined by Western blots. (B) Quantification of LC3 I and LC3 II band intensities normalized to tubulin are shown. LC3 I and II values of cells treated with CQ was set as 1 (**p<0.01, t-test, mean±SEM, n=4), AU, arbitrary units. (C) Western blot showing LC3 I and LC3 II levels in C22 mouse SCs, treated as in (A). A longer exposure (high exp.) blot for LC3 is shown to visualize LC3 I levels. (D) Quantification of LC3 I and LC3 II band intensities in C22 samples is shown. (*p<0.05, t-test, mean±SEM, n=3). (E) The steady-state levels of slow-migrating poly-ubiquitinated proteins (pUb) in lysates of SCs from Wt and C22 mice treated with vehicle (-) or RM (+) are shown. Mono-ubiquitin (mUb) is marked by concave arrowhead. GAPDH is a loading control. Molecular mass, in kDa. (F) Quantification of pUb/GAPDH in A. The value of pUb/GAPDH in Wt was set as 1 (*p<0.05, **p<0.01, t-test, mean±SEM, n=3), AU, arbitrary units.

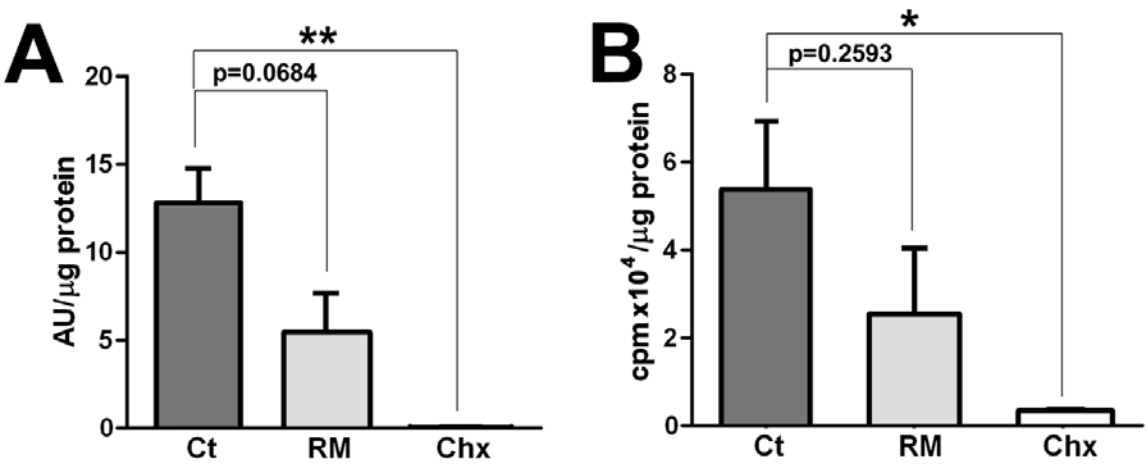

Figure 3-4. Protein synthesis in rapamycin treated SCs. (A) Wt mouse SCs were treated with vehicle (Ct), 25 nM RM for 48 h or 100μg/ml cyclohexamide (Chx) for 12 h followed by 35S pulse labeling. Equal amounts of protein were resolved by a SDS-PAGE and autoradiographs were obtained. Quantification of autoradiographs is shown (p=0.0684, **p<0.01, t-test, mean±SEM, n=3). (B) In a subset of samples, the proteins were precipitated and counts per minute (cpm) of protein-bound 35S-radioactivity was measured and normalized to μg of protein (p=0.2593, *p<0.05, t-test, mean±SEM, n=3).

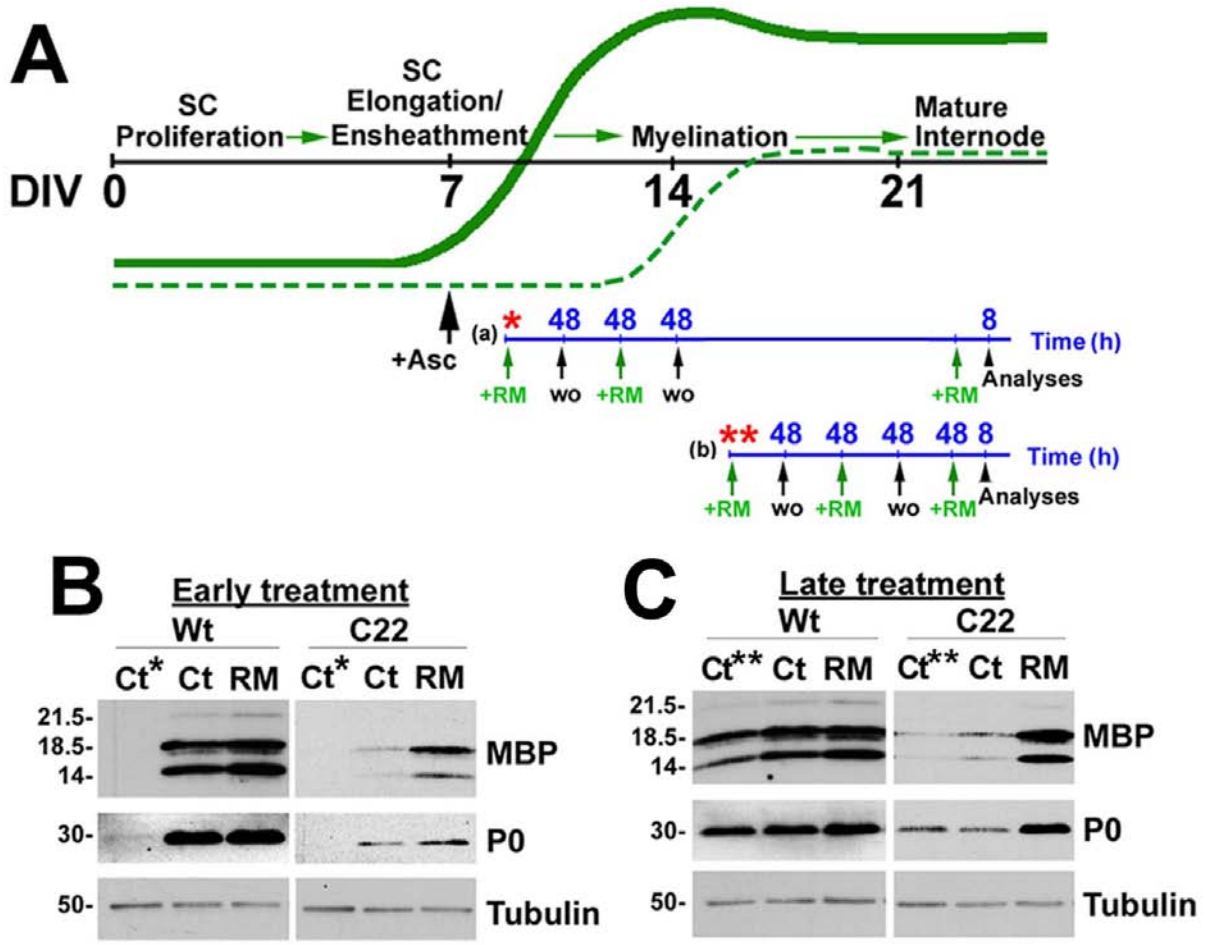

Figure 3-5. Rapamycin promotes myelination by SCs. (A) Schematic representation of the RM treatment paradigms. The black line indicates DIV, while the green lines represent the expression profile of myelin proteins in Wt (bold green) and neuropathic (dashed green) samples. The blue line indicates the time-scale for RM treatment in hours (h). Asterisks indicate the DIV at which the control samples Ct* and Ct** were obtained. For early RM treatment (a), starting on DIV9, or for late treatment (b) starting on DIV15, a pulse of RM (green arrows) was given for 48 h, followed by 48 h washout (wo, black arrows). This sequence was repeated and a third RM treatment (8 h) was given prior to analysis (arrowhead). (B, C) DRG explants from Wt and C22 mice were treated with RM as indicated and whole protein lysates were analyzed for the myelin proteins, MBP and P0. The main isoforms of MBP are marked. Tubulin is shown as protein loading control. Molecular mass, in kDa.

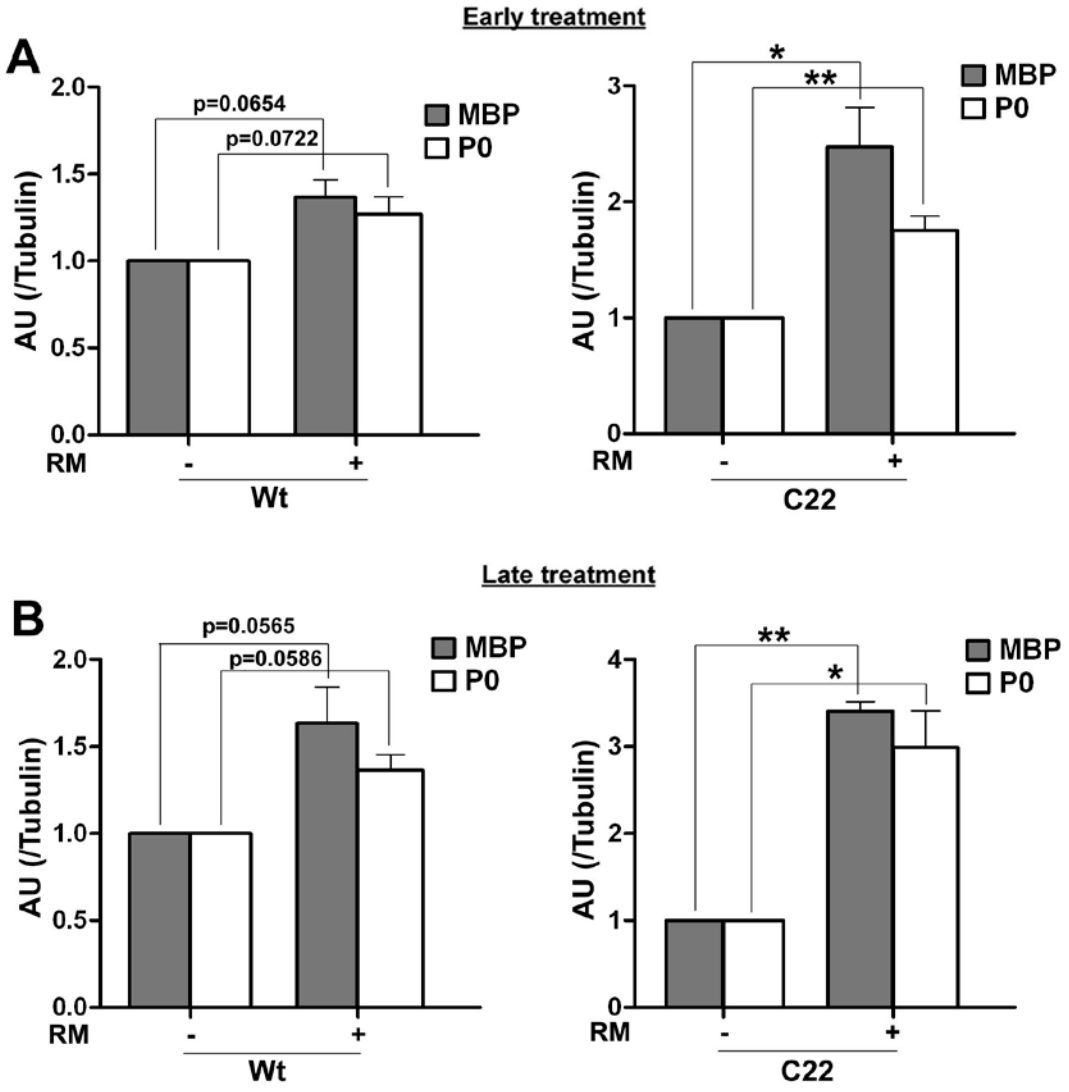

Figure 3-6. Late treatment of rapamycin improves myelin protein expression better than early treatment in C22 samples. (A) Quantification of myelin protein levels (MBP and P0) in Wt and C22 DRG explants following early treatment with vehicle (-) or RM (+) in Fig.3B. MBP and P0 values after normalizing to tubulin in vehicle-treated (-) samples were set as 1. AU, arbitrary units. (p= 0.0654, p=0.0722, *p<0.05, **p<0.01, t-test, mean±SEM, n=3-4). (B) Quantification of MBP and P0 band intensities in Wt and C22 samples after late RM treatment paradigm in Fig. 3C. MBP and P0 values after normalizing to tubulin in Ct (-) samples were set as 1. AU, arbitrary units. (p=0.0565, p= 0.0586, *p<0.05, **p<0.01, t-test, mean±SEM, n=3-4).

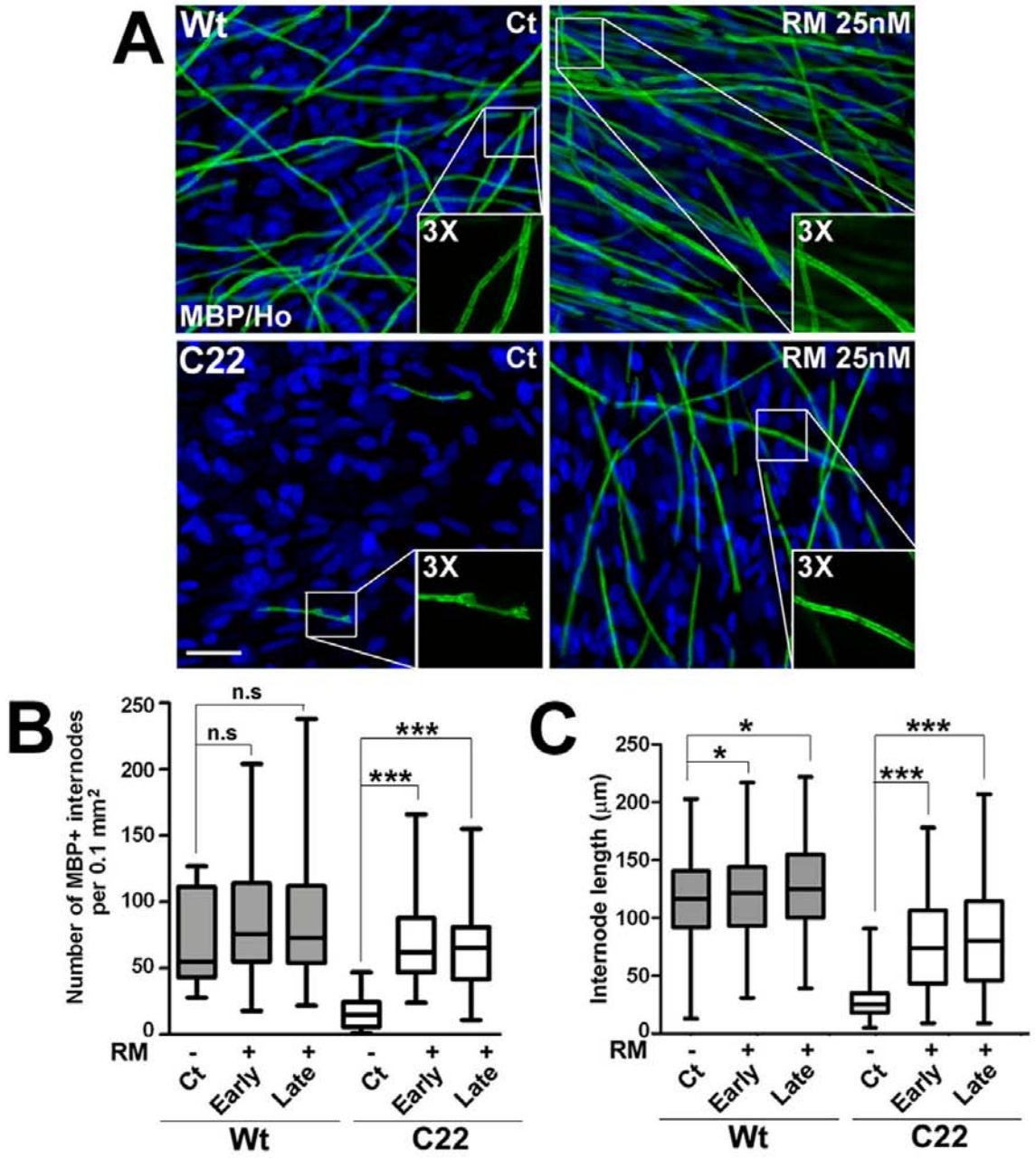

Figure 3-7. The abundance and length of myelin internodes are increased by rapamycin. (A) Explant cultures from Wt and C22 mice were treated with Ct or RM at late stage, as described in Fig. 3A, and stained for MBP (green) to visualize myelin. Scale bar, 40 μm. Hoechst dye stains the nuclei (blue). (B) The abundance of myelin internodes was quantified in a fixed area ($p>0.2$, n.s; non-significant; ***$p<0.001$, t-test, mean±SEM, n=3). (C) The lengths of the myelin internodes (n=130-260) were measured and quantified in three independent experiments (*$p<0.05$, **$p<0.01$, ***$p<0.001$, t-test, mean±SEM).

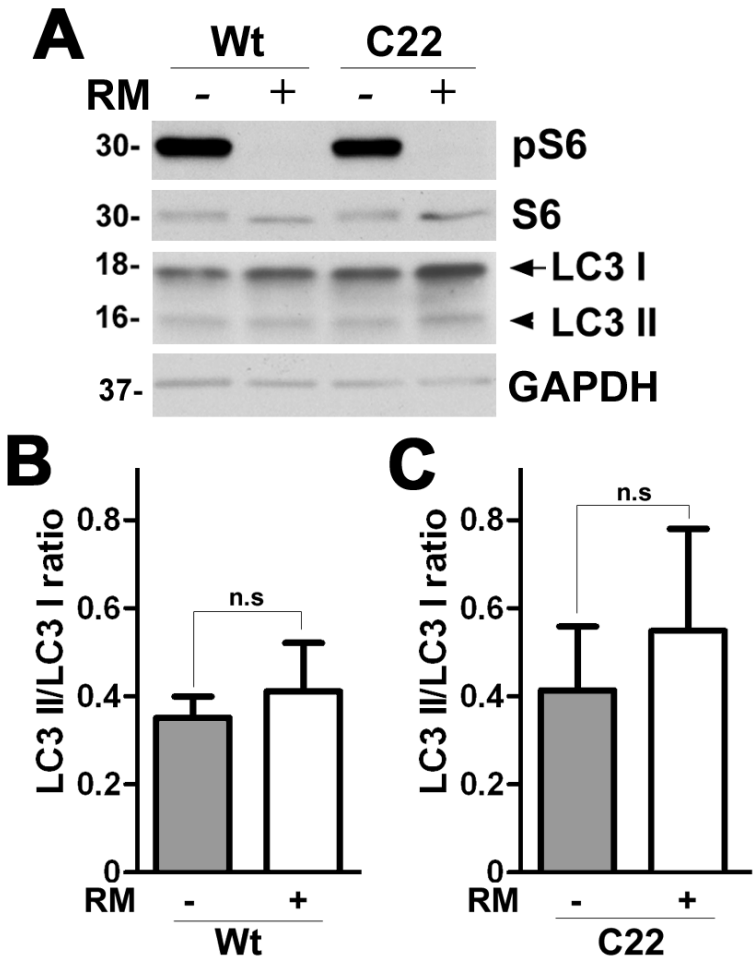

Figure 3-8. Activation of autophagy by rapamycin is negligible in DRG neurons. (A) SC-depleted DRG neurons from Wt and C22 embryos were treated with vehicle (-) or 25 nM RM for 48 h (+) and analyzed for the protein levels of pS6, S6, LC3 I and II by Western blots. GAPDH, loading control. Molecular mass, in kDa. (B, C) The ratio of LC3 II to LC3 I steady-state protein levels was measured from Western blots of Wt and C22 DRG neurons treated with vehicle (-) or 25 nM RM for 48 h (+) is shown. (n.s, not significant, t-test, mean±SEM, n=3).

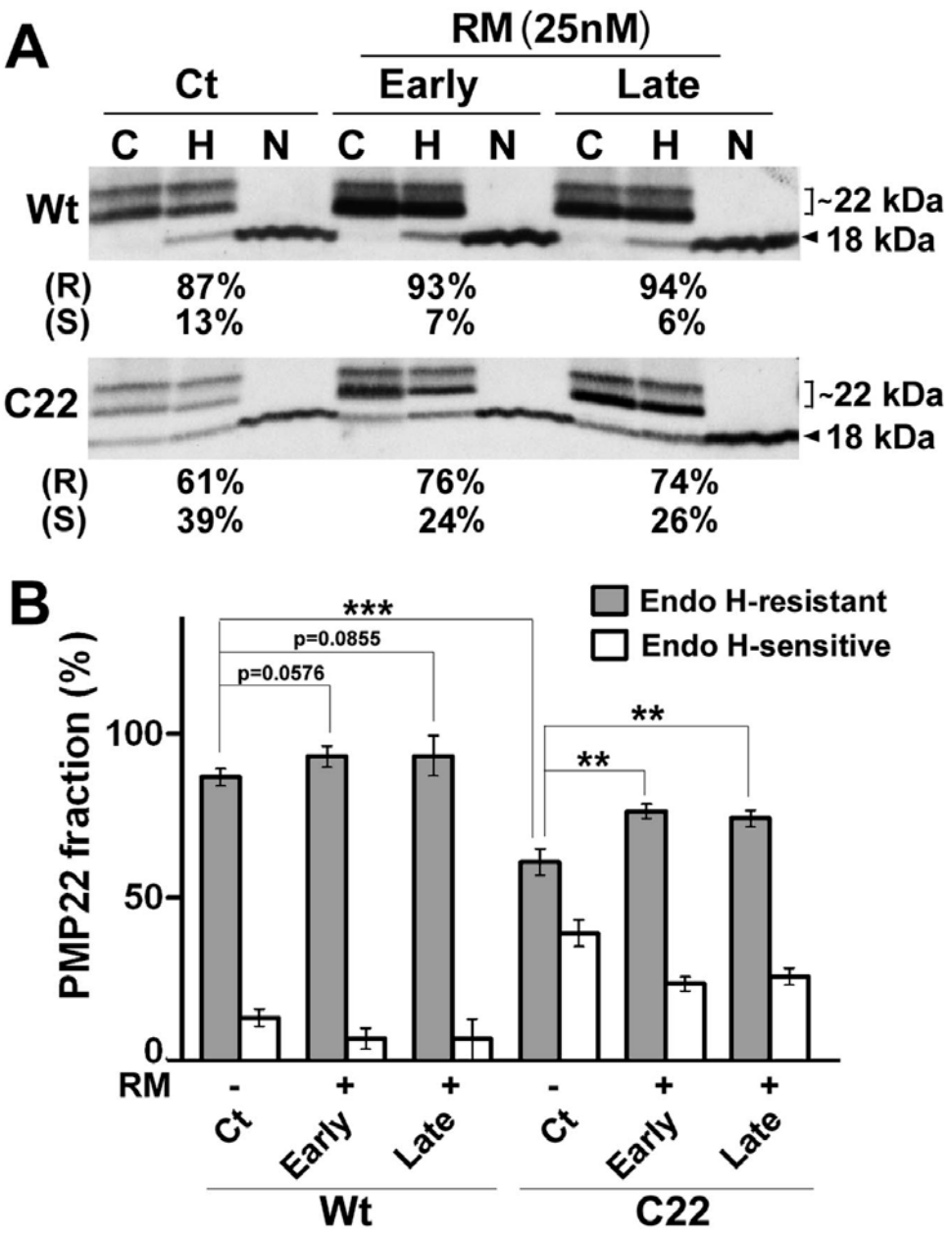

Figure 3-9. The processing of PMP22 in myelinating SCs. (A) Total protein lysates of DRG explants from Wt and C22 mice after treatment with vehicle (Ct) or RM were incubated with endo H (H) or PNGase F (N) and PMP22 was detected by Western blots. Endo H-resistant (R) (square bracket, ~22 kDa) and endo H-sensitive (S) (18 kDa) fractions of PMP22 are marked. Control (C) protein lysates for each sample without enzymatic treatment are also shown. (B) Quantitative analysis of data from three independent experiments are shown ($p=0.0576$, $p=0.0855$, $^{**}p<0.01$, $^{***}p<0.001$, t-test, mean±SD).

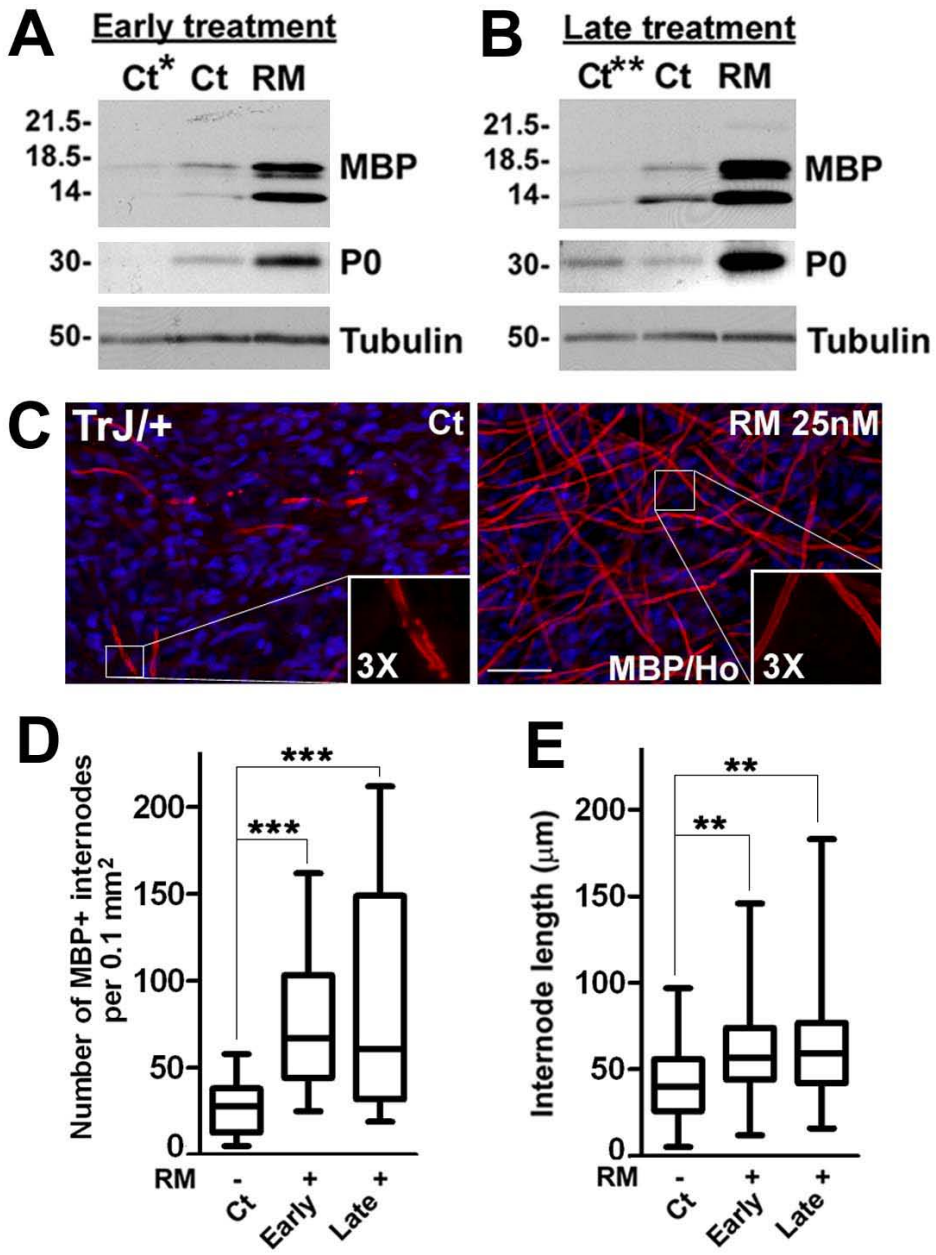

Figure 3-10. Rapamycin enhances myelination in cultures from TrJ mice. (A, B) DRG explants from TrJ mice were treated as described in Fig. 3A and whole protein lysates analyzed for the levels of myelin proteins, MBP and P0. Tubulin is shown as loading control. Molecular mass, in kDa. (C) Cultures from TrJ mice were treated with vehicle Ct or RM at late stage as described in Fig. 3A, and stained with an anti-MBP (red) antibody. Scale bar, 40 μm. Hoechst dye stains the nuclei (blue). (D) The abundance (***$p<0.001$, t-test, mean±SEM) and (E) the lengths of the myelin internodes (n=150-200) were quantified in explant cultures from TrJ mice treated without (-) or with (+) early or late RM treatment, (**$p<0.01$, t-test, mean±SEM, n=3).

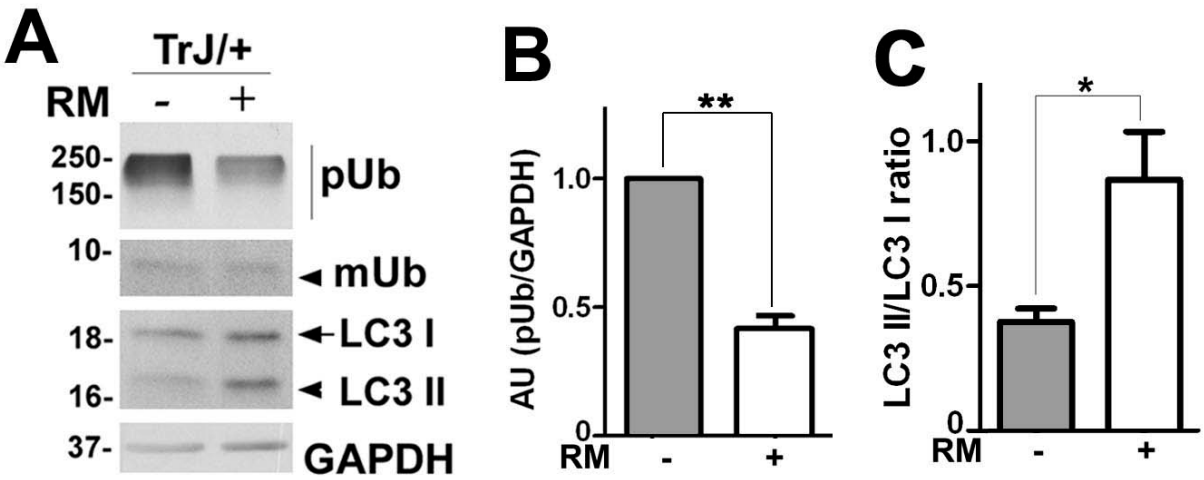

Figure 3-11. Exposure to rapamycin reduces the accumulation of poly-ubiquitin substrates in TrJ mouse SCs. (A) A representative blot for the steady-state levels of slow-migrating pUb proteins and mUb in lysates of SCs from TrJ mice treated with vehicle (-) or RM (+). LC3 I and II and GAPDH loading control were detected. Molecular mass, in kDa. (B) Quantification of pUb/GAPDH in A. The value of pUb/GAPDH in Ct sample was set as 1. AU, arbitrary units. (**$p<0.01$, t-test, mean±SEM, n=3). (C) Quantification of the ratio of LC3 II to LC3 I band intensities is shown. (*$p<0.05$, t-test, mean±SEM, n=3).

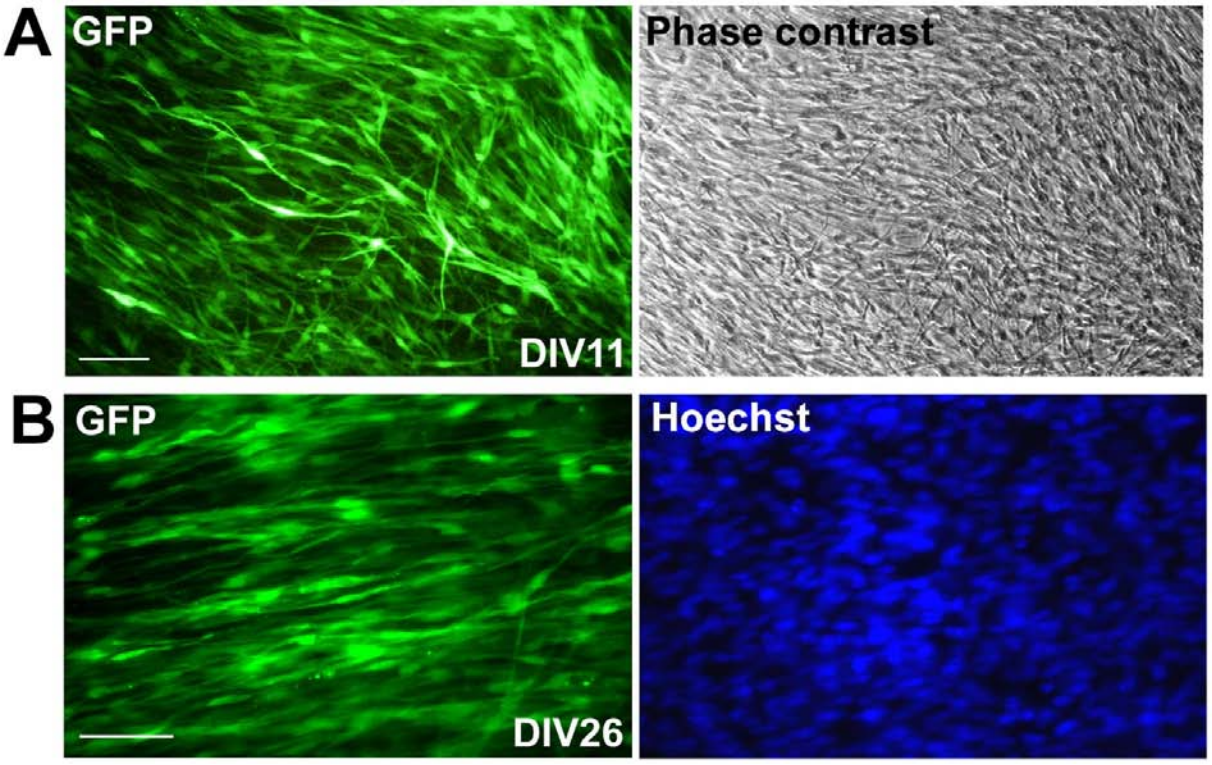

Figure 3-12. Determination of lentiviral transduction efficiency. TrJ DRG explants were transduced with GFP lentiviral particles. (A) Live GFP fluorescence (left panel) and phase contrast (right panel) images of DRG explants in culture on DIV11 are shown. (B) Direct GFP fluorescence after fixation (left panel) and Hoechst (right panel) staining are shown on DIV26. Scale bars, 40 µm.

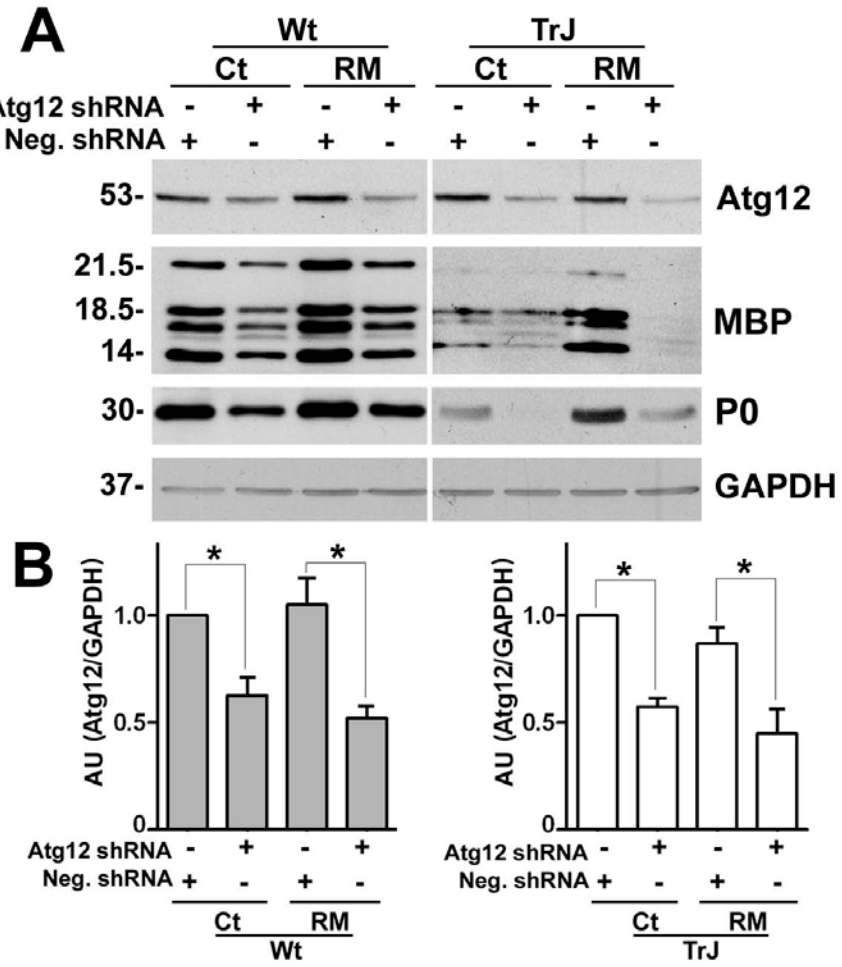

Figure 3-13. Atg12 is necessary for the myelin improvement by rapamycin. (A) Wt and TrJ DRG explants were transduced with scrambled negative (Neg.) shRNA or Atg12 shRNA. The shRNA transduced DRGs were given a late treatment with vehicle control (Ct) or RM, as indicated. Western blot analyses for Atg12 and myelin proteins MBP, P0 are shown. GAPDH serves as protein loading control. Molecular mass, in kDa. (B) Quantification of Atg12 protein levels in Wt (left panel) and TrJ (right panel) cultures after normalizing to GAPDH. The value of Atg12/GAPDH in Ct samples transduced with Neg. shRNA was set as 1 (*$p<0.05$, t-test, mean±SEM, n=3). (C) Quantitative analysis of MBP protein levels in Wt (left panel) and TrJ (right panel) explants normalized to GAPDH. The value of MBP/GAPDH in Ct samples transduced with Neg. shRNA was set as 1 (n.s, not significant, $p=0.0569$, *$p<0.05$, **$p<0.01$, t-test, mean±SEM, n=3). (D) Quantitative analysis of P0 protein levels in Wt (left panel) and TrJ (right panel) samples normalized to GAPDH. The value of P0/GAPDH in Ct samples transduced with Neg. shRNA was set as 1 (n.s, not significant, $p=0.0540$, *$p<0.05$, t-test, mean±SEM, n=3); AU, arbitrary units.

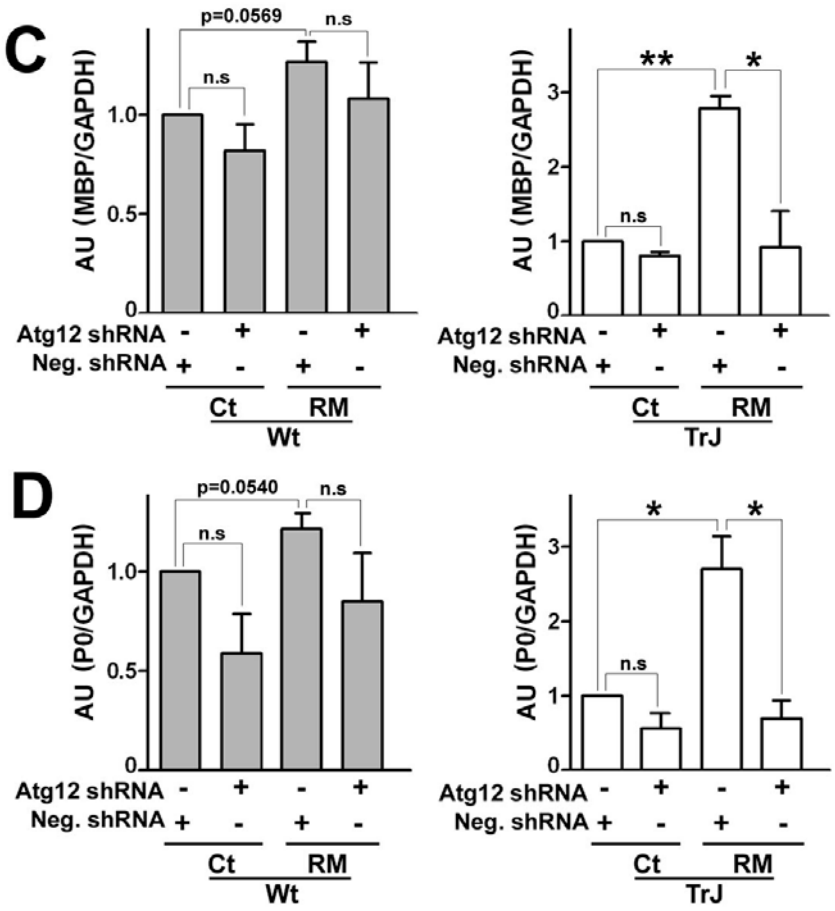

Figure 3-13. Continued

Table 3-1. Primary antibodies used in this study. WB, Western Blot; IS, Immunostaining

Species	Antigen	Source and Catalog #	Dilution	
			WB	IS
Rat	MBP	Chemicon, Temecula; MAB386	1:500	1:500
Mouse	GAPDH	Encor Biotechnology Inc.; MCA-1D4	1:5000	n/a
Mouse	Tubulin	Sigma-Aldrich;T 6199	1:5000	n/a
Rabbit	Ubiquitin	Dako, Carpenteria, CA; Z0458	1:500	n/a
Rabbit	pAkt (Ser473)	Cell Signaling Technology, Inc.; 9271	1:1000	n/a
Rabbit	Akt	Cell Signaling Technology, Inc.; 2938	1:1000	n/a
Rabbit	pS6 (Ser235/236)	Cell Signaling Technology, Inc.; 2211	1:800	n/a
Mouse	S6	Cell Signaling Technology, Inc.; 2317	1:800	n/a
Rabbit	Atg12	Cell Signaling Technology, Inc.; 2011	1:800	n/a
Rabbit	LC3	Cell Signaling Technology, Inc; 2775	1:1000	n/a

CHAPTER 4
MOLECULAR ARCHITECTURE OF MYELINATED PERIPHERAL NERVES IS SUPPORTED BY CALORIE RESTRICTION WITH AGING

Introduction

Aging is associated with structural, functional and biochemical alterations in the nervous system. Neurons with long processes are particularly vulnerable to degeneration (Mattson and Magnus, 2006), which makes peripheral nerves susceptible to age-related modifications. Signal propagation along axons is facilitated by myelin, a lipid-rich membranous structure formed by SCs. Distinct domains within the myelin and the axonal plasma membrane are maintained by complex signaling events between neurons and glia (Garbay et al., 2000). Therefore, degenerative changes in either cell type have global influences on overall nerve structure and function. Myelinated peripheral nerves from aged animals show fiber loss and morphological irregularities (Verdu et al., 2000), as well as a notable reduction in the expression of myelin and neurofilament genes and proteins (Parhad et al., 1995; Melcangi et al., 1999; Melcangi et al., 2000; Uchida et al., 2004). There is evidence for axonal demyelination and occasional remyelination in aged rat sciatic nerves, associated with nerve fiber degeneration (Sharma et al., 1980; Grover-Johnson and Spencer, 1981; Adinolfi et al., 1991). In response to demyelination, SCs increase in number (Gregson and Hall, 1973) and dedifferentiate (Zanazzi et al., 2001). Age-associated functional changes include decline in nerve conduction velocity and muscle strength, and decreases in sensory discrimination, autonomic responses and endoneurial blood flow (Verdu et al., 2000). Together, these alterations contribute to decline in neuromuscular function and impact physical performance.

Reduction in the expression of functional proteins and the accumulation of damaged and misfolded proteins have been observed in a variety of organisms with age (Sitte et al., 2000; Squier, 2001; Calabrese et al., 2004; Keller et al., 2004; Grune et al., 2005). The extent to which damaged proteins accumulate is highly dependent upon the cell's capacity to repair or remove them by subcellular homeostatic mechanisms (Stadtman, 2001), namely chaperones and protein degradation. Chaperones (also referred to as HSPs) transiently interact with proteins to aid their folding, trafficking and degradation (Frydman, 2001; Sherman and Goldberg, 2001). Cellular degradative pathways include the UPS and the autophagy-lysosomal pathway (also referred to as autophagy). With an age-related decline in the activity of these homeostatic mechanisms, damaged proteins and organelles can accumulate and lead to cellular dysfunction and cell death (Macario and Conway de Macario, 2002; Bergamini et al., 2004). Metabolically active and postmitotic cells (Boulton et al., 2004; Weissman et al., 2007) such as neurons and myelinating SCs are particularly sensitive to the accumulation of damaged proteins.

One approach to slow the aging process and prolong lifespan is through dietary modulation, such as calorie restriction (CR) (Johnson et al., 2006). Dietary restriction can induce HSPs (Heydari et al., 1996; Selsby et al., 2005) and autophagy (Bergamini et al., 2003; Wohlgemuth et al., 2007) and therefore support the maintenance of healthy cells and organs. While much work concerning dietary modulation has focused on the CNS, peripheral organs and lifespan (Feuers et al., 1989; Mattson et al., 2001; Jolly, 2004), little is known about the effects of such approach on peripheral nerves. In the CNS, life-long reduction in calorie intake has been shown to preserve long-term

potentiation (Hori et al., 1992) and ameliorate age-related cognitive decline (Pitsikas and Algeri, 1992). In the periphery, the decline in muscle mass and strength with age is ameliorated with a life-long CR diet (Marzetti et al., 2008; Xu et al., 2008), which in part might be underlined by improved neural function.

Here we examine the chaperone and autophagic responses of SCs isolated from young and aged nerves, and relate the findings to age-related biochemical and cellular alterations in peripheral nerves. Our results indicate that a life-long CR regimen supports the maintenance of the molecular architecture of myelinated axons, including the expression of essential axonal and glial proteins.

Materials and Methods

Animals and Diets

To establish rat SC cultures, we used male Fischer 344 rats from National Institute on Aging colony at Harlan Sprague Dawley Inc (Indianapolis, IA) (Norris et al., 1996). For dietary modulation studies, Male Fisher 344 x BN (Brown Norway) rats of four distinct ages 8-, 18-, 29- and 38-months (mo) and specified diets were obtained from the National Institute on Aging colony. AL fed rats had free access to NIH-31 average nutrient composition pellets, whereas the calorie restricted (CR) group received fortified pellets once daily, 1 h before the onset of the dark period. The dietary restriction was initiated at 14 weeks of age with 10% restriction, increased to 25% at 15 weeks, and continued at 40% from 16 weeks of age. Both the AL and CR rats had access to water at all times. The use of animals in this study was approved by an Institutional Animal Care and Use Committee of the University of Florida.

Primary Culture of Schwann Cells from Young and Old Rats

SC cultures were established from the sciatic nerves of postnatal day 2 (P2) 5-mo and 25-mo old rats using established procedures (Notterpek et al., 1999a). Nerves were dissected and gently stripped of connective tissue and epineurium, chopped into small pieces and digested over a period of 1 h for P2 (young) and 5 h for the adult samples, at 37 °C in a humidified atmosphere of 5% CO_2. The digestion medium consisted of Dulbecco's Modification of Eagle's Medium (DMEM) (Gibco, Grand Island, NY), 15% Fetal Bovine Serum (FBS) (Hyclone, Logan, UT), penicillin streptomycin (Gibco) and an enzyme cocktail of 0.03% collagenase type III (Worthington, Lakewood, NJ), 0.1% hyaluronidase (Sigma-Aldrich), 1.25 units/mL dispase (Worthington). Following digestion, cell suspensions were washed once and resuspended in culture medium (DMEM containing 10% FBS). Cells were then plated in small drops on poly-L-lysine (Sigma-Aldrich) coated glass cover slips or on plastic petri-dishes and allowed to adhere overnight. The next day, cells were washed with DMEM followed by addition of DMEM containing 10% FBS, 10 µM of antimitotic agent cytosine β-D-arabinofuranoside (Sigma-Aldrich), to eradicate contaminating fibroblasts. After four 24 h periods of antimitotic treatments, given on alternate days, standard growth medium (DMEM containing 10% FBS, 10 µg/mL bovine pituitary extract [Biomedical Technologies, Inc., Stroughton, MA] and 5 µM forskolin [Calbiochem, La Jolla, CA]) was added and the cells were allowed to proliferate for 7-8 days. For the HS treatments, the cells were incubated at 45 ^{o}C for 20 min, followed by a recovery for 6 h (Cristofalo et al., 2004). Stv medium (amino acid- and serum-free) was used to stimulate autophagy (Fortun et al., 2003; Fortun et al., 2007). To estimate the autophagic flux, CQ (50 µM) was added

simultaneously with Stv condition for 4 h. After the specified treatments, samples were processed for biochemical or immunochemical studies.

Biochemical Studies

Sciatic nerves isolated from AL and CR rats (n=3) were frozen immediately and stored in liquid nitrogen. Cultured SCs were washed twice with ice cold PBS followed by lysis. Cell or nerve lysates were prepared in sodium dodecyl sulfate (SDS) sample buffer (62.5 mM Tris, pH 6.8, 10% glycerol, 3% SDS) supplemented with phosphatase inhibitors, PMSF (both from Sigma-Aldrich, St. Louis, MO) and complete protease inhibitor (Roche, Indianapolis, IN). Protein concentrations were determined using the BCA protein assay kit (Pierce Chemicals, Rockford, IL). Protein samples (5-25 µg/lane) were separated on 7.5%, 10%, 12.5% or 15% SDS-polyacrylamide gels under reducing conditions and proteins were transferred to nitrocellulose or Polyvinylidene Flouride (PVDF) membranes (for LC3) (both from Bio-Rad Laboratories, Hercules, CA). Membranes were blocked in 5% non-fat milk in PBS and incubated overnight with primary antibodies (See Table 1). After washing, anti-mouse, anti-rabbit (both from Cell Signaling Technology), anti-chicken or anti-rat (both from Sigma-Aldrich) HRP-linked secondary antibodies were added for 2 h. Bound antibodies were visualized using an enhanced chemiluminescence detection kit (PerkinElmer Life Sciences, Boston, MA). Films were digitally imaged using a GS-710 densitometer (Bio-Rad Laboratories) and were formatted for printing by using Adobe Photoshop 5.5. Semi-quantitative analysis of protein levels was performed using Scion image software. The relative densitometric units were determined after normalizing with a protein loading control. For the nerves, the value of 8-mo old AL sample was set to 1 and the values of other age-diet combination were determined with respect to this. One way ANOVA followed by Fisher's

PLSD analysis was performed using the StatView program, to compare the normalized densitometric values of proteins (dependent variables) between AL and CR diet with age (factor). To determine statistical significance between samples, unpaired t-test was performed using GraphPad Prism v5.0 software.Graph pad Prism software.

Immunochemistry

SCs on glass coverslips were fixed with 4% paraformaldehyde (10 min) and permeabilized with ice-cold 100% methanol (5 min). Sciatic nerves from rats were dissected and frozen by immersion in liquid nitrogen. Frozen nerves were longitudinally sectioned (5 μm thickness) using Leica CM1850 cryostat and were dried on Superfrost/Plus microslides (Fisher, Pittsburgh, PA) for 1 h. Dried tissue sections were fixed with 4% paraformaldehyde for 1 h, permeabilized with ice-cold 100% methanol (5 min) or acetone (2 min) and processed for immunostaining (Ryan et al., 2002). After an overnight incubation at 4 °C, bound antibodies (see Table 1) were detected using Alexa Fluor 594-conjugated (red) anti-rabbit and Alexa Fluor 488-conjugated (green) anti-mouse secondary antibodies (Molecular Probes, Eugene, OR). To visualize the nuclei, Hoechst dye (Molecular Probes) was included with the secondary antibodies. Control samples without primary antibodies were processed in parallel. Cover slips were mounted using the Prolong Antifade kit (Molecular Probes). Images were acquired with a SPOT digital camera attached to a Nikon Eclipse 800 microscope Leica TCS SP2 confocal laser scanning microscope and processed for printing by using Adobe Photoshop 5.5.

Colocalization of LC3 and LAMP1

For analysis of colocalization of LC3 and LAMP1, images were acquired on a 63X water immersion lens using the Leica confocal microscope and z-stack images

were captured. The 2D cytofluorograms in Figure 4-3C were created using Leica software with the same exposure settings for red and green channels for P2 and 25-mo samples. The software quantifies the extent of colocalization by creation of a binary mask for all of the pixels that are double positive for both LC3 and LAMP1 fluorescence so that colocalizing elements will appear in the diagonal of the cytofluorogram (Fig. 4-3C, outlined in green). Colocalization of LC3 and LAMP1 was then quantified by comparing the colocalization mask areas (in μm^2), normalized per cell, between P2 and 25-mo samples treated with Stv+CQ from three independent experiments (n=8 random visual fields per condition). Statistical significance was determined by unpaired t-test using GraphPad Prism v5.0 software.

Nuclei Count

The nuclei (stained with Hoechst) of non-epineurial and non-endoneurial cells were counted in longitudinal sections (5 µm thickness) of sciatic nerves from two different depths and eight random visual fields ($0.1mm^2$) per animal (n=3). Statistical significance was determined by unpaired t-test using GraphPad Prism v5.0 software.

Results

Chaperone Response of Schwann Cells Isolated from Nerves of Aged Rats

We isolated SCs from postnatal day 2 (P2) and aged (25-mo) rats to investigate the subcellular mechanisms underlying the age-related alterations in the molecular architecture of myelinated peripheral nerves (Verdu et al., 2006). SCs from young (P2-6) animals respond to *in vitro* manipulation of protein degradative and chaperone pathways and allow for mechanistic studies (Fortun et al., 2003; Fortun et al., 2007). We examined the chaperone response of the cells to Stv and HS stimuli (Fig. 4-1A). Under control culture conditions (Ct), both cell populations express similar levels of HSP90,

HSP70 and HSP40. Incubation of the cells in Stv medium is associated with a notable increase in HSP70 (Plakidou-Dymock and McGivan, 1994), particularly in young cells. Similarly, stimulation of HSPs by incubating the cells at 45 °C for 20 min (Cristofalo et al., 2004; Fortun et al., 2007) leads to a pronounced increase in the expression of HSP70 and a slight increase in HSP90 and HSP40 (Fig. 4-1A). Quantifications from three independent experiments indicate a nearly 5-fold greater HSP70 induction in P2 cells, as compared to cells from 25-mo old rats (*$p<0.05$). GAPDH levels are similar among the cells and paradigms tested.

To further investigate the muted chaperone response of the aged cells, we performed immunostaining with anti-HSP70 antibodies (Fig. 4-1B). As suggested by the biochemical data (Fig. 4-1A), SCs cultured from P2 nerves show a robust induction of HSP70 (Fig. 4-1B, green), which is nearly uniform among all the cells. The low level of HSP70-like immunoreactivity in control cells is shown in the inset. In comparison, cells isolated from the 25-mo old rats exhibit notable heterogeneity in their ability to respond to HS, with only a fraction of the cells showing elevated HSP70 expression (Fig. 4-1B, green). Quantification of three independent experiments indicates that 42.48±6.14% of 25-mo cells respond to HS in comparison to over 90.45±2.47% of young (P2) cells (mean ± SEM; ***$p<0.001$). Therefore, the reduced level of HSP70 on the Western blots (Fig. 4-1A) is a reflection of the inability of a fraction of aged cells to respond to stress stimuli.

The Autophagic Response of Glial Cells is Altered with Age

Next, we tested SCs isolated from P2 and 25-mo old rats for their autophagic capacity (Fig. 4-2). To stimulate autophagy, the cells were incubated in medium

deprived of amino acids and serum (Stv medium) (Fortun et al., 2003) for 4 h followed by lysis. In a subset of samples, we simultaneously added CQ (50 μM) to evaluate differences in the autophagic flux under conditions that inhibit lysosomal enzyme activity (Mizushima and Yoshimori, 2007). CQ is a lysosomotropic alkaline that increases the pH within lysosomes thereby inhibiting their proteolytic activity (Rocca et al., 2001). As a biochemical measure of autophagy, we evaluated the levels of Atg7 and lipidation of LC3 (Fig. 4-2A). The young (P2) cells respond to nutrient deprivation (Stv) by activating the autophagic pathway, as revealed by an increase in Atg7 and the conversion of LC3 I to LC3 II (lipidated form) (Kabeya et al., 2000; Mizushima and Yoshimori, 2007). In the old cells, the response to Stv is lessened, which is particularly notable for Atg7. Upon co-treatment with Stv medium and CQ, the levels of LC3 II further increase, indicating ongoing autophagic flux (Mizushima and Yoshimori, 2007; Klionsky et al., 2008). This trend is significantly (*$p<0.05$) more robust in cells from young, as compared to those from aged rats (Fig. 4-2B). Furthermore, in young cells (P2), the phosphorylated form of ribosomal protein S6 (pS6) disappears completely upon Stv (Blommaart et al., 1995), whereas in 25-mo old cells it does not (Fig. 4-2A). As expected, compared to Stv alone, the levels of pS6 slightly increase in the Stv+CQ co-treatment paradigm in both samples, confirming the specificity of this marker for the Stv-induced autophagy. Both young and old cells respond to Stv as seen by significant decline in the ratio of pS6 and S6 (Fig. 4-2C), a value that is used as a marker of autophagic activity (Blommaart et al., 1995). However, the ratio in 25-mo old samples is significantly higher (**$p<0.01$) than in P2 cells, indicating defective autophagy (Fig. 4-2C).

We also examined the expression of lysosomal proteins within the same samples and detected a slowed mobility of LAMP1 in aged cells (Fig. 4-2D, asterisk) To obtain insight into lysosomal proteolytic potential (Fusek and Vetvicka, 2005), we studied the expression of cathepsin D (cath D). The levels of pro-cathepsin D (pro-cath D) and active cath D under control conditions are lower in 25-mo cells as compared to P2 (Fig. 4-2D, E). There is a decrease in the active cath D upon CQ treatment in both ages, as this lysosomotropic agent increases the secretion of pro-cath D and prevents the processing of the active cath D (Samarel et al., 1989). Under Stv conditions, the active form of cath D is notably higher in young, as compared to 25-mo cells (Fig. 4-2E, $^{**}p<0.01$). This active form is depleted when Stv is combined with CQ treatment, thereby confirming the specificity of the Stv response in processing cath D. These results are consistent among three independent experiments (Fig. 4-2E) and suggest alterations in the autophagy-lysosomal activity of SCs isolated from nerves of aged rats.

To examine the fusion of autophagic vacuoles with lysosomes, we double immunostained SCs with LC3 and LAMP1 antibodies (Fig. 4-3). SCs from P2 rats contain small LAMP1-positive lysosomes and relatively few LC3- reactive autophagosomes dispersed within the cytosol (Fig. 4-3A, panel on left, Ct). Subjecting the young cells to Stv increases the size of lysosomes (Fig. 4-3A, Stv, arrow) and the number of autophagosomes. On the other hand, SCs from 25-mo rats show visibly large lysosomes under control conditions (Fig. 4-3A, panel on right, Ct, arrows) and only a modest increase in LAMP1-positive lysosomes upon Stv. In agreement with the biochemical results (Fig. 4-2A), the abundance of LC3-positive autophagosomes remains low in Stv-treated 25-mo SCs (insets on right). To evaluate the autophagic flux,

we analyzed the Stv+CQ treated cells by confocal microscopy (Fig. 4-3B). On representative single plane images, there are several fusion events of LC3-positive autophagosomes and LAMP1-positive lysosomes in SCs from P2 rats (Fig. 4-3B, yellow spots). The fusion of lysosomes (green) with autophagosomes (red) is resolved in more detail on single plane sections (Fig. 4-3B, x and y sections). In agreement with the defective autophagosome-lysosome fusion hypothesis in old cells (Cuervo et al., 2005), there are fewer colocalization of LAMP1 and LC3 (yellow spots) within SCs isolated from the old rats. 2D-cytofluorograms reveal more yellow pixels in young, as compared to old cells (Fig. 4-3C). Quantification of colocalization mask area shows a significant (*$p<0.05$) reduction in autophagosome-lysosome fusion events in 25-mo cells (Fig. 4-3D). We completed a similar set of studies in cells isolated from the peripheral nerves of 5-mo old rats which behave similar to the P2 rats (data not shown). Together, these results indicate that SCs isolated from aged nerves respond less vigorously to HS and Stv stimuli, as compared to neonatal (P2) or young-adult (5-mo) cells.

Protein Homeostatic Mechanisms are Maintained in Nerves of Diet Restricted Rats

Protein homeostatic mechanisms that maintain tissue health and repair damage are known targets of age-related alterations (Rattan, 2004). To examine how age and diet affect the steady-state expression of protein chaperones within myelinated nerves, we focused on the HSP90/HSP70 network (Fig. 4-4A). HSF1, a key regulator of this pathway, is held in an inactive state in the cytosol by HSP90. (Ohtsuka and Suzuki, 2000; Voellmy and Boellmann, 2007) and upon release it translocates to the nucleus, where it promotes the expression of HSP70, HSP27 and αB-crystallin (Pirkkala et al., 2001). The levels of HSF1 and HSP90 gradually increase with age in the AL group, a

trend which is significant at 38-mo (Fig. 4-4A, B). The CR diet attenuates this pattern and is associated with sustained low level of HSF1. Upon analysis of the corresponding chaperones, we observe a significant increase in HSP90-like reactivity, while the steady-state levels of HSP70 and αB-crystallin appear to decline with age (Fig. 4-4A). Quantification of the data confirms the changes for HSP90 (Fig. 4-4B), but not for HSP70 and αB-crystallin (data not shown). The steady-state expressions of HSP40 and of the small chaperone HSP27 are sustained across the studied samples.

Demyelination of nerves and accumulation of damaged proteins within SCs elicits a proteolytic response, which is reflected by activation of the autophagy-lysosomal pathway (Notterpek et al., 1997; Fortun et al., 2003). In agreement with the known degenerative changes in peripheral nerves of aged rodents (Melcangi et al., 1999; Verdu et al., 2000; Uchida et al., 2004), we found a gradual increase in the steady-state levels of LAMP1 and the autophagic protein Atg7 with age (Fig. 4-4C). The semi-quantitative analysis shows that this trend is lessened by the intervention, leading to balanced expression of both these proteins (Fig. 4-4C, D). Similarly, the age-associated increase in the levels of pS6 and total S6, are diminished by the intervention. The ratio of these two species (Blommaart et al., 1995) is significantly higher in the samples from the AL-fed 18-mo and 38-mo rats as compared to CR (Fig. 4-4E). However, the differences in the pS6/S6 ratios between AL and CR samples at 8- and 29-mo ages are not significant ($p=0.823$ and $p=0.526$, respectively). Overall, these data suggest that the degenerative changes are muted with CR, which decreases the demand on protein homeostatic mechanisms, including the autophagy-lysosomal pathway.

The Expression of Myelinated Schwann Cell Proteins in Diet Restricted Rats

Efficient functioning of peripheral nerves is supported by myelin-forming SCs. To examine the influence of the dietary restriction on peripheral nerve health, we prepared tissue lysates from sciatic nerves and studied the expression of glial and axonal proteins by Western blots (Fig. 4-5). Our results confirm earlier findings (Melcangi et al., 1999; Melcangi et al., 2000) in a wide age group, where we detect gradual decline in three structural myelin proteins, including protein zero (P0), PMP22 and MBP (Fig. 4-5A). The decreases are pronounced by 29-mo of age, and reach statistical significance for all three proteins at 38-mo (Fig. 4-5B). In comparison, in nerve lysates from diet restricted animals, the levels of these proteins are maintained (Fig. 4-5A, B). We previously reported that rats kept on the CR diet display significantly better functional performance in the grip strength task (Ingram et al., 2007; Xu et al., 2008). Within the AL-fed group, there is a positive correlation between the decline in fore-limb grip strength and MBP expression ($p<0.001$), and an emerging trend for strength and PMP22 ($p=0.096$). Neither association is present in the CR-fed group ($p>0.05$). These data suggest that age-related loss of myelin is correlated with a decline in strength, and interventions such as CR, which slow myelin loss, may also preserve functional performance (Ingram et al., 2007; Xu et al., 2008).

In response to demyelination SCs re-enter the cell cycle and proliferate (Jessen and Mirsky, 2005). Change in the differentiation state of SCs is reflected by the re-expression of the p75 neurotrophin receptor ($p75^{NTR}$) (Jessen and Mirsky, 2005). In agreement, immunoblotting the nerve lysates with an anti-$p75^{NTR}$ antibody shows higher levels of this protein in the samples from 38-mo old AL-fed rats (Fig. 4-5C, D), as compared to the younger ages. This increase in expression is attenuated by the CR

regimen, supporting the maintenance of the differentiated SC phenotype (Fig. 4-5D). In accordance, the levels of the mitotic marker, phosphorylated histone-3 (pHH3) (Ribalta et al., 2004) are higher in the AL-group as compared to CR (Fig. 4-5C, D). We also labeled nerve sections with Hoechst dye and counted the number of supernumerary SC nuclei, excluding epineurial and endoneurial cells (Fig. 4-5E). The average number of nuclei within fixed tissue area of 18-mo old AL-fed rats is 42.80 ± 0.98 (n=3, mean ± SEM) whereas there is a small but statistically significant decrease in response to the intervention (39.88 ± 1.24 nuclei, *$p<0.05$). Significantly, there is a nearly 3-fold increase in the number of nuclei in the oldest samples (117.9 ± 6.08 vs. 42.80 ± 0.98), which is remarkably alleviated by CR (Fig. 4-5E). Together, these results indicate that a life-long dietary restriction supports the maintenance of the differentiated SC phenotype, which is beneficial for myelin and axonal structure.

Axonal Constituents in Myelinated Peripheral Nerves of Diet Restricted Rats

SCs provide support for the functional integrity of myelinated axons (Nave and Trapp, 2008). Therefore, under conditions of myelin loss as seen in the aged nerves (Fig. 4-5A) alterations in axonal and structural proteins are expected. We corroborated the biochemical analysis of myelin proteins (Fig. 4-5) by double immunolabeling longitudinal nerve sections from 18- and 38-mo old rats with anti-MBP and neurofilament light chain (NF-L) protein antibodies (Fig. 4-6A). In agreement with the pronounced reduction in MBP in the nerve lysates (Fig. 4-5A) in samples from AL 38-mo old animals there are NF-L antibody-reactive axons devoid of myelin (Fig. 4-6A, arrowheads). In contrast, nerves of 38-mo old CR rat show a remarkable maintenance of MBP-positive internodes (Fig. 4-6A, red) and only few axons without myelin (arrowheads). Immunostaining for NF-heavy (NF-H) and -medium (NF-M) chain protein

shows similar pattern (data not shown). Nerve sections from 18-mo old rats are included for comparison (Fig. 4-6A, insets in top panels).

Since there seem to be fewer NF-reactive fibers in AL-fed 38-mo old samples (Fig. 4-6A), we analyzed the levels of the three major NF proteins (Fig. 4-6B). In agreement with previous reports (Parhad et al., 1995; Uchida and Brown, 2004; Uchida et al., 2004), nerves from 38-mo old rodents show reduction in the steady-state expression of NF-H, -M and -L (trend for NF-H and significant for NF-M and NF-L) (Fig. 4-6B, C). Strikingly, their levels are maintained in rats on the intervention (Fig. 4-6C), corresponding to the immunolabeling studies (Fig. 4-6A). In sciatic nerve samples from our oldest AL-fed rats, vimentin, an intermediate filament protein expressed by SCs and neurons (Toth et al., 2008), appears to undergo proteolytic degradation (Fig. 4-6B, square bracket). This aberrant phenotype, which may be a reflection of enhanced caspase activity in aged nerves (Byun et al., 2001), is absent from independent samples on the dietary regimen (Fig. 4-6B). Together these results show that the CR intervention supports maintained expression of glial and axonal gene products, including myelin and neurofilament proteins.

Demyelination of nerve fibers with age and disease leads to spreading of voltage-gated ion channels in the axonal membrane (Adinolfi et al., 1991; Verdu et al., 2000; Amici et al., 2007). To determine if the CR diet supports the expression of channel proteins at nodes of Ranvier, we performed biochemical and immunohistochemical analyses of pan-voltage gated sodium channels (Na_v) and voltage gated potassium channels (Kv1.1) (Fig. 4-7). While the steady-state levels of both Na_v and Kv1.1 dramatically increase with age in the AL-fed group, especially at 38-mo (6-fold increase

for Na_v and 7-fold increase for Kv1.1), in nerves from CR animals such changes are muted (*$p<0.05$ for both Na_v and Kv1.1) (Fig. 4-7A). Furthermore, proteolytic cleavage of the α-subunit of Na_v channels (Zwerling et al., 1991; Benz et al., 1997), most notable in the 38-mo sample (Fig. 4-7A, arrowhead), is lessened by the intervention.

We confirmed the biochemical results by co-immunolabeling nerve sections with antibodies against Na_v or Kv1.1 channels, and MBP (Fig. 4-7B, C). As suggested by the higher expression level of the channel proteins (Fig. 4-7A) and the abundance of unmyelinated fibers (Fig. 4-6A), Na_v channel-like immunoreactivity is prominent and diffuse along unmyelinated axons in nerves from 38-mo old AL-fed rats (Fig. 4-7B). Furthermore, there is wider distribution of Na_v at nodes of Ranvier (Fig. 4-7B, asterisks and insets in top panel), likely due to segmental demyelination. In comparison, focal localization of Na_v channel is maintained in samples from 38-mo old rodents on the regimen (Fig. 4-7B, asterisks and insets in bottom panel). Similarly, the Kv1.1 channel-like immunoreactivity is spread along axons in nerve sections from 38-mo AL rats (Fig. 4-7C), instead of being confined to the paranodal region. Again, in response to dietary restriction, spatial localization of Kv1.1 is maintained to the paranodal region (Fig. 4-7C). Together, these results show a beneficial effect of CR on the molecular architecture of myelinated peripheral nerves, including the expression and localization of glial and axonal proteins (Figs. 5-5 to 5-7).

Discussion

Glial cells isolated from aged rats have muted response to stress stimuli, which may in part underlie the degenerative changes observed with age in myelinated peripheral nerves. Reduction in calorie intake, the most widely accepted and effective method of defying age-related alterations (Everitt et al., 2006), preserves the molecular

architecture of myelinated axons likely by supporting SC function. The benefits are evident by maintained expression and correct localization of glial and axonal molecules, including myelin, neurofilament and ion channel proteins. Constituents of protein homeostatic mechanisms remain leveled in nerves from diet restricted rats, potentially reflecting lower demand on these pathways.

While CR diet affects specific physiologic parameters and cellular pathways in different organs (Mattson et al., 2001), here we focused on two protein homeostatic mechanisms, namely chaperones and autophagy. We isolated SCs from myelinated nerves of young and old rats and found notable differences in their chaperone responses (Fig. 4-1). The muted response of old glial cells at least in part is reminiscent of the findings from the nerves of AL-fed aged animals (Fig. 4-4). In sciatic nerve lysates, we detected a prominent increase in the steady-state expression of HSF1 at 38-mo (Fig. 4-4), which may indicate a compensatory attempt for compromised signaling of the HSP90/HSF1 pathway (Ohtsuka and Suzuki, 2000; Voellmy and Boellmann, 2007). In agreement, while there is an increase in HSP90-like reactivity, the steady-state levels of HSP70 and αB-crystallin are low. Age-related increase in HSF1 levels have been previously reported in isolated rat hepatocytes and is associated with a decline in binding activity of HSF1 with heat shock elements (HSE) (Heydari et al., 2000). A crucial role for chaperones in myelinated nerves is supported by the ATP-dependent interaction of HSP70 with MBP (Lund et al., 2006). Constitutive expression of HSC70 appears to be also necessary for the correct expression of MBP during the differentiation of oligodendrocytes (Aquino et al., 1998), suggesting HSP70 is involved in the proper folding and trafficking of this myelin protein. Furthermore, *hsf1* knock-out mice exhibit a

demyelinating phenotype in the CNS, likely due to defective oligodendrocyte differentiation, or myelin synthesis and assembly (Homma et al., 2007). Complimentarily, the enhancement of HSPs improves myelination in a neuropathic model (Rangaraju et al., 2008). Thus, the decline in the ability of SCs to induce chaperones may impair their ability to sustain and repair myelin with age. CR diet has the ability to prevent the aforementioned decrease in HSF1 binding activity (Heydari et al., 1996), and support the expression of chaperones.

In aged cells, macroautophagy is known to be defective both in the formation and clearance of autophagosomes (Cuervo et al., 2005). Poor elimination of autophagosomes could result from a decrease in lysosomal enzyme activity and/or impaired fusion of lysosomes with autophagosomes (Cuervo et al., 2005). Our data support these hypotheses, as SCs from old rats show low levels of the lysosomal endoprotease, cath D with Stv, and prominent swollen lysosomes and few fusion events of autophagosomes and lysosomes (Figs. 5-2 and 5-3). Although the overall levels of LAMP1 are unchanged by the modulation, the mobility of LAMP1 is slowed in old cells, possibly due to altered glycosylation, or compromised pathway activity. Indeed, SCs isolated from old rats contain visibly larger lysosomes under basal conditions (Fig. 4-3A), as compared to young cells. In addition, the described alterations in biochemical markers of the autophagy-lysosome pathway (Atg7, LC3 and pS6/S6 ratios) suggest that autophagy becomes less efficient with age. It has been previously shown that phosphorylation of S6 and inhibition of autophagy have a linear relationship in rat hepatocytes (Blommaart et al., 1995). In our model, based upon the levels of pS6 in response to Stv the activation of autophagy is minimal in SCs from 25-mo old rats (Fig. 4-

2A). The maintenance of autophagy with diet restriction in sciatic nerves is likely mediated via S6 kinase (Klionsky et al., 2005), which is reflected upon the lower levels of pS6 in 38-mo CR rat nerves as compared to AL.

Peripheral nerves serve as long cables connecting the CNS with distal targets, such as skeletal muscle. The function of peripheral nerves is affected by age and is associated with morphologic (Verdu et al., 2000) and biochemical myelin abnormalities (Fig. 4-5 to 4-6). Defective myelin and segmental demyelination are coupled with dedifferentiation of SCs (Gregson and Hall, 1973; Saito et al., 1990; Zanazzi et al., 2001). We observed this switch in phenotype in the aged nerves from AL-fed rats by re-expression of $p75^{NTR}$ (Fig. 4-5C), which is detected only at low levels when the cells are in a myelinating state (Jessen and Mirsky, 2005; Amici et al., 2007). In nerves from rats on the diet-regimen, myelin maintenance is associated with subdued expression of $p75^{NTR}$ and the mitotic marker, pHH3 (Fig. 4-5). Prevention of demyelination and hyperproliferation of SCs with age suggest better axo-glial communication in diet restricted animals, which supports the maintenance of the major structural proteins of axons. Together, the prevention of glial and axonal changes preserves the functional architecture of myelinated nerves (Figs. 5-5 to 5-7) and is associated with improved motor performance (Xu et al., 2008).

Demyelination of axons leads to a decrease in nerve conduction velocity and reorganization of voltage-sensitive ion channels has been suggested as an underlying cause (Adinolfi et al., 1991; Verdu et al., 2000). The cross-talk between axons and glia is responsible for maintaining the proper localization of ion channels (Novakovic et al., 2001; Hinman et al., 2006). In this study, we found segmental demyelination in nerves

from AL-fed aged rats and a corresponding redistribution of ion channels (Fig. 4-7). In transgenic mice, when SCs are selectively killed by diphtheria toxin, a demyelinating phenotype is associated with overexpression and redistribution of sodium channels (Vabnick et al., 1997). Similarly, a knock-out mouse with deletion of MBP shows a strikingly high density of Na channels along hypomyelinated axons (Noebels et al., 1991; Westenbroek et al., 1992), likely as a compensatory mechanism to support signal propagation. Nonetheless, the redistribution in ion channel proteins associated with defective myelination is not an effective replacement of myelinated internodes and can lead to sensory and motor dysfunction (Novakovic et al., 2001). Our study shows that the CR regimen has the ability to minimize the changes in expression and organization of the Na_v and Kv channel at the node of Ranvier (Fig. 5-7), likely by preservation of internodal myelin segments.

Together, the muted responsiveness of stress induced pathways in aged SCs might exacerbate the observed molecular and structural defects in myelinated peripheral nerves. Approaches to limit the demand on protein homeostatic pathways, such as dietary restriction appear to provide benefits for maintenance of nerve health.

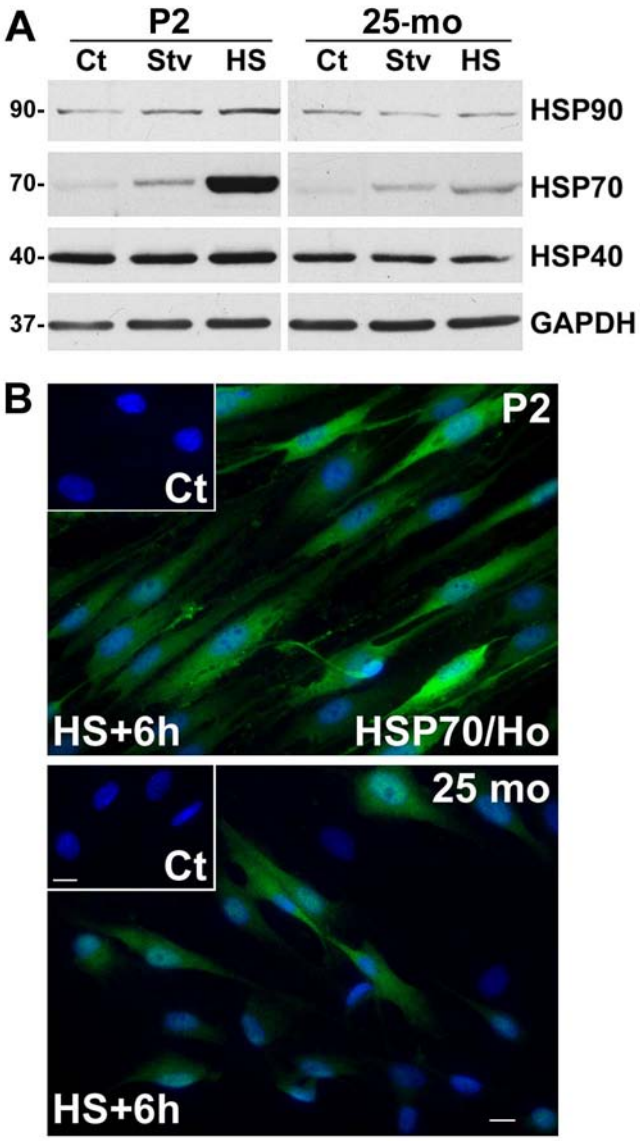

Figure 4-1. The chaperone response of SCs from aged rats. (A) SCs isolated from P2 and 25-mo rats were treated with amino acid and serum-deficient (Stv) medium, or subjected to HS and allowed to recover at 37 ºC for 6 h. Steady-state expression of HSP90, HSP70 and HSP40 were analyzed in whole cell lysates (15 µg/lane) of untreated control (Ct), Stv- or HS-treated samples. Blots were reprobed with anti-GAPDH antibody as a protein loading control. Molecular mass at the left, in kDa. (B) SCs isolated from P2 and 25-mo old rats were subjected to HS (45 °C; 20 min) and allowed to recover at 37 °C for 6 h (HS+6h). Control untreated cells (Ct) and HS+6h samples were immunolabeled with anti-HSP70 (green) antibody. Hoechst dye (blue) was used to visualize nuclei. Scale bar, 10 µm.

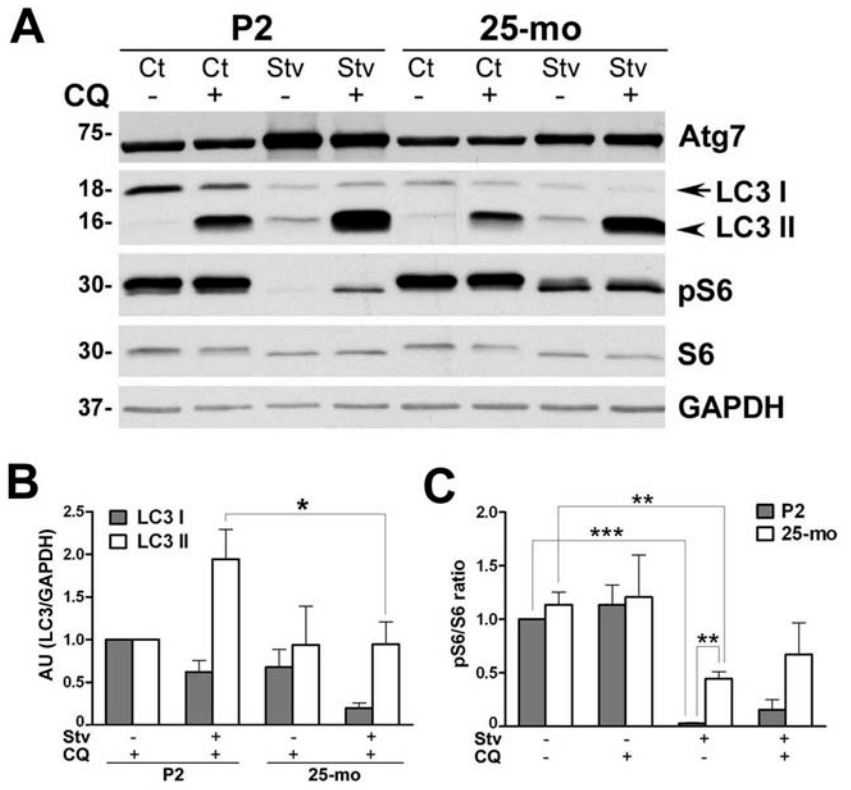

Figure 4-2. The response of glial cells to Stv stimulus. (A) Primary rat SCs from postnatal day 2 (P2) and 25-mo old rats were maintained in normal (Control, Ct), or amino acid and serum-deficient Stv medium for 4 h, with (+) or without (-) CQ. The levels of autophagy markers, Atg7, LC3 I and II, pS6 and S6 were determined by Western blots (15 µg/lane). (B) Quantification of LC3 I and LC3 II band intensities in the presence of CQ normalized to GAPDH from three independent experiments are shown. LC3 I and II values of P2 cells treated with CQ was set as 1. AU:arbitrary units. (*$p<0.05$, unpaired t-test, mean ± SEM, n=3). (C) Levels of pS6 and S6 from three independent experiments were quantified and the values are represented as ratio of pS6/S6. The value of P2 Ct sample was set as 1. (D) The expression of lysosome-associated membrane protein 1 (LAMP1) and cathepsin D were determined by Western blots. The shift in LAMP1 mobility in 25-mo samples is indicated by an asterisk. The bands representing pro-cathepsin D (pro-cath D) and active form of cathepsin D (active cath D) are marked with arrows. (E) Semi-quantitative analysis of pro-cath D and active-cath D protein levels after normalization to GAPDH from three independent experiments. The values of pro- and active-cath D in P2 Ct sample were set as 1. AU:arbitrary units. (**$p<0.01$, ***$p<0.001$, unpaired t-test, mean ± SEM). (A and D) GAPDH is shown as a protein loading control. Molecular mass at left, in kDa.

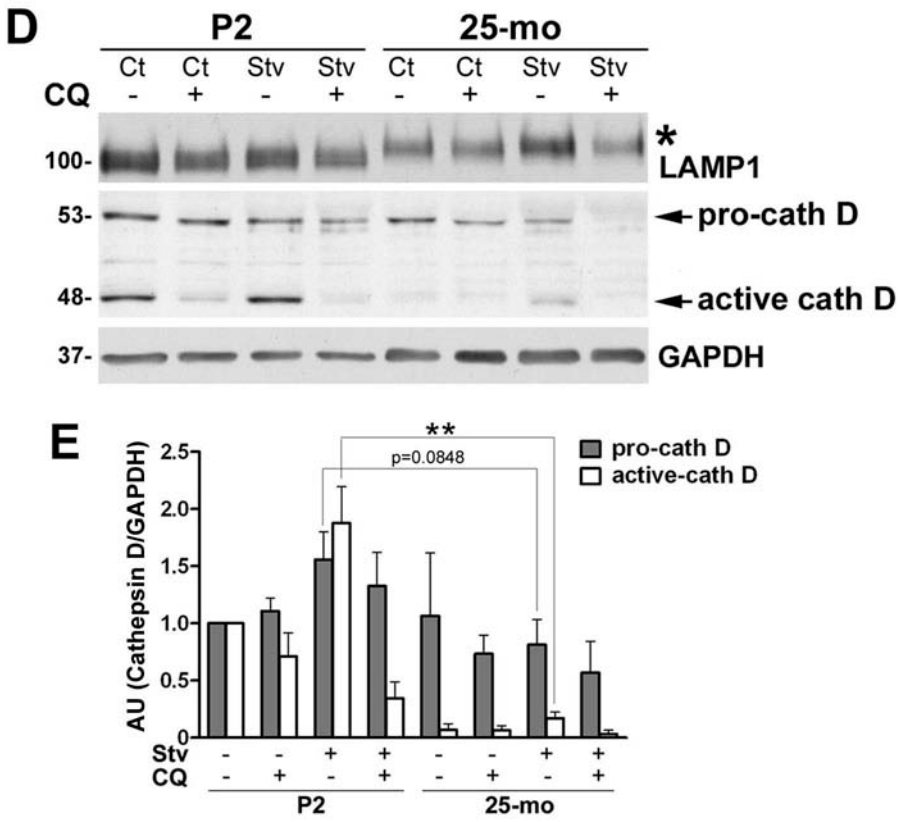

Figure 4-2. Continued

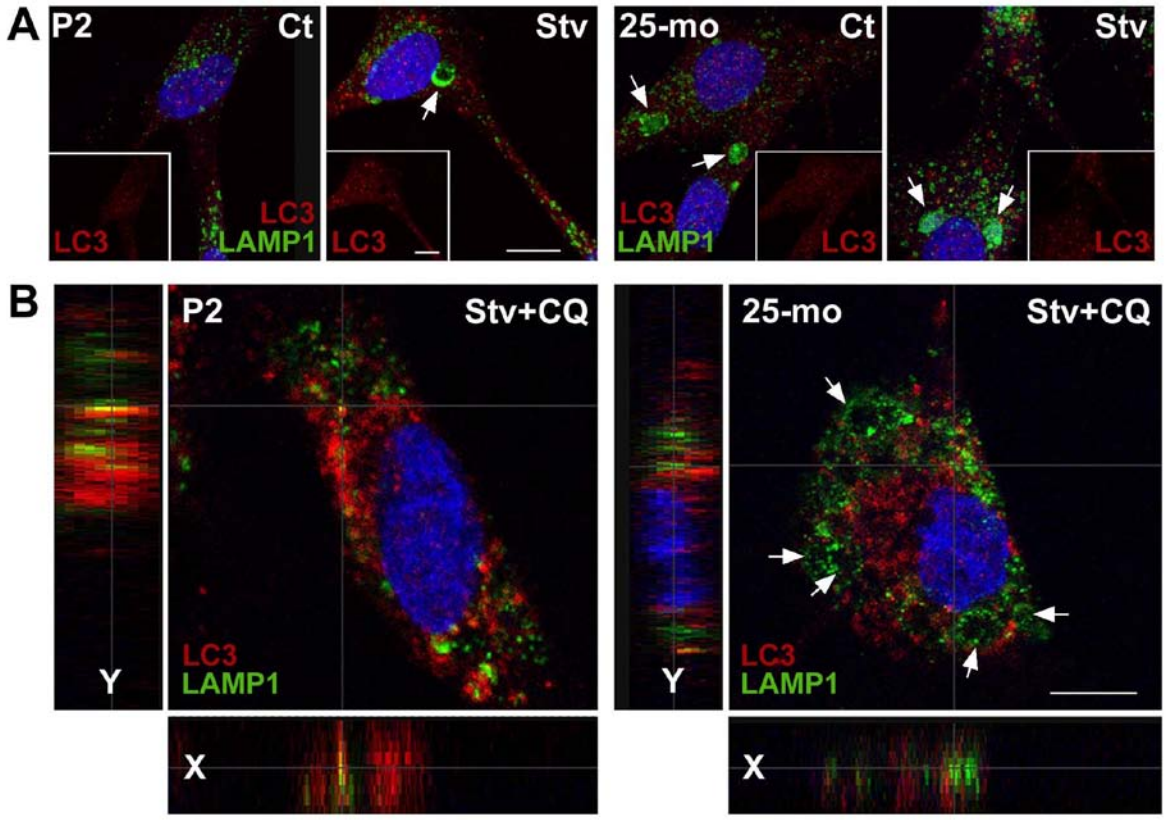

Figure 4-3. The fusion of autophagosomes with lysosomes in SCs. (A) Composite confocal images of control (Ct) and Stv-treated (Stv) SCs from postnatal day 2 (P2) and 25-mo old rats, double immunostained with anti-LC3 (red) and anti-LAMP1 (green) antibodies. Insets show LC3-like (red) staining alone. Enlarged lysosomes positive for LAMP1 (green) are indicated by arrows. (B) Mid z-stack images of cells after treatment with CQ, in Stv medium. Single x and y plane sections are shown at the left to reveal the interaction of autophagosomes (red) with lysosomes (green), in yellow. In cells from 25-mo old rats, swollen LAMP1-positive lysosomes (green) are indicated by arrows. Nuclei are visualized by Hoechst dye (blue). Scale bars, 10 µm. (C) 2D cytofluorograms for LC3 and LAMP1 colocalization in Stv+CQ treated P2 and 25-mo samples in which the interaction between the red channel (x-axis) and the green channel (y-axis) is highlighted in green in the diagonal region. (D) The area of colocalization (mask area) per cell was estimated using Leica software from P2 and 25-mo cells (n=200) treated with Stv+CQ from three independent experiments, and eight random visual fields per condition (*$p<0.05$, unpaired t-test, mean ± SEM).

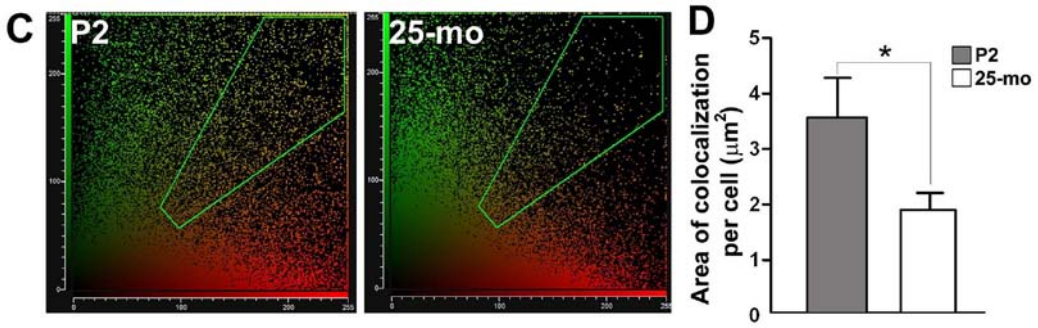

Figure 4-3. Continued

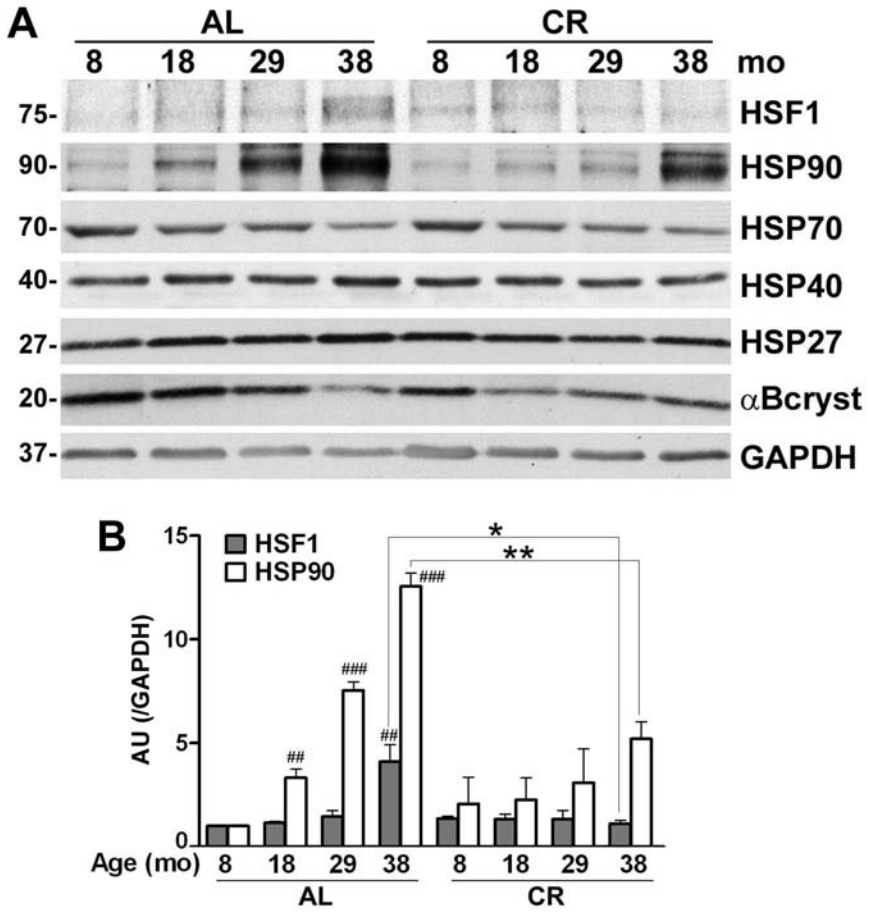

Figure 4-4. Age-associated alterations in chaperones and autophagic proteins in myelinated peripheral nerves. (A) Total sciatic nerve lysates (25 µg/lane) from the indicated ages and diet were analyzed with anti-HSF1 antibody. The same nerve lysates (20 µg/lane) were also probed with antibodies against HSP90, HSP70, HSP40, HSP27 and αB-crystallin. (B) Quantification of HSF1 and HSP90 protein levels normalized to GAPDH from three independent experiments ($^{\#\#}p<0.01$, $^{\#\#\#}p<0.001$, Fisher's PLSD, mean ± SEM), AU: arbitrary units. The effect of CR on these proteins was analyzed by comparing HSF1 or HSP90 protein values with age-matched AL counterparts (*p<0.05, **p<0.05, unpaired t-test, mean ± SEM). (C) Steady-state levels of LAMP1, Atg7, pS6 and S6 proteins in sciatic nerves from AL and CR rats were analyzed by Western blots. Blots were reprobed with anti-GAPDH antibody as protein loading control. Molecular mass at the left, in kDa. (D) Quantification of LAMP1 and Atg7 protein levels normalized to GAPDH from three independent experiments ($^{\#}p<0.05$, $^{\#\#\#}p<0.001$, Fisher's PLSD analysis, *p<0.05, unpaired t-test, mean ± SEM). (E) Blots of pS6 and S6 from three independent experiments were quantified and the values are represented as ratio of pS6/S6. The pS6/S6 ratio of 8-mo old AL sample was set as 1 (*p<0.05, unpaired t-test, mean ± SEM). A-D, n=3 rats per condition.

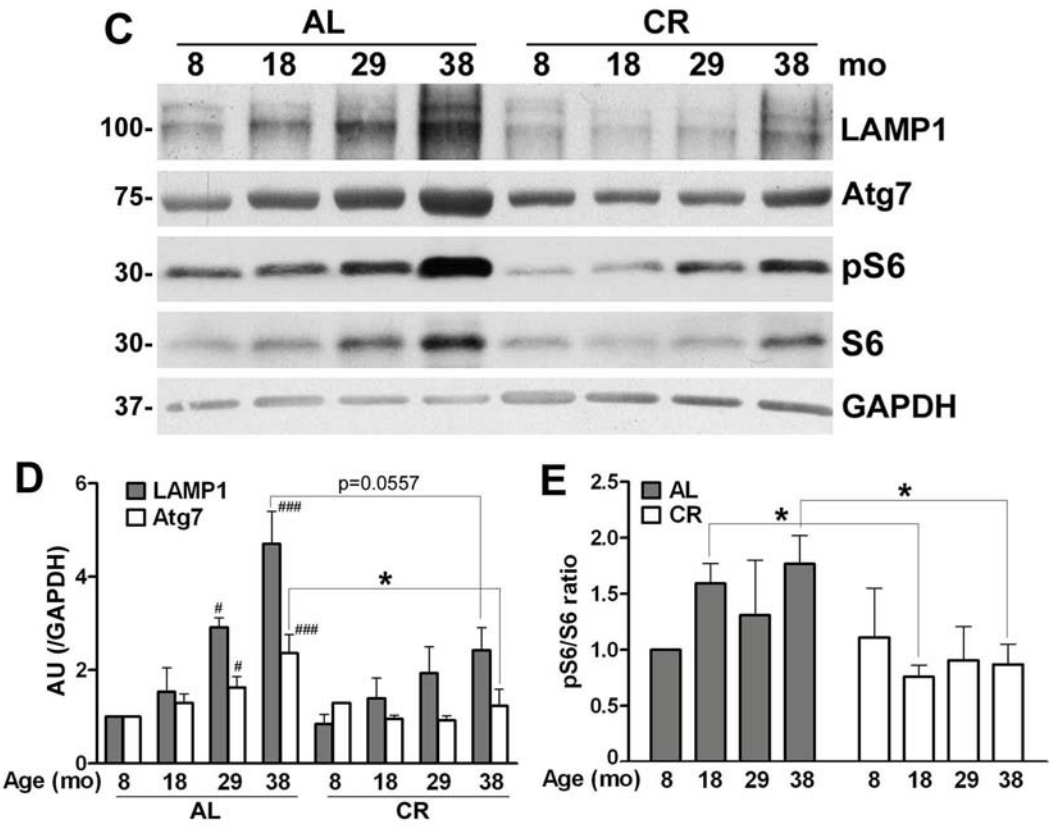

Figure 4-4. Continued

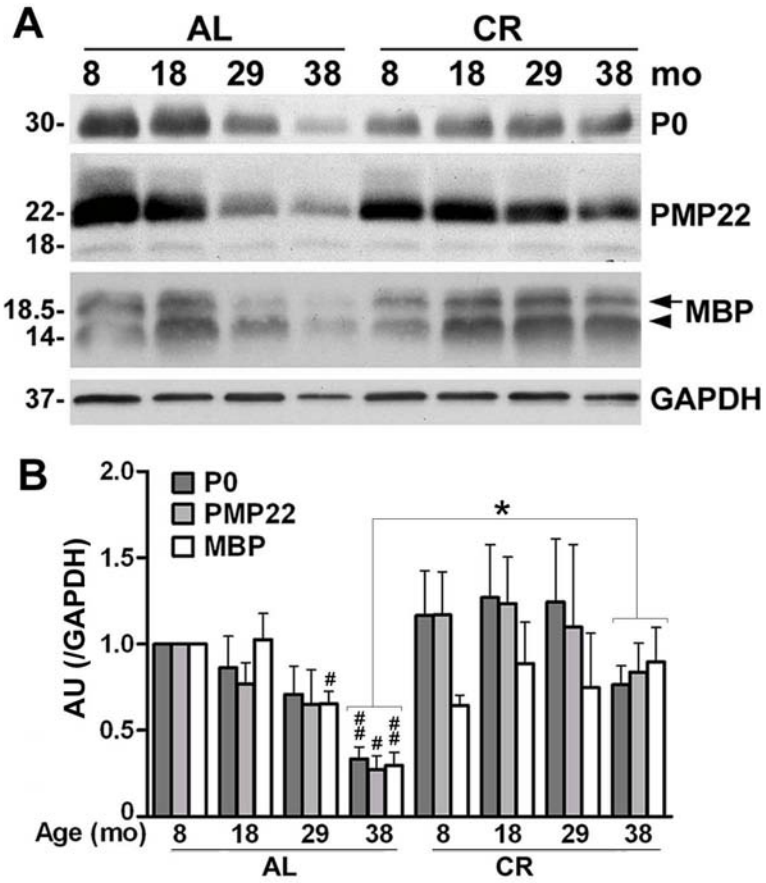

Figure 4-5. CR preserves myelin protein expression and myelinating SC phenotype. (A) Total sciatic nerve lysates (10 µg/lane) from AL and CR rats at 8, 18, 29 and 38-mo ages were analyzed with antibodies against protein zero (P0), PMP22 and MBP by Western blots. The arrow and arrowhead on the right indicate the 18.5 and 14 kDa of isoforms of MBP. GAPDH serves as a protein loading control. (B) Densitometric analysis of myelin proteins P0, PMP22 and MBP normalized to GAPDH (#p<0.05, ##p<0.01 [Fisher's PLSD], *p<0.05 [unpaired t-test], mean ± SEM). (C) Total sciatic nerve lysates (20 µg/lane) from rats under AL and CR diet were analyzed by Western blotting with polyclonal anti-p75NTR and monoclonal anti-pHH3 antibodies. The blots were reprobed with anti-tubulin to monitor protein loading. Molecular mass at left, in kDa. (D) Quantification of p75NTR and pHH3 normalized to GAPDH (###p<0.001 [Fisher's PLSD], *p<0.05, *p<0.01, ***p<0.001 [unpaired t-test]). (E) The nuclei of SCs were counted in longitudinal sections of sciatic nerves from two different depths and eight random visual fields (0.1mm2) per animal. (*p<0.05, ***p<0.001, unpaired t-test, mean ± SEM). A-E, n=3 rats per condition.

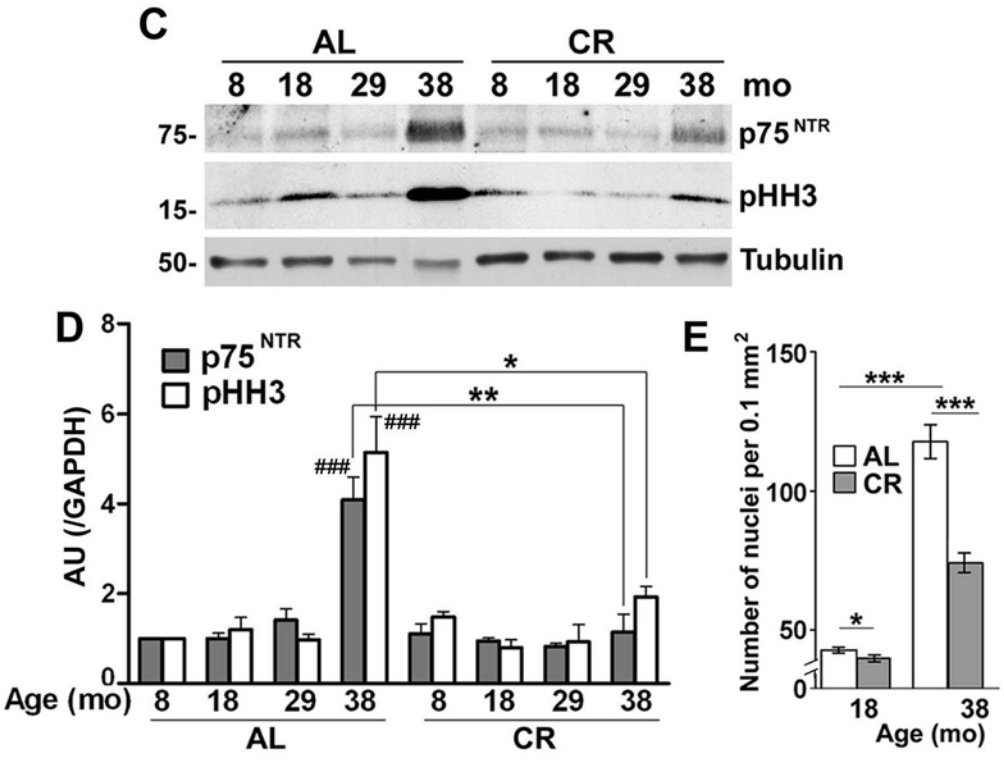

Figure 4-5. Continued

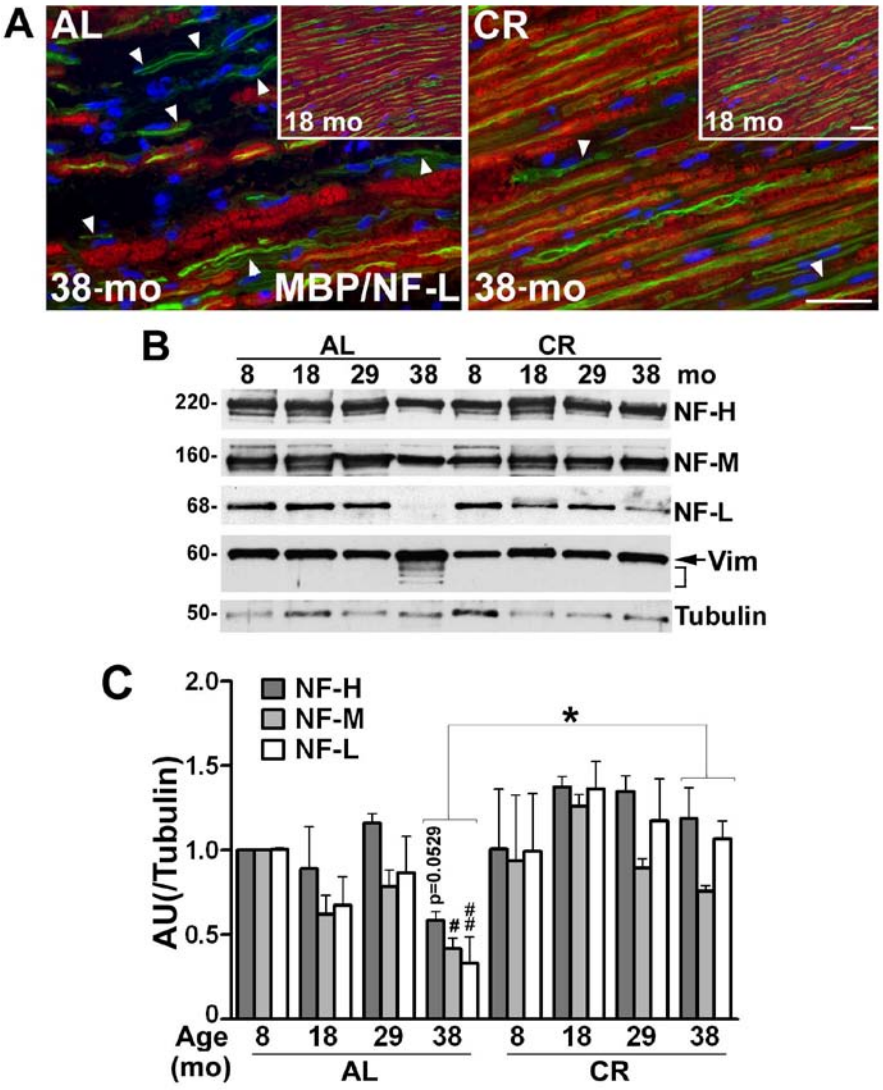

Figure 4-6. The expression of axonal proteins is supported by CR diet. (A) The severe reduction in MBP-like (red) as well as NF-L-like (green) staining is shown on longitudinal sections of sciatic nerves of 38-mo old AL-fed rats. Arrowheads indicate nerve fibers positive for neurofilaments but devoid of MBP-reactive myelin. Nerves from 18-mo old AL and CR rats are shown in the insets on the right. Nuclei are stained with Hoechst dye (blue). Scale bars, 40 µm. (B) Total sciatic nerve lysates (10 µg/lane) of AL and CR rats from the indicated ages were analyzed with antibodies against neurofilament proteins, NF-H, NF-M, NF-L and the intermediate filament protein, vimentin. The arrow indicates the full-length form (60 kDa) and the bracket shows the proteolytic cleavage products of vimentin. Tubulin serves as a protein loading control. Molecular mass at left, in kDa. (C) Densitometric analysis of neurofilament proteins NF-H, -M and -L normalized to tubulin from three independent sets of blots (#p<0.05, ##p<0.01 (Fisher's PLSD), *p<0.05 (unpaired t-test), mean ± SEM, n=3 rats). AU:arbitrary units.

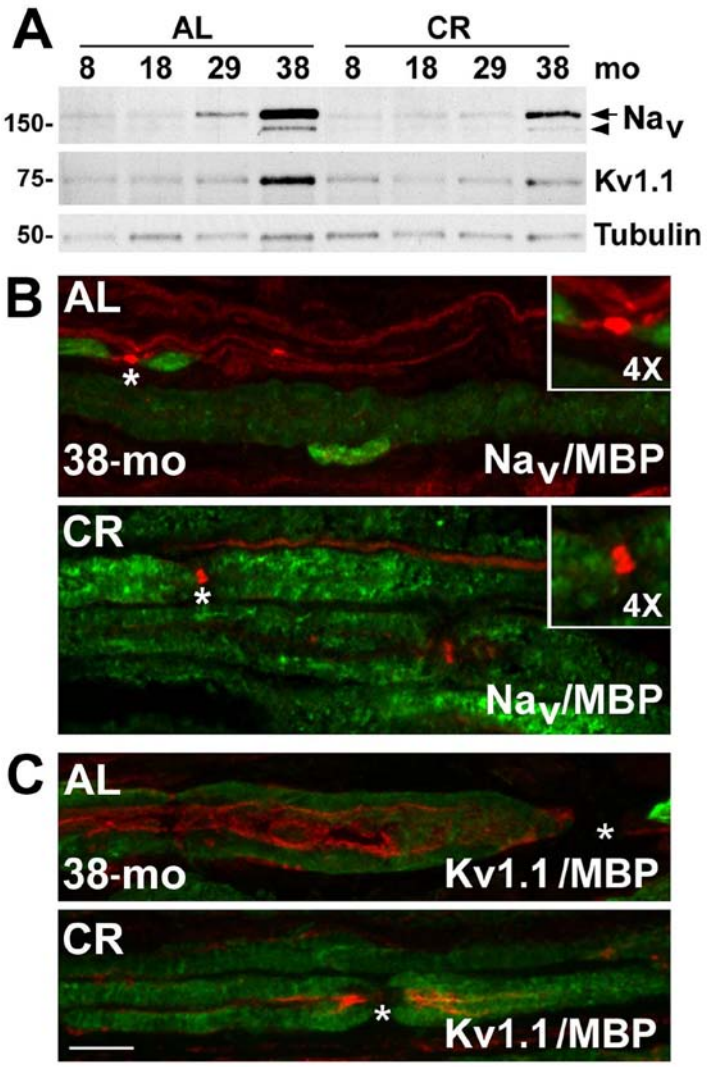

Figure 4-7. The expression and localization of Na+ and K+ channel proteins in myelinated nerves of aged rats. (A) Lysates of sciatic nerves (25 µg/lane) from the indicated ages and diet regimen (AL and CR) were assayed by Western blots for the expression of pan-voltage gated sodium channels (Nav) and a subtype of voltage gated potassium channel (Kv1.1) with polyclonal anti-pan Nav and anti-Kv1.1 antibodies, respectively. The arrow indicates the full length α-subunit of Nav and the arrowhead points to its proteolytic cleavage product. Tubulin serves as a protein loading control. Molecular mass at left, in kDa. (B) Longitudinal sciatic nerve sections were co-immunolabeled with anti-pan Nav (red) and anti-MBP (green) antibodies (panel on right). The node of Ranvier, as marked by clustered Nav channel-like staining (asterisk) is enlarged 4X in the inset. (C) Localization of Kv1.1 channel was visualized in longitudinal sciatic nerve sections from 38-mo old AL and CR rats by co-immunolabeling with anti-Kv1.1 (red) and anti-MBP (green) antibodies (panel on right). The nodes of Ranvier are marked by asterisks. Scale bar, 10 µm.

Table 4-1. Primary antibodies used in this study. WB, Western Blot; IS, Immunostaining

Species	Antigen	Source and catalog numbers	Dilution	
			WB	IS
Chicken	P0	Gift from Dr Gerry Shaw, UF	1 : 10000	1 : 500
Rabbit	PMP22	Pareek *et al.*, 1997; n/a	1 : 1000	n/a
Rat	MBP	Chemicon, Temecula; MAB386	1 : 5000	n/a
Mouse	GAPDH	Encor Biotechnology Inc.; MCA-1D4	1 : 5000	n/a
Mouse	NF-H	Encor Biotechnology Inc.; MCA-NAP4	1 : 500	n/a
Chicken	NF-M	Encor Biotechnology Inc.; CPCA-NF-M	1 : 5000	n/a
Chicken	NF-L	Encor Biotechnology Inc.; CPCA-NF-L	1 : 5000	1 : 1000
Mouse	Vimentin	Sigma, St Louis, MO, USA; clone VIM 13.2	1 : 1000	1 : 500
Chicken	MBP	Encor Biotechnology, Inc.; CPCA-MBP	n/a	1 : 500
Rabbit	$p75^{NTR.}$	Chemicon; AB1554	1 : 10000	n/a
Mouse	pHH3 (Ser10)	Millipore, Temecula; 05–598	1 : 500	1 : 200
Rabbit	Pan-Na_v (α-subunit)	Chemicon; AB5210	1 : 250	1 : 100
Rabbit	Kv1.1	Chemicon; AB5174	1 : 250	1 : 100
Rabbit	HSF1	Stressgen; Victoria British Columbia; SPA-901	1 : 500	1 : 250
Rat	HSP90	Stressgen, SPA-835	1: 2000	n/a
Rabbit	HSP70	Stressgen; SPA-812	1 : 1000	1 : 500
Rabbit	HSP40	Stressgen; SPA-400	1: 2000	n/a
Goat	HSP27	Santa Cruz Biotechnology, Inc.; sc-1049	1: 2000	n/a
Rabbit	αB-crystallin	Stressgen; SPA-223	1 : 1000	n/a
Rabbit	LAMP1	Gift from Dr William Dunn Jr, UF	1: 2000	n/a
Rabbit	Atg7	Gift from Dr William Dunn Jr, UF	1 : 3000	n/a
Rabbit	pS6 (Ser235/236)	Cell Signaling Technology, Inc., 2211	1 : 800	n/a
Mouse	S6	Cell Signaling Technology, Inc.; 2317	1 : 800	n/a
Mouse	HSP70	Stressgen; SPA-810	1 : 1000	1 : 250
Mouse	LAMP1	Stressgen; VAM-EN001	n/a	1 : 250
Rabbit	Cathepsin-D	Cortex Biochem, San Leanardo, CA, USA; CP3090	1 : 1000	n/a
Rabbit	LC3	Cell Signaling Technology; 2775	1 : 1000	1 : 200

CHAPTER 5
LIFE-LONG CALORIE RESTRICTION ALLEVIATES AGE-RELATED OXIDATIVE DAMAGE IN PERIPHERAL NERVES

Introduction

Aging of organ systems is associated with the accumulation of oxidatively damaged polynucleotides, proteins, carbohydrates and lipids which compromise cellular function. This is considered the “Oxidative Stress Theory of Aging” whereby age-related loss of proper physiological function is due to the accumulation of oxidative damage (Bokov et al., 2004). Long-lived postmitotic cells such as neurons are at higher risk and accrue greater amounts of damaged waste than short-lived cells (Agarwal and Sohal, 1994; Sohal et al., 1994). In addition, SCs, the myelinating glia of the PNS, are rich in polyunsaturated fatty acids (Garbay et al., 2000) which serve as a substrate for ROS-mediated lipid peroxidation (Smith et al., 1999; Blair, 2001). Together, the buildup of age-related damaged material along with their inefficient removal by homeostatic mechanisms become a concern in the vulnerable neurons and SCs of peripheral nerves.

Intracellular proteolytic mechanisms, including the UPS and the autophagy-lysosomal pathway (macroautophagy) are responsible for degradation and removal of damaged cellular material. The accumulation of waste material is not only harmful due to its interference with biological functions, but also for imparting toxicity via lipid peroxidation products such as malondialdehyde (MDA), 4-hydroxynonenal (HNE) and nitrotyrosine (Levine and Stadtman, 2001; Grune and Davies, 2003).

Although the precise mechanisms underlying the “Oxidative Stress Theory of Aging” are still largely unknown, there is accumulating evidence to support the involvement of the inflammatory response (Chung et al., 2009). An increase in the

levels of serum cytokines, such as TNF-α, interleukin-6 and interferon are commonly associated with senescence and play integral roles in activating inflammation and innate immunity (Spaulding et al., 1997). Free radicals are known to modulate this stress-induced activation of inflammation through the regulator of innate immunity and of the macrophage inflammatory response, the nuclear factor κB (NF-κB) (Seo et al., 2006; Salminen et al., 2008; Wang et al., 2008) Activation of NF-κB by degradation of its bound inhibitory protein, IκB, has also been found to upregulate the expression of the oxidizing agent, inducible nitric oxide synthase (iNOS) (Seo et al., 2006; Chung et al., 2009).

Restriction of calorie-intake is a widely accepted approach to lower levels of oxidative stress and slow age-associated changes, as well as to extend lifespan in mammals (Sohal and Weindruch, 1996; Martin et al., 2006). Previous studies have shown that calorie restriction (CR) decreases mitochondrial ROS generation and oxidative damage to DNA, protein and lipids (Lambert et al., 2004). CR has been found to activate the autophagic protein degradative pathway in aging rats (Wohlgemuth et al., 2007; Rangaraju et al., 2009) and to reduce markers of age-related chronic inflammation, like TNF-α, NF-κB and iNOS (Martin et al., 2006; Chung et al., 2009) . Although there have been extensive studies on the ability of CR to reduce age-related oxidative damage in the CNS (Martin et al., 2006), little is known about the beneficial effects of CR on age-associated oxidative stress and inflammation within the PNS.

In this study, we asked whether CR can relieve the oxidative stress placed upon the PNS during aging. We found that a life-long CR diet decreases the steady-state levels of undegraded poly-ubiquitinated substrates and oxidative damage markers of

proteins and lipids in myelinated peripheral nerves. Furthermore, CR relieves the chronic inflammation commonly associated with age.

Materials and Methods

Animals and Diet

The use of animals in this study was approved by the Institutional Animal Care and Use Committee (IACUC) of the University of Florida. AL fed and calorie-restricted (CR) male Fischer 344 x BN (Brown Norway) rats (n=3 per group) of ages 8-, 18-, 29- and 38-mo were obtained from the National Institute on Aging colony at Harlan Sprague Dawley Inc. (Indianapolis, IN). The animals were housed in a temperature and light controlled environment and had water available at all times. AL fed rats had free access to NIH-31 nutrient composition pellets, while the CR group received fortified pellets once daily 1 h before the onset of the dark cycle. Calorie reduction began at 14 weeks of age with 10% restriction, increased to 25% at 15 weeks, and was maintained at 40% from 16 weeks of age until sacrificed at 8-, 18-, 29- and 38-mo of age. Data on survival characteristics and physical performance of the same colony of rats have been previously reported (Turturro et al., 1999; Xu et al., 2008). The survival percentages of the male Fischer 344 x BN rats in the AL group for the ages 8-, 18-, 29- and 38-mo are, 100, 98, 70 and 30%, respectively. In comparison, those for the CR group for the same ages are 100, 100, 90 and 70% respectively (Turturro et al., 1999).

Biochemical Analyses

Rats of above mentioned ages kept under AL or CR diets were sacrificed as per IACUC protocols. The proximal ends (approximately 5 cm long piece) of the left and right sciatic nerves were surgically removed within 5 minutes of decapitation and frozen

immediately and stored in liquid nitrogen. The nerves from the right sides were used for biochemical analysis. Whole nerve lysates (including myelin and axonal proteins) were prepared separately from individual nerves in sodium dodecyl sulfate (SDS) sample buffer (62.5 mM Tris, pH 6.8, 10% glycerol, 3% SDS) supplemented with phosphatase inhibitors, PMSF (both from Sigma-Aldrich, St. Louis, MO) and complete protease inhibitor (Roche, Indianapolis, IN). The lysates were assayed for protein content using the BCA kit (Pierce, Rockford, IL) and then separated on polyacrylamide gels and transferred to nitrocellulose membranes for Western blotting. Primary antibodies in blocking buffer (5% milk in phosphate buffered saline (PBS) were applied to the membranes overnight at 4°C (see Table 1). Membranes were then incubated with horseradish peroxidase-conjugated secondary antibodies directed against the primary antibody, including anti-rabbit, anti-mouse (Cell Signaling technology, Inc., Danvers, MA), anti-rat or anti-goat (Sigma-Aldrich, St. Louis, MO). Membranes were then reacted with an enhanced chemiluminescent substrate (Perkin Elmer, Boston, MA). A GS-800 densitometer (Bio-Rad, Hercules, CA) was used to digitally image the films. In each experiment the densitometric value of AL 8-mo sample was set as 1 and the values of other age-diet combination were determined with respect to this. One way ANOVA followed by Fisher's PLSD analysis was performed using the StatView program, to compare the normalized densitometric values of proteins (dependent variables) between AL or CR diet with age (factor). For each analysis, the p-value and significance (#, ##, ###) for Fisher's PLSD analysis was determined by comparing the densitometric values of 8-mo-old AL samples with the older ages (18-, 29- or 38-mo) of the AL group. Similarly in the CR group, the 8-mo-old CR sample was compared with older ages.To

determine statistical significance between samples, unpaired t-test was performed using GraphPad Prism v5.0 software. Differences were considered significant at $p<0.05$. For each analysis, nerve samples from 3 individual rats were used.

Immunolabeling of Nerve Samples

The proximal ends of each left sciatic nerve (n= 3 animals for each age and diet group) were sectioned at 5 μm thickness and dried for 1 h at room temperature on Superfrost/Plus microslides (Fisher Scientific, Pittsburg, PA). Sections for HNE staining were fixed and permeabilized with 1% paraformaldehyde and 90% ethanol for 2 min at 25°C. Sections analyzed for lysosome-associated membrane protein 1 (LAMP1), pUb, CD11b and NF-κB were fixed with 4% paraformaldehye in PBS for 30 min followed by permeabilization with ice cold methanol for 5 min (Rangaraju et al., 2009). Following fixation, slides were blocked in 20% normal goat serum in PBS, and then incubated with primary antibodies overnight at 4°C (see Table 1). Bound antibodies were detected using Alexa Fluor 594 or Alexa Fluor 488 goat anti-rabbit or anti-mouse IgG secondary antibodies (Molecular Probes, Eugene, OR). Hoechst dye (Molecular Probes) was included with the secondary antibodies to visualize nuclei. Slides were mounted with coverslips using the ProLong Antifade kit (Molecular Probes) and imaged with a SPOT camera attached to a Nikon Eclipse E800 microscope (Melville, NY). Images were formatted using Adobe Photoshop 5.5. For quantification of macrophages, CD11b-positive cells were counted per field of view in longitudinal sections (5 μm thickness) of sciatic nerves from two different depths and eight random visual fields ($0.1mm^2$) per animal (n=3). To determine statistical significance between samples, unpaired t-test was performed using GraphPad Prism v5.0 software. Differences were considered significant at $p<0.05$.

Di-8 ANEPPS Labeling

For labeling of accumulated oxidized material, 4-(2-(6-dibutylamino)-2-naphthalenyl)ethenyl)-1-(3-sulfopropyl) hydroxide (di-8 ANEPPS), a lipophilic dye that recognizes lipofuscin adducts (Grune et al., 2004) was used. Frozen nerve sections (as above) were fixed with 4% paraformaldehye in PBS for 10 min followed by permeabilization with 0.2% Triton X-100 in PBS for 15 min at 25^{o}C. Samples were blocked in 20% normal goat serum in PBS then incubated with 2 nM di-8 ANEPPS in PBS for 30 min at 25°C. Slides were mounted with coverslips and imaged, as above. Mean di-8 ANEPPS pixels per fixed area (0.1mm^2) were determined using the mean gray value tool in the NIH Image J software. Statistical analysis was performed by unpaired t-test using GraphPad Prism software v5.0 and differences were considered significant at $p<0.05$.

Results

A Calorie-Restricted Diet Slows Protein Damage within Peripheral Nerves During Aging

As a marker of damaged and/or aggregated proteins we compared the steady-state levels of anti-ubiquitin reactive molecules between sciatic nerve lysates from 8-18-, 29- and 38-mo-old rats (Fig. 5-1A). There is a gradual accumulation of slow-migrating poly-ubiquitinated substrates in the nerves of AL fed rodents, which becomes prominent by 29-mo (Fig. 5-1A). In comparison, the levels of ubiquitin-reactive proteins remain remarkably low in nerves of CR-fed rats, even at 38-mo (Fig. 5-1A). Quantification of blots after correcting for GAPDH from three independent experiments reveals a significant increase in poly-ubiquitin reactive proteins by 29-mo of age in the AL group, which is absent from the CR animals (Fig. 5-1B).

To examine if lysosomes are recruited to ubiquitin aggregates in aged nerves, we coimmunolabeled longitudinal sciatic nerve sections for ubiquitin and LAMP1 (Fig. 5-1C). As suggested by the Western blots (Fig. 5-1A), nerves samples from 38-mo AL fed rats contain numerous ubiquitin-positive protein aggregates (Fig. 5-1C), as well as enlarged lysosomes and vacuoles (Fig. 5-1C, green, arrows) (Rangaraju et al., 2009). Many of the ubiquitin-reactive aggregates are surrounded by LAMP1-positive lysosomes, which are revealed by yellow color on merged images (Fig. 5-1C, 3X magnifications). On sections from 38-mo-old CR animals, the abundance and apparent size of ubiquitin-positive aggregates are dramatically lower (Fig. 5-1C, red, arrows), which agree with the biochemical data (Fig. 5-1A). Correspondingly, these nerves show an overall decrease in LAMP1-like immunoreactivity and fewer vacuoles (Fig. 5-1C, bottom panel). The CR diet also attenuates the age-related increase the number of nuclei per fixed area of nerve tissue (Fig. 5-1C, blue), as shown previously (Rangaraju et al., 2009).

In aged postmitotic mammalian tissues, besides undegraded ubiquitin-tagged substrates, there is a build-up of oxidized and crosslinked proteins and lipids, known as lipofuscin (Jung et al., 2007). In accordance, sciatic nerve sections from 38-mo-old AL fed rodents stain prominently with di-8 ANEPPS (Fig. 5-2A, arrows), a lipophilic dye that recognizes lipofuscin adducts (Grune et al., 2004), as compared to samples from 18-mo-old rats (Fig. 5-2A). Nerve tissues of diet-restricted rats contain fewer and apparently smaller di-8 ANEPPS-positive structures at both ages examined (Fig. 5-2A, arrowhead). Quantification of the mean di-8 ANEPPS pixels per fixed area shows a statistically significant increase with age from 18- to 38-mo in samples from AL rats (Fig.

5-2B). When compared across ages and diet groups, the accrual is significantly reduced by CR diet (Fig. 5-2B, *p<0.05, ***p<0.001). Together, these results emphasize that a life-long CR diet is effective in reducing the accumulation of oxidized and cross-linked substances in peripheral nerves, either by lowering damage across lifespan and/or enhancing the activity of protective mechanisms, such as the ubiquitin-proteasome and/or autophagy-lysosomal pathways.

Lipid Oxidation-Mediated Protein Damage within Myelinated Peripheral Nerves

Oxidation of polyunsaturated fatty acids of myelin lipids (Garbay et al., 2000) results in the formation of hydroperoxides and hydroxyalkenals, like malondialdehyde (MDA) and 4-hydroxynonenal (HNE), which then can react with proteins and alter their surface hydrophobicity (Adams et al., 2001; Davies, 2001). To examine lipid modification during aging of myelinated nerves, we analyzed tissue lysates with antibodies to MDA (Fig. 5-3A). As shown on the Western blot, there is a gradual increase in MDA adducted proteins with age, detected as a smear, in AL samples (Fig. 5-3A, square bracket). In addition, the mobility of MDA-positive proteins is slowed in the AL 38-mo-old lysate likely representing aggregates (Fig. 5-3A). In comparison, we find a marked decrease in MDA adducted proteins within nerves from animals on CR diets (Fig. 5-3A, square bracket). Quantification after correction for tubulin, reveals a significant increase ($^{###}$p<0.01) in MDA adducted proteins in sciatic nerves of AL fed animals from 29- to 38-mo, a trend that is attenuated by the CR intervention (Fig. 5-3B). Furthermore, the differences are significant when comparing across diet groups at the 38-mo time point (Fig. 5-3B, *p<0.05). We also measured the levels of protein nitrosylation within whole nerve lysates and found a similar increasing pattern across the ages in AL samples (Fig. 5-3C, D, $^{##}$p<0.01). In contrast, significantly lower levels

(*p<0.05) of nitrosylated proteins are detected in nerves of animals maintained on a life-long CR (Fig. 5-3D). As both axonal and glial proteins are vulnerable to HNE modification (Gard et al., 2001), we also quantified HNE adducts by biochemical analysis and found a significant increase from 29- to 38-mo in the AL fed group (Fig. 5-3E, F, $^{\#\#}$p<0.01). While the CR diet lowers the levels of HNE-reactive proteins across lifespan, statistical analysis between AL and CR 38-mo samples did not yield significance (p=0.0697) (Fig. 5-3F).

To examine the distribution of oxidatively damaged proteins within peripheral nerves, we immunostained sciatic nerves with the same anti-HNE antibody that was used for the Western blots (Fig. 5-3G). There is a prominent increase in HNE-like immunoreactivity with age within the nerve tissues of AL fed rats, with diffuse localization throughout axonal and glial compartments (Fig. 5-3G). As suggested by the Western blots, there are fewer HNE-positive areas within the 38-mo CR counterpart. While the anti-MDA and anti-nitrotyrosine antibodies are unsuitable for immunolocalization studies, we predict that those antibodies would show a similar diffuse immunoreactivity.

Age-related activation of pro-inflammatory pathways is attenuated by a life-long CR diet

The inflammatory response appears to play a critical role in decreasing redox status and increasing oxidative damage observed with aging (Beckman and Ames, 1998; Salminen et al., 2008). Therefore, we analyzed sciatic nerve lysates for the levels of markers of chronic inflammation, including TNF-α, the p50 and p65 subunits of pro-inflammatory NF-κB and for phospho-IκB. For each of these proteins, we found an increasing trend with age, which is attenuated by the CR intervention (Fig. 5-4A).

Quantification of blots from three different group of animals revealed a significant increase in TNF-α from 8-mo to 38-mo ($^{\#\#}p<0.01$) in animals receiving an AL diet (Fig. 5-4B). In contrast, the expression of TNF-α remains low in the CR group, with only significant increase in the oldest animals ($^{\#\#}p<0.01$). Additionally, diet restriction significantly reduced TNF-α levels in 29- and 38-mo-old nerves when compared to their AL fed counterparts (Fig. 5-4B, $^{*}p<0.05$).

Similar to TNF-α, there is an increase in the expression of both p50 and p65 subunits of pro-inflammatory NF-κB with age ($^{\#\#\#}p<0.001$ between 8-mo and 38-mo, Fig. 5-4A, C, D) in the AL group. Strikingly, the steady-state levels of p50 subunit of NF-κB in sciatic nerve of 38-mo-old CR rats is significantly lower ($^{*}p<0.05$) as compared to age matched AL-fed rats. An analogous trend is observed for the p65 subunit of NF-κB protein in nerves of AL rats with age, and the attenuation of this rise with diet restriction, (Fig. 5-4D, $^{*}p<0.05$). We analyzed the steady-state levels of phosphorylated IκB (phospho-IκB), which also shows an increasing pattern with age (Fig. 5-4E). In the CR group the increase is still significant at the oldest age examined ($^{\#\#}p<0.01$), however a marked reduction in normalized phospho-IκB protein level is apparent when compared across diet groups ($^{**}p<0.01$) (Fig. 5-4E).

The main source for inflammatory mediators within myelinated peripheral nerves are infiltrating macrophages (Hartung et al., 1992). Hence we tested whether a CR diet would influence the number of infiltrating immune cells associated with aging in sciatic nerves. We used an anti-CD11b antibody to stain for macrophages (Misko et al., 2002), which appear to increase in numbers from 18 to 38-mo on longitudinal nerve sections from AL fed rats (Fig. 5-5A). Quantification of CD11b-positive immune cells reveals a

significant age-related increase (***p<0.001) in the AL group from 18- to 38-mo-old (Fig. 5-5B). On the other hand, the number of macrophages is low in nerves of the CR rats, particularly when compared at the 38-mo time point (***p<0.001) (Fig. 5-5B). Accordingly, Western blot analysis of whole nerve lysates reveals a pronounced increase in CD11b protein levels in 38-mo-old AL samples as compared to 8-mo (Fig. 5-5C), while the levels remain low across the tested ages in the diet-restricted group (Fig. 5-5C, D). In agreement with the increased inflammatory response, biochemical studies with an anti-rat IgG antibody detect a marked increase in endogenous nerve immunoglobulins, specifically IgG- heavy chain (-HC) and light chain (-LC) with age. The dietary modulation notably alleviates the increase in the levels of endogenous nerve IgGs (Fig. 5-5C, E, F).

Discussion

As physical barriers against circulating toxic oxidants such as capillary endothelia and the choroid plexus are absent within the periphery (Samson and Nelson, 2000), the PNS is a vulnerable target for oxidative damage. Here we show a pronounced accumulation of ubiquitinated and oxidatively damaged proteins with age within myelinated peripheral nerves, which prompts an immunologic response from the host. In comparison, nerves of rats kept on a life-long CR diet accumulate lower levels of modified proteins and the inflammatory response is muted. While a life-long CR might not be practical for humans, this study clearly shows the power of this intervention in preventing age-associated damage in peripheral nerves. Based on the findings presented here, we hypothesize that the PNS would also respond to a more acute, short-term CR, or a long-term mild CR. Both of these approaches have been explored in

other organ systems with success (Seo et al., 2006; Ingram et al., 2007) but their effects on peripheral nerves is not known.

Proteomics studies of aging rat brain have revealed a decrease in proteins required for proper ubiquitin-proteasomal degradation, resulting in a build-up of undegraded substrates (Klionsky et al., 2008). While due to sample size limitations we were unable to test the levels of proteasomal constituents, we detected the accumulation of slow-migrating poly-ubiquitinated substrates within nerves of AL-fed aged rats, suggestive of compromised proteasome activity. Significantly, the levels of such ubiquitin-reactive proteins are reduced in nerves of CR rats (Fig. 5-1). This effect could be due to less protein damage throughout lifespan, and/or sustained proteasomal processing of ubiquitinated substrates and/or their removal by an alternative mechanism, such as autophagy. Although we do not know yet which of these possibilities are influenced by the life-long diet restriction, a contribution from the autophagy-lysosomal pathway is likely (Rangaraju et al., 2009). With normal aging, lysosomes overwhelmed with lipofuscin still receive proteolytic enzymes, which leads to their depletion and decrease in overall autophagic capacity of the cell (Brunk and Terman, 2002). Diet restriction is known to activate the autophagy-lysosomal pathway and assist in removal of damaged proteins (Wohlgemuth et al., 2007; Madorsky et al., 2009). Accordingly, transgenic mice with compromised autophagic activity accumulate high levels of aggregated proteins that are reactive for ubiquitin (Komatsu et al., 2005; Mizushima and Hara, 2006). These findings together with our previous reports (Wohlgemuth et al., 2007; Madorsky et al., 2009; Rangaraju et al., 2009) suggest that dietary restriction is

beneficial for the activity of protein degradative pathways, such as the UPS and the autophagy-lysosomal system.

High levels of HNE, nitrotyrosine, and other irreversible protein adducts have been observed in age-related neurodegenerative conditions of the CNS (Beal, 2002), yet their contribution to peripheral nerve disease is unclear. Given that lipids are sensitive to free radical damage (Pamplona et al., 2000), myelinated nerves provide an opportune environment for lipid peroxidation mediated oxidative damage to organelles and proteins. Indeed, we observed a gradual increase in lipid peroxidation products in our AL samples with age, including MDA, HNE and nitrotyrosine (Fig. 5-3). Oxidative modifications in cellular proteins lead to increased proteolytic susceptibility due to the hydrophobicity (Davies, 2001; Grune and Davies, 2003; Grune et al., 2003). This increase in proteolytic recognition, however, functions only for mildly oxidized substrates as extensively oxidized proteins tend to aggregate and covalently cross-link (Davies, 2001; Merker et al., 2001; Farout and Friguet, 2006). Such changes are suggested by the accumulation of slow-migrating proteins in nerve samples from old AL rodents (Fig. 5-1 and 5-3). Beside protein degradation mechanisms, cells utilize antioxidant cascades to modulate oxidative damage. With age, both of these processes become less efficient, which can lead to further accumulation of lipid peroxidation, protein oxidation and other deleterious cellular modifications (Merker et al., 2001; Grune et al., 2004). Our results suggest that a CR diet attenuates lipid peroxidation (Fig. 5-3) and thereby decreases oxidative damage within peripheral nerves with age.

Age-associated oxidant stress is known to activate the inflammatory process via the NF-κB transcription factor and associated target genes, including TNF-α (Chung et

al., 2009). In human and rodent studies, the circulating levels of this pro-inflammatory cytokine TNF-α increase with age, which in rodents is significantly attenuated by CR (Phillips and Leeuwenburgh, 2005; Bruunsgaard, 2006). In agreement with these findings, we found age-associated increase in TNF-α expression in peripheral nerves, a trend that was attenuated up to 38-mo of age by CR (Fig. 5-4). One of the upstream modulator of NF-κB activity is IκB kinase which is activated by redox imbalance and oxidative stress (Chung et al., 2009). The phosphorylation of the IκB subunit of NF-κB/IκB complex triggers the degradation of IκB, which then leads to the activation of NF-κB (Zandi et al., 1997; Karin, 2006). Studies in different organ systems have shown an increase in NF-κB activity with age and in disease (Chandrasekar and Freeman, 1997; Chung et al., 2009). Corresponding to the increase in NF-κB binding activity with age, the levels of p65 and p50 subunits of NF-κB, as well as phospho-IκB also elevated (Kim et al., 2002a), a pattern that is reproduced in myelinated peripheral nerves (Fig. 5-4). The upregulation of NF-κB in sciatic nerves of old AL fed rats could be a response to the severe demyelination (Rangaraju et al., 2009), in combination with an inflammatory response (Fig. 5-5) (Andorfer et al., 2001). In inflammatory demyelinating neuropathies, macrophages infiltrated into the nerves are the primary expressors of NF-κB (Andorfer et al., 2001) and are the likely source for this cytokine in aged nerves, as well. While due to antibody binding specificities we could not perform colocalization studies for macrophages and NF-κB in our rat nerve samples, the significant attenuation of macrophages in CR samples in association with a decrease in pro-inflammatory NF-κB levels supports this theory.

Infiltration of peripheral nerve tissue by CD11b-positive macrophages in inflammatory nerve disease and hereditary demyelinating neuropathies take part in the pathogenic cascade (Ceballos et al., 1999; Andorfer et al., 2001; Misko et al., 2002). Upon analyses of longitudinal sections of sciatic nerves, we observed a significant increase (***p<0.001) in the number of CD11b-positive macrophages in AL fed animals from age 18- to 38-mo (Fig. 5-5), which could contribute to the pronounced morphologic changes observed (Rangaraju et al., 2009). Indeed, ultrastructural studies of senescent paranodal junctions of rat peripheral nerves have detected myelin fragment-filled macrophages between the ages of 24- and 31-mo (Sugiyama et al., 2002). In addition to a possible role in myelin damage, a pronounced inflammatory response is also evidenced by accumulation of immunoglobulins within nerves, targets of which antibodies are unknown. Together, our studies support the activation of the inflammatory response through oxidative damage within aged peripheral nerves, a detrimental cascade that is muted in nerves of calorie-restricted rodents.

In summary, our studies show evidence of pronounced oxidative damage within myelinated peripheral nerves with age and associated activation of pro-inflammatory events. In comparison, life-long CR thwarts such detrimental changes likely by attenuating the levels of damaging molecules and allowing the cells to maintain endogenous protective mechanisms (Martin et al., 2006; Rangaraju et al., 2009). These findings offer novel insights into possible mechanisms of age-associated decline in neural function and provide targets for therapeutic interventions.

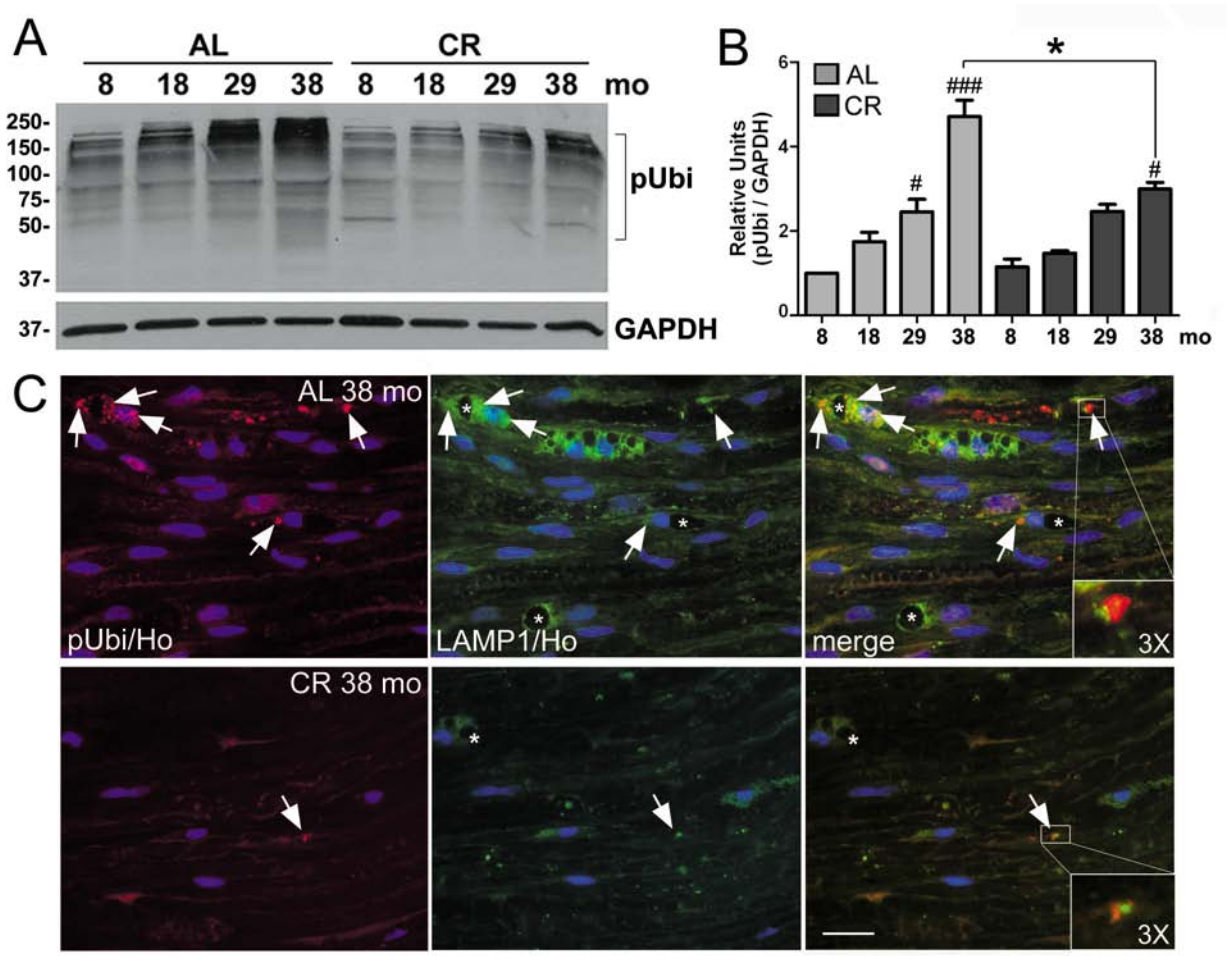

Figure 5-1. A calorie-restricted diet minimizes accrual of damaged proteins within peripheral nerves during aging. (A) Western blot analysis of whole sciatic nerve lysates (20 µg/lane) from rats of the indicated months (mo) fed AL or CR diets probed with an anti-ubiquitin antibody. Slow-migrating poly-ubiquitinated (pUbi) protein substrates are marked by a square bracket. GAPDH is shown as a protein loading control. Molecular mass in kDa, on the left. (B) Quantification of pUbi band intensity normalized to GAPDH is shown (#p<0.05, ###p<0.001, Fisher's PLSD analysis; *p<0.05, unpaired t-test, mean±SEM, n=3). In this and subsequent figures, the p-value for Fisher's PLSD analysis is determined by comparing the 8-mo-old sample with the older ages (18-, 29-, or 38-mo) for each diet group. (C) Longitudinal sciatic nerve sections from 38-mo-old animals fed AL or CR diets were analyzed for ubiquitin- (red) and LAMP1-like (green) immunoreactivity. Arrows point to ubiquitin-positive protein aggregates adjacent to LAMP1-positive lysosomes (magnified 3X in insets). Asterisks indicate intracytoplasmic vacuoles. Nuclei are labeled with Hoechst dye (blue). Scale bar, 20 µm.

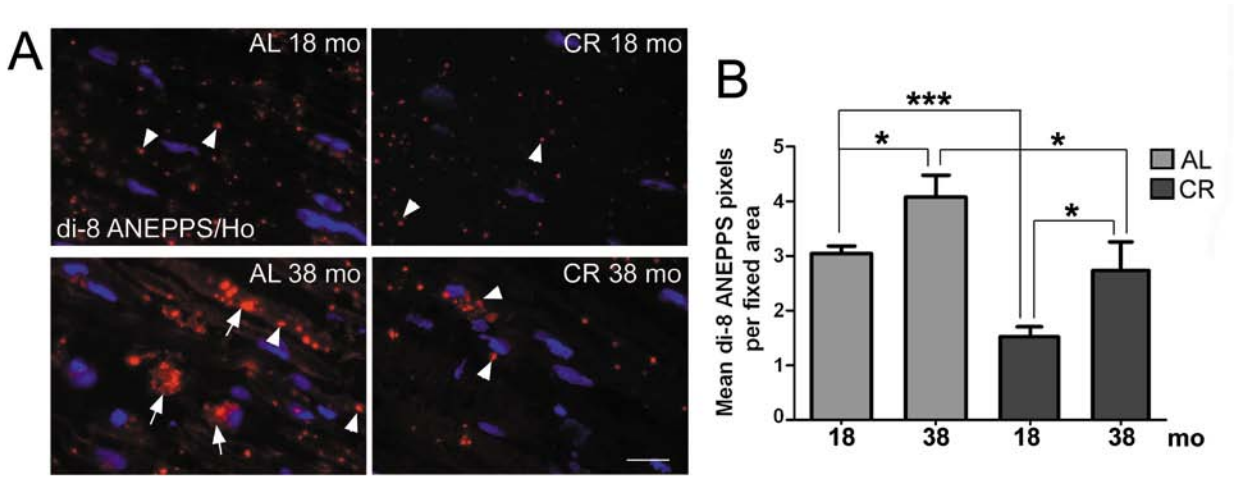

Figure 5-2. Accumulation of lipofuscin is curtailed by CR diet with aging. (A) Sciatic nerve sections from 18-mo and 38-mo-old animals fed AL or CR diets were stained with di-8 ANEPPS dye, which labels lipofuscin content (red). Large (~10 μm) and smaller (<10 μm) di-8 ANEPPS-positive adducts are marked with arrows and arrowheads, respectively. Nuclei are labeled with Hoechst dye (blue). Scale bar, 20 μm. (B) Quantification of mean di-8 ANEPPS dye-positive pixels per fixed area is shown (*p<0.05, ***p<0.001, unpaired t-test, mean±SEM, n=3).

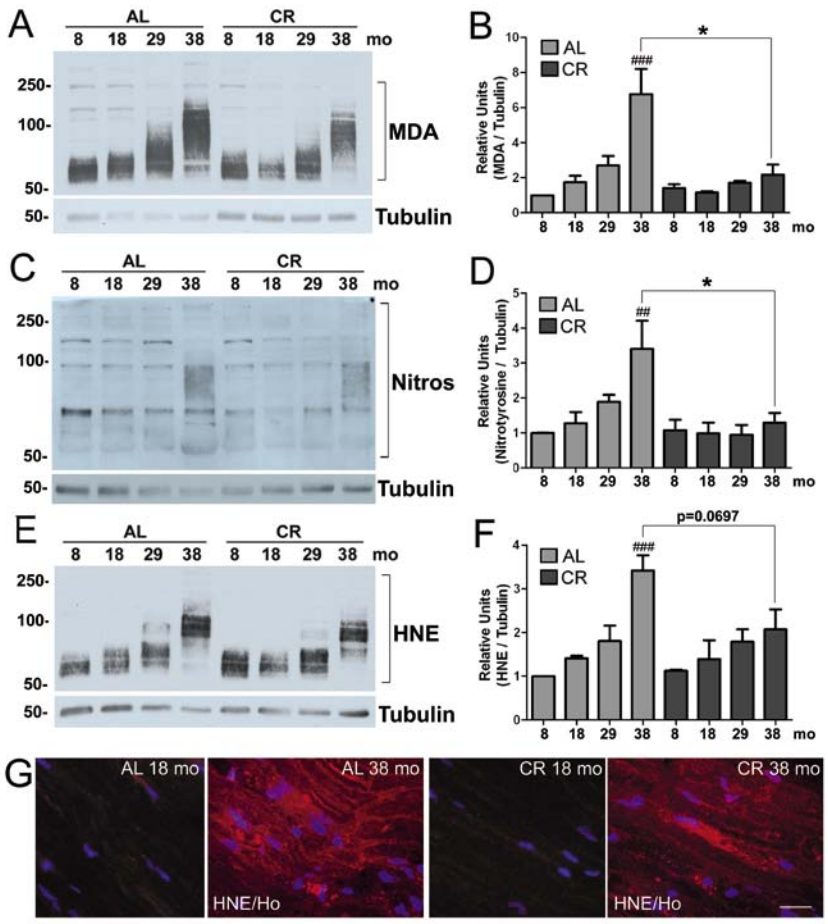

Figure 5-3. Lipid peroxidation-associated modifications of proteins with age are relieved in sciatic nerve with a CR diet. (A) Whole rat sciatic nerve lysates (20 µg/lane) were probed with a rabbit anti-malondialdehyde (MDA) antibody to detect MDA adducts to proteins (square bracket). Tubulin is shown as a protein loading control. (B) Quantification of MDA adduct band intensities normalized to tubulin is shown ($^{###}p<0.001$, Fisher's PLSD analysis; *p<0.05, unpaired t-test, mean±SEM, n=3). (C) Biochemical analysis of tyrosine residues (Nitros) on proteins (square bracket) using an anti-nitrosylation antibody in the same lysates as in A.. Tubulin is shown as a protein loading control. (D) Quantification of nitrotyrosine band intensities from Western blots normalized to tubulin is shown ($^{##}p<0.01$, Fisher's PLSD analysis; *p<0.05, unpaired t-test, mean±SEM, n=3). (E) Western blot analysis of 4-hydroxynonenal (HNE) in the same lysates used in A and C. Tubulin is shown as a protein loading control. In A, C and E molecular mass is in kDa, on the left. (F) Quantification of HNE adduct band intensities from Western blots normalized to tubulin is shown ($^{###}p<0.001$, Fisher's PLSD analysis; p=0.0697, unpaired t-test, mean±SEM, n=3). (G) Immunohistochemical staining of sciatic nerve from 18-mo and 38-mo-old animals fed AL and CR diets with an antibody against 4-hydroxynonenal (HNE). Nuclei are labeled with Hoechst dye (blue). Scale bar, 20 µm.

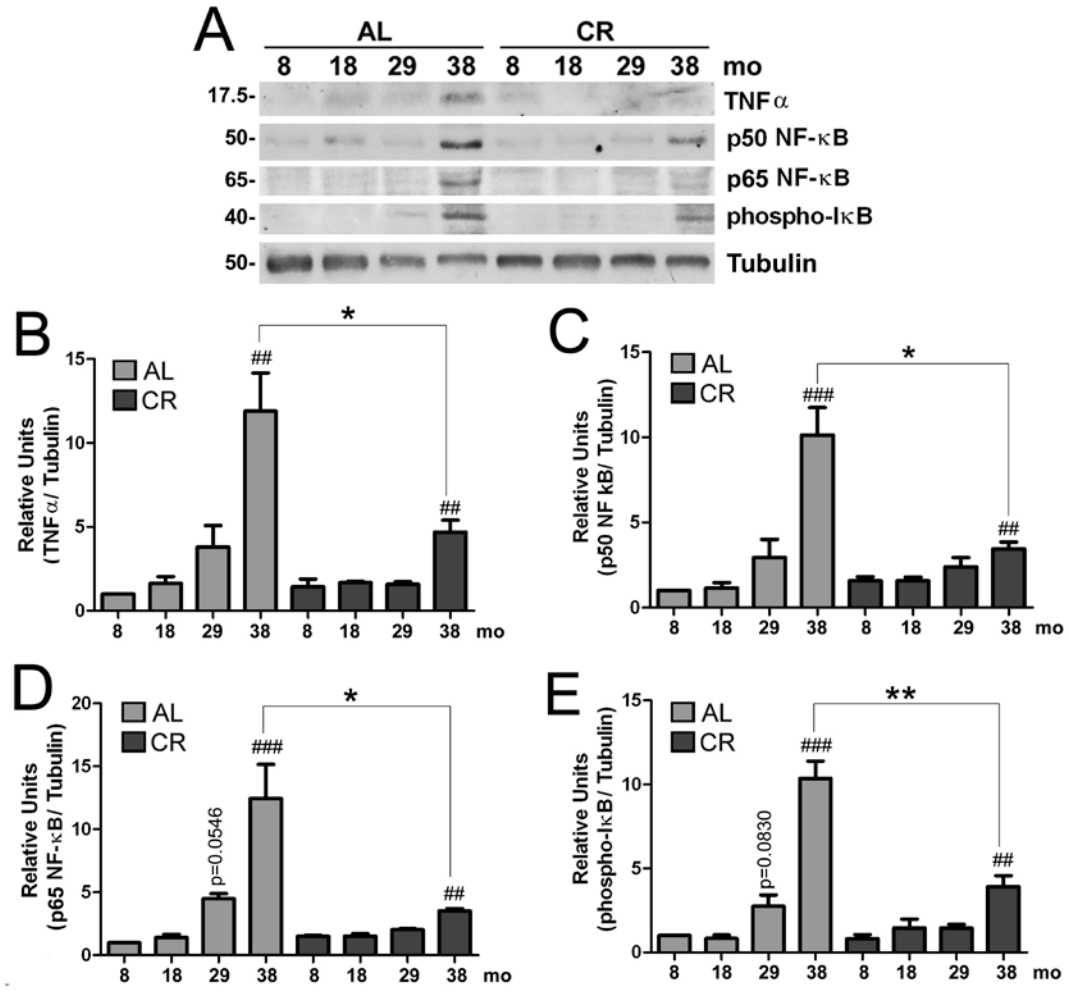

Figure 5-4. Age-related increase in pro-inflammatory mediators is attenuated by a life-long CR diet. (A) Total sciatic nerve lysates (20 µg/lane) from the indicated ages and diet were analyzed with antibodies against TNFα, p50 and p65 subunits of NF-κB and phospho-IκB. Tubulin is shown as a loading control. Molecular mass is in kDa, on the left. (B) Quantification of TNFα band intensities after normalization to tubulin is represented ($^{\#\#}$p<0.01, Fisher's PLSD analysis; *p<0.05, unpaired t-test, mean±SEM, n=3). (C) Quantification of the p50 subunit of NF-κB band intensities normalized to tubulin is shown ($^{\#\#}$p<0.01, $^{\#\#\#}$p<0.001, Fisher's PLSD analysis; *p<0.05, unpaired t-test, mean±SEM, n=3). (D) Quantification of the p65 subunit of NF-κB band intensities normalized to tubulin is shown (p=0.0546, $^{\#\#}$p<0.01, $^{\#\#\#}$p<0.001, Fisher's PLSD analysis; *p<0.05, unpaired t-test, mean±SEM, n=3). (E) Phospho-IκB levels were also analyzed within the same lysates and quantification of band intensities normalized to tubulin was performed (p=0.0830, $^{\#\#}$p<0.01, $^{\#\#\#}$p<0.001, Fisher's PLSD analysis; **p<0.01, unpaired t-test, mean±SEM, n=3).

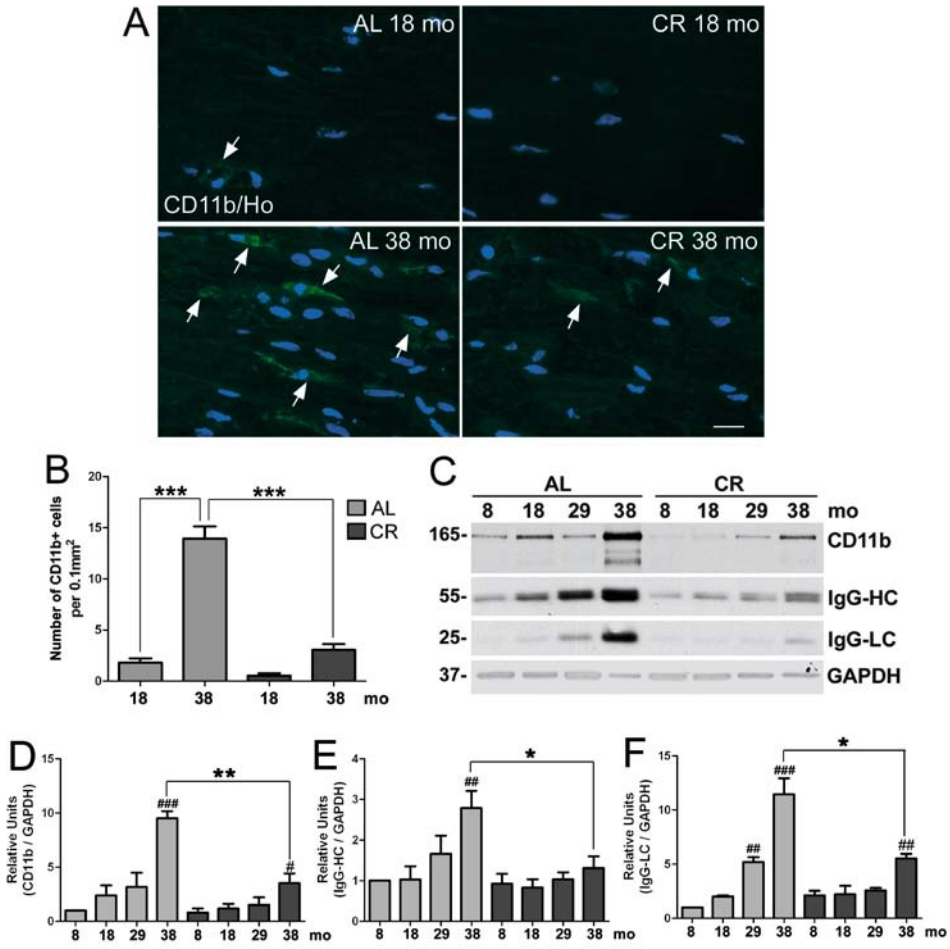

Figure 5-5. A calorie-restricted diet diminishes macrophage infiltration of peripheral nerves with age. (A) Cryosections of sciatic nerves from 18-mo and 38-mo-old rats either maintained on AL or CR diet were immunostained with an antibody against CD11b (green). Nuclei are stained with Hoechst dye (blue). Scale bar, 20 μm. (B) Quantification of CD11b-positive cells per 0.1 mm^2 of nerve tissue area is shown for 18- and 38-mo-old animals fed AL or CR diets (***$p<0.001$, unpaired t-test, mean±SEM, n=3). (C) Western blot analysis of sciatic nerve lysates (20 μg/lane) for steady-state levels of CD11b and endogenous IgG [heavy chain (-HC) and light chain (-LC)] from AL and CR rats is shown. GAPDH is used as a protein loading control. Molecular mass in kDa, on the left. (D) Quantification of the CD11b band intensities normalized to GAPDH from Western blot analyses from whole sciatic nerve lysates is shown ($^{\#}p<0.05$, $^{\#\#\#}p<0.001$, Fisher's PLSD analysis; **$p<0.01$, unpaired t-test, mean±SEM, n=3). (E) Quantification of the IgG-HC band intensities normalized to GAPDH from whole sciatic nerve lysates of AL and CR rats of the indicated ages is shown ($^{\#\#}p<0.01$, Fisher's PLSD analysis; *$p<0.05$, unpaired t-test, mean±SEM, n=3). (F) Quantification of band intensities of IgG-LC normalized to GAPDH was performed ($^{\#\#}p<0.01$, $^{\#\#\#}p<0.001$, Fisher's PLSD analysis; *$p<0.05$, unpaired t-test, mean±SEM, n=3).

Table 5-1. Primary antibodies used in this study. WB, Western Blot; IS, Immunostaining

Species	Antigen	Source and catalog number	Dilution	
			WB	IS
Rabbit	Nitrotyrosine	Calbiochem, San Diego, CA, 487924	1:400	n/a
Rabbit	Malondialdehyde (MDA)	Abcam, Cambridge, MA, 27642	1:400	n/a
Mouse	4-Hydroxynonenal (HNE)	Abcam, 48506	1:80	n/a
Mouse	GAPDH	Encor Biotechnology Inc., FL, USA; MCA-1D4	1:5000	n/a
Mouse	Tubulin	Sigma, St Louis, MO, USA, T6199	1:5000	n/a
Mouse	CD11b	Serotec, Raleigh, NC, MCA275GA	n/a	1:500
Rabbit	NF-κB	Stressgen; Victoria British Columbia, Canada; KAP-TF112	1:1000	n/a
Mouse	NF-κB	Santa Cruz Biotechnology, Inc., CA, USA; sc-109	1:1000	n/a
Mouse	Phospho-IκB (Ser 32/36)	Cell Signaling Technology, Inc. Boston, MA, USA; 9246	1:1000	n/a
Rabbit	TNF-α	Millipore, Temecula, CA, USA; AB1837P	1:2000	n/a
Rabbit	Ubiquitin	Dako, Carpinteria, CA, Z0458	1:500	1:100
Mouse	LAMP1	Stressgen, VAM-EN001	1:2000	1:500
Rat	CD11b	Serotec, Raleigh, NC, MCA711	1:500	n/a

CHAPTER 6
CONCLUSIONS

Misexpression and intracellular retention of PMP22 is associated with hereditary neuropathies in humans, namely, CMT1A (Fig. 6-1A [1]). In neuropathic SCs from both the mouse models of this disease, C22 and TrJ mice, the turnover of the newly-synthesized PMP22 by the proteasome is decreased (Fig. 6-1A [2]), leading to the formation of cytosolic protein aggregates (Fortun et al., 2003; Fortun et al., 2006). In these models, impaired PMP22 trafficking has been proposed to play a role in the disease process which eventually leads to demyelination (Fig. 6-1A [4]) (Sanders et al., 2001). Currently, there is no cure for CMT1A neuropathies and treatment is limited to rehabilitation and corrective surgery (Pareyson and Marchesi, 2009). In this study, two protein quality control pathways of therapeutic interest were explored for aiding the folding and/or degradation of misfolded proteins and improve myelination, namely chaperones (Chapter 2) and autophagy (Chapter 3) (Fig. 6-1B [1,3]). Our investigations in Chapter 2 and Chapter 3 directly stem from our previous proof-of-principle studies. First, the HS-induced chaperones and nutrient deprivation-induced autophagy are able to suppress the formation of PMP22 aggregates in a toxin-induced cellular model (Fortun et al., 2003; Fortun et al., 2007). Secondly, intermittent fasting, a dietary approach to induce both chaperone and autophagy pathways improve locomotor performance and myelination in TrJ mice (Madorsky et al., 2009).

Pharmacological stimulation of the expression of protein chaperones by synthetic small-molecule inhibitors of HSP90 in DRG explants from C22 neuropathic mice leads to an improvement in myelin formation, increase in myelin internodes and correct processing of PMP22 (Chapter 2)(Fig. 6-1B [1,2,5,7]). This treatment was performed

during late stage of myelination which is 10-14 days after initiating myelination with ascorbate (Fig. 2-5). Preliminary results from our lab show that exposure of DRGs from C22 neuropathic mice with HSP90 inhibitors at early timepoints (i.e) 2 days after initiation of myelination also leads to improvement in myelin protein expression (data not shown). In addition to the improved myelin in C22 model, first round of results show that activating chaperones using HSP90 inhibitor in DRGs from TrJ mice, also leads to enhanced myelination (data not shown). Together, these results warrant further studies with HSP90 inhibitors as potential therapeutic candidates, *in vivo*, for both overexpressor (C22) and point mutation (TrJ) mouse models of hereditary demyelinating neuropathies.

With regards to the autophagy pathway, the treatment of DRG explant cultures from neuropathic mice with RM (25 nM) to activate autophagy, improves the processing of PMP22 through the secretory pathway (Chapter 3) (Fig. 6-1B [3,5]). Furthermore, RM increases the abundance and length of myelin internodes, as well as the expression of myelin proteins (Chapter 3) (Fig. 6-1B [7]). The improvement in myelination was observed for early and late treatment paradigms in both disease models. These results signify that the beneficial effect of autophagy on myelination, similar to that of the chaperone pathway, overlaps among distinct genetic models of PMP22 neuropathies. Abolishment of the improvement in myelination by lentivirus-mediated knockdown of the autophagy-related gene 12 (*Atg12*) in the TrJ model further reinstates the fact that autophagic activity is critical for the observed benefits. Together, these results support the potential use of RM and other autophagy-enhancing compounds as therapeutic agents for PMP22-associated demyelinating neuropathies and necessitate the testing of

RM *in vivo* in the mouse models. In all of the studies in Chapter 2 and 3, late treatment with chaperone- or autophagy-inducing compounds was consistently better in improving myelination compared to early treatment, *in vitro*. The fact that pharmacological activation of chaperones and autophagy independently improves myelination in C22 and TrJ models (Chapters 2 and 3) prompts us to test whether combined treatment of these pathway activators would be additive for improvement in myelination.

The commonality between the C22 and TrJ mouse models is the misfolding of PMP22 associated with accumulation of pUb substrates (Fig. 6-1A [2]). Protein aggregates could interfere with essential cellular functions, such as myelination in the case of SCs (Fig. 6-1A [4]). Myelination is a highly energy- and quality control-demanding process that requires massive synthesis and processing of myelin proteins by SCs (D'Antonio et al., 2009). Hence it is not surprising that a defect in the trafficking of one extremely hydrophobic glycoprotein, namely PMP22, would affect the expression and trafficking of other myelin proteins such as P0 and MBP, in our mouse models. Furthermore, in addition to endogenous activation of chaperones and autophagy (Fortun et al., 2003; Fortun et al., 2006), the quality control mechanism that is commonly affected in these two models is the proteasomal machinery (Fortun et al., 2005; Fortun et al., 2006) (Fig. 6-1A [3]) which is the major pathway for turn-over of myelin proteins such as PMP22 (Pareek et al., 1997) and MBP (Akaishi et al., 1996). Intriguingly, MBP is one of the unrelated proteasome substrates that is trapped in with the PMP22 inclusions in nerves of neuropathic mice (Fortun et al., 2005) (Fig. 6-1A [2]). On the otherhand, P0 is thought to be turned-over by the endosomal-lysosomal pathway (Yin et al., 2000). There is an emerging body of evidence for the cross-talk

between these quality control pathways (Ryhanen et al., 2009). When inefficiency in one pathway occurs, activation of another pathway has the capacity to protect the overall proteostatic balance of the system (Ryhanen et al., 2009). In our studies, activation of chaperones (Chapter 2) and autophagy (Chapter 3) independently show reduction in pUb substrates in SCs from both neuropathic models (Fig. 6-B [4]). Due to limited samples, we could not directly measure the proteasomal activitiy in these studies (Chapters 2 and 3). However, accumulation of pUb substrates has been previously shown to correlate with impaired proteasome activity (Fortun et al., 2005; Fortun et al., 2006) (Fig. 6-1A [3]). Hence, the reduction in the accumulation of pUb substrates achieved by activating chaperones and autophagy in this study (Chapter 2 and 3; also see Chapter 5) (Fig. 6-1B [4]) likely reflects the alleviation of the burden on the proteasomal pathway (Fortun et al., 2005; Fortun et al., 2006) (Fig. 6-1B [6]). Such a restoration of protein homeostasis would possibly provide a more conducive environment for improvement in PMP22 processing and myelination by SCs from neuropathic mice (Fig. 6-1B [5,7]). In addition to the improved protein expression and trafficking of our protein of interest, PMP22, the total levels of other myelin proteins namely P0 and MBP improved as well, leading to an overall increase in myelination. This result could be explained by taking into account of the facts that *P0* and *MBP* genes are coexpressed with *PMP22* in myelinating SCs (Kuhn et al., 1993) and at the protein level, PMP22 and P0 are coregulated (Hagedorn et al., 1999; Notterpek et al., 1999a) and they interact (D'Urso et al., 1999; Hasse et al., 2004). Hence, the improvement in PMP22 processing by chaperones (Chapter 2) and autophagy (Chapter

3) most likely contributed to the concomitant increase in the protein expression of its associated partners, P0 and MBP, in the both C22 and TrJ neuropathic samples.

The onset of CMT1A in humans is ~35 years and is progressive with age (Shy et al., 2008; Verhamme et al., 2009a) (Fig. 6-1A). The big question remains, as to why, a person born with a defective *PMP22* gene manifests disease symptoms only after ~35 years. To address whether normal aging contributes to the onset and disease progression of CMT1A, we focused on the molecular changes in quality control pathways in the PNS with normal aging (Chapter 4 and 5). The responsiveness of SCs isolated from aged nerves to stress stimuli such as HS and starvation is weakened (Chapter 4), likely accounting for the observed accrual of damaged molecules including pUb substrates in sciatic nerves with age (Chapter 5) (Fig. 6-1A [2]). The defective chaperone, autophagy (Chapter 4) and proteasomal pathways (Chapter 5) in the nerves of aged rats, is associated with a loss of myelination, degeneration of axons, and drastic expansion of ion channels at the nodes of Ranvier (Chapter 4) (Fig. 6-1A [4,5,6]). These results indicate that age is possibly a contributing factor in peripheral neuropathies.

We employed a well-defined diet restriction method namely life-long CR, known to slow the aging process and activate chaperone and autophagy pathways in many organ systems (Heydari et al., 1993; Bergamini et al., 2003; Selsby et al., 2005; Wohlgemuth et al., 2007), to determine its influence on the peripheral nerves (Chapter 4) (Fig. 6-1B [1,3]). Age-associated reduction in the expression of the major myelin proteins, neurofilaments and widening of the nodes of Ranvier are attenuated by the dietary intervention, which is paralleled with the maintenance of a differentiated SC phenotype (Fig. 6-1B [7,8,9]). Notably, the improvement in nerve architecture with diet restriction

are underlined by sustained expression of protein chaperones and markers of the autophagy-lysosomal pathway (Fig. 6-1B [1,3,9]) similar to the other studies (Heydari et al., 1996; Bergamini et al., 2003; Selsby et al., 2005; Wohlgemuth et al., 2007) in other organ systems as well. In an independent study from our lab, an intermittent fasting diet is able to activate chaperones and autophagy, decrease pUb substrates, improve myelination and alleviate neuropathic behavioural phenotype (Madorsky et al., 2009). Together, the *in vitro* and *in vivo* results in Chapter 4 suggest that there might be an age-limit by which dietary intervention or a similarly effective pharmacological intervention needs to be initiated to elicit a beneficial response on peripheral nerve health, in the context of aging and disease (Fig. 6-1B).

In addition to the myelin and protein quality control pathway defects, normal aging is associated with oxidative damage in the PNS (Chapter 5). The age-related alterations in cellular protein homeostatic mechanisms (Chapter 4) likely lead to a build-up of oxidatively-modified damaged proteins with age, which is associated with the conglomeration of distended lysosomes and lipofuscin adducts. These results underscore the close relationship with which these pathways function (Chapter 5). The occurrence of these detrimental structures is notably less frequent within nerves of age-matched rodents kept on a life-long reduced calorie diet, likely by reducing the accumulation of damage buildup or by a sustained activation of protein quality control pathways. Myelination is a highly energy-demanding process that likely becomes less efficient due to oxidative damage. CMT1A is an age-related disease and oxidative stress is known to take place with age in a variety of organ systems (Bokov et al., 2004). There are currently no reports about oxidative damage in neuropathic mouse

models and human patients. Little is known about the involvement of oxidative stress with disease progression in CMT1A. Although, the antioxidant ascorbic acid has been tried as a therapeutic intervention for CMT1A neuropathies (Pareyson et al., 2006; Verhamme et al., 2009b). We looked at the oxidative stress pathway with aging in the PNS, since a major effort in the development of therapeutics for CMT1A, in the past 5 years, was turning towards administration of ascorbic acid, an antioxidant (Pareyson et al., 2006; Micallef et al., 2009). The results from Chapter 6 show that there is significant oxidative damage to axonal and glial proteins of sciatic nerves with age (Fig. 6-1A). Restricting diet by life-long CR is able to alleviate the age-related oxidative damage. Clinical studies with ascorbic acid that showed promise in rodent models did not yield positive results in human trials (Micallef et al., 2009). It is possible that a combined pharmacological treatment that can activate more than one quality control pathway and simultaneously alleviate oxidative damage to mimick diet restriction will be cumulatively beneficial for myelin improvement and associated defects for the disease in humans (Fig. 6-1B).

In CMT1A disease, dedifferentiation of SCs, aberrant expression and reorganization of axonal ion channels, pronounced damage to axonal cytoskeleton and transport as well as recruitment of macrophages have been reported (Kohl et al., ; Kohl et al., ; Maier et al., 2002; Misko et al., 2002; Devaux and Scherer, 2005; Martini et al., 2008) and similar changes have been documented with normal aging in this study (Chapter 4 and 5) (Fig. 6-1A [5,6,7]). Strikingly, food restriction is able to attenuate all of the above mentioned deleterious processes with age (Fig. 6-1B [8,9,10]). In the human disease as well as in CMT1A mouse models, macrophages have been shown to be the

primary immune cell type exacerbating the disease (Kohl et al., ; Hartung et al., 1992; Misko et al., 2002). They are likely activated and recruited due to the degenerating myelin fragments. With CR, prevention of the age-related degeneration of myelin sheaths due to sustained chaperone, autophagy and proteasomal pathways, as well as minimal oxidative damage, likely leads to decline in macrophage recruitment (Fig. 6-1B [1,3,6]). Since CMT1A disease has an immune component, RM which is an FDA-approved immunosuppressant is expected to provide additional benefits for curtailing the macrophage cell infiltration. Also, a recent study shows that RM extends lifespan of aged mice and this could offer further advantage in the treatment of neuropathy without toxic side effects (Harrison et al., 2009).

In CMT1A, the early disease manifestations include muscle loss, weakening of extremities and reduction in nerve conduction velocity (Verhamme et al., 2009a). These disease characteristics are replicated by neuropathic mice as well (Huxley et al., 1996; Huxley et al., 1998; Notterpek and Tolwani, 1999). In order to analyze the disease progression with aging in humans, a 5-year-long study has recently been completed with adult CMT1A patients (*PMP22* gene duplication) and age-matched controls (Verhamme et al., 2009a). The results of this study show that there is significant physical disability in CMT1A patients but not in controls over the 5-year period, as expected (Fig. 6-1A [8]). However, decline in nerve conduction velocity and muscle strength is detected even in control subjects with normal aging (mean age, 40 years; median age, 25-65 years; n=26) and is at a similar rate compared to patients (mean age, 41 years; median age, 17-69 years; n=44) (Verhamme et al., 2009a). Hence, it is possible that the reduction in nerve conduction velocity and muscle strength with normal

aging (Verhamme et al., 2009a) combined with the decline in functional glial and axonal proteins and the accumulation of damaged proteins with age seen in our study (Chapters 4 and 5) together become additive for the progression of the neuropathy. Thus, the physical diability seen in CMT1A patients seems to be a combination of having a defective *PMP22* gene and the events triggered by normal aging (Fig. 6-1A [8]). Studies from our collaborators (Marzetti et al., 2008; Xu et al., 2008) as well as our correlation studies (Chapter 4) indicate a significant decline in forelimb grip strength with age which is a measure of muscle strength (Xu et al., 2008). This result in our rodent study, with normal aging, is comparable to the decline in muscle strength observed in the human study (Verhamme et al., 2009a). Significantly, a CR diet that is able to minimize aberrant changes in quality control pathways (Chapters 4 and 5) correlates with maintenance of grip strength (Fig. 6-1B [11]) in age-matched rodents (Chapter 4; also see (Xu et al., 2008)). Thus, there is evidence from humans as well as from rodent studies that normal aging contributes to the progressive nature of this disease to a considerable extent. This could explain why the onset of the disease takes place after the individuals with the disease mutations have lived asymptomatic upto mid-life.

Together, these studies described in this dissertation support our hypothesis that, activating quality control pathways such as HSR and autophagy by pharmacological or dietary means is indeed beneficial for the processing of PMP22 and associated myelin proteins. Overall, activating protein homeostatic pathways has the ability to improve myelination in the context of disease and aging (Fig. 6-1B), which shows great potential for therapeutic benefits for a neurodegenerative disease such as CMT1A. Although, it is hard to decipher the specific sequence of events through which CR thwarts age-related

changes in quality control mechanisms, the results in Chapter 4 and 5 show that dietary restriction is an efficient means of defying age-related oxidative damage and maintaining a younger-state in peripheral nerves. As a matter of fact, it becomes a “chicken-or-the-egg” question of whether sustained activation of quality control pathways by CR prevents damaged protein accumulation or a decrease in accumulation of undesirably modified proteins with CR leads to better functioning of the proteostatic mechanisms. Either way, the end result of CR is the maintenance of myelinated phenotype and better nerve health. Since adverse dietary means such as intermittent feeding and calorie reduction might not be suitable therapeutic options in humans, the pharmacological approaches described in Chapters 2 and 3 are desirable.

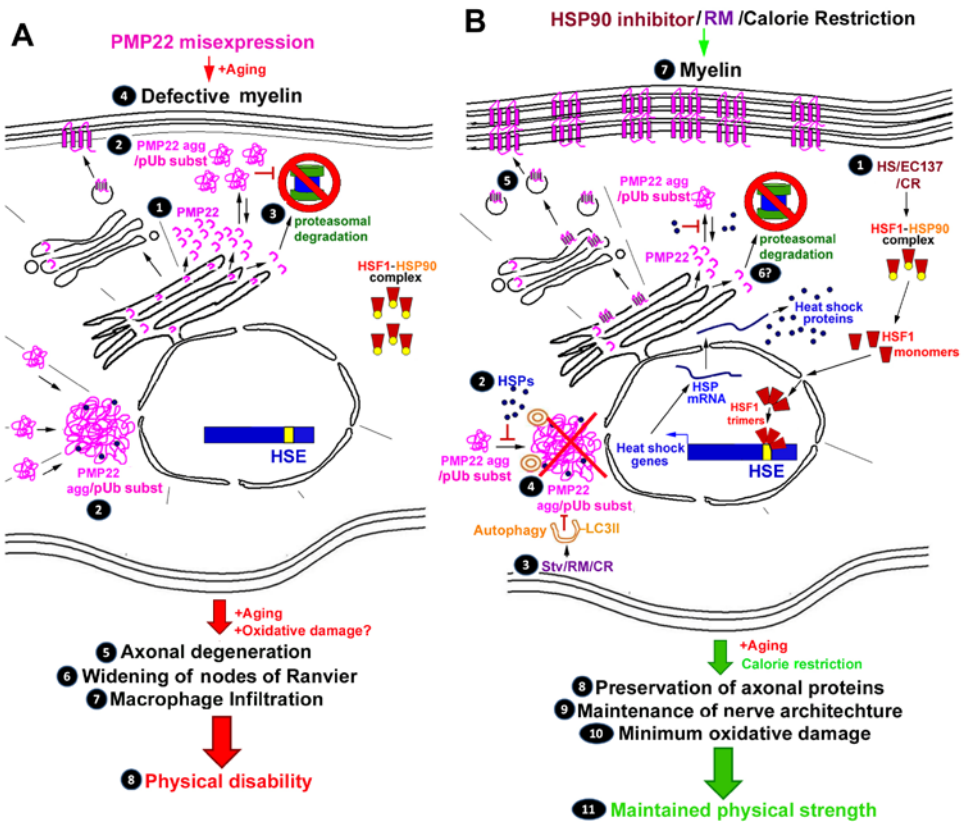

Figure 6-1. Working model: Quality control mechanisms with disease and age in the PNS. (A) In SCs from animals with disease mutation or normal aging [1], there is an accumulation of PMP22 aggregates (PMP22 agg) and pUb substrates (pUb subst) [2], respectively. This is associated with an impairment of protein degradation by the proteasome [3]. As a result, the trafficking of PMP22 as well as other myelin proteins to the plasma membrane is affected, leading to defects in myelination [4]. With disease and aging, myelination decreases and correspondingly axonal degeneration [5], widening of nodes of Ranvier [6] and macrophage infiltration [7] take place. In normal aging, oxidative damage has a contributing role to these deleterious processes. Together, these events lead to physical disability with disease and age [8]. (B) Exposure of SCs to HSP90 inhibitor/RM/CR promotes the sustained activation of the chaperone [1, 2] and autophagy [3] pathways. The induction of these protein homeostatic pathways by pharmacological or dietary means prevent the aggregation of damaged pUb substrates [4] and subsequently promote the correct processing and trafficking of PMP22 [5], as well as other myelin proteins [7]. Restoration of subcellular proteostasis with CR diet improves myelin formation [7] along with preservation of axonal proteins including neurofilaments and channel proteins [8] and maintenance of nerve architechture and differentiated SC phenotype [9]. These improvements are are associated with minimum oxidative damage in the normal aging process [10]. These beneficial effects likely lead to a maintained physical strength [11].

LIST OF REFERENCES

Adams S, Green P, Claxton R, Simcox S, Williams MV, Walsh K, Leeuwenburgh C (2001) Reactive carbonyl formation by oxidative and non-oxidative pathways. Front Biosci 6:A17-24.

Adinolfi AM, Yamuy J, Morales FR, Chase MH (1991) Segmental demyelination in peripheral nerves of old cats. Neurobiol Aging 12:175-179.

Adlkofer K, Naef R, Suter U (1997a) Analysis of compound heterozygous mice reveals that the Trembler mutation can behave as a gain-of-function allele. J Neurosci Res 49:671-680.

Adlkofer K, Martini R, Aguzzi A, Zielasek J, Toyka KV, Suter U (1995) Hypermyelination and demyelinating peripheral neuropathy in Pmp22-deficient mice. Nat Genet 11:274-280.

Adlkofer K, Frei R, Neuberg DH, Zielasek J, Toyka KV, Suter U (1997b) Heterozygous peripheral myelin protein 22-deficient mice are affected by a progressive demyelinating tomaculous neuropathy. J Neurosci 17:4662-4671.

Agarwal S, Sohal RS (1994) DNA oxidative damage and life expectancy in houseflies. Proc Natl Acad Sci U S A 91:12332-12335.

Akaishi T, Shiomi T, Sawada H, Yokosawa H (1996) Purification and properties of the 26S proteasome from the rat brain: evidence for its degradation of myelin basic protein in a ubiquitin-dependent manner. Brain Res 722:139-144.

Amaral MD, Kunzelmann K (2007) Molecular targeting of CFTR as a therapeutic approach to cystic fibrosis. Trends Pharmacol Sci 28:334-341.

Amici SA, Dunn WA, Jr., Notterpek L (2007) Developmental abnormalities in the nerves of peripheral myelin protein 22-deficient mice. J Neurosci Res 85:238-249.

Amici SA, Dunn WA, Jr., Murphy AJ, Adams NC, Gale NW, Valenzuela DM, Yancopoulos GD, Notterpek L (2006) Peripheral myelin protein 22 is in complex with alpha6beta4 integrin, and its absence alters the Schwann cell basal lamina. J Neurosci 26:1179-1189.

Andorfer B, Kieseier BC, Mathey E, Armati P, Pollard J, Oka N, Hartung HP (2001) Expression and distribution of transcription factor NF-kappaB and inhibitor IkappaB in the inflamed peripheral nervous system. J Neuroimmunol 116:226-232.

Aquino DA, Peng D, Lopez C, Farooq M (1998) The constitutive heat shock protein-70 is required for optimal expression of myelin basic protein during differentiation of oligodendrocytes. Neurochem Res 23:413-420.

Archelos JJ, Roggenbuck K, Schneider-Schaulies J, Toyka KV, Hartung HP (1993a) Detection and quantification of antibodies to the extracellular domain of P0 during experimental allergic neuritis. J Neurol Sci 117:197-205.

Archelos JJ, Roggenbuck K, Schneider-Schaulies J, Linington C, Toyka KV, Hartung HP (1993b) Production and characterization of monoclonal antibodies to the extracellular domain of P0. J Neurosci Res 35:46-53.

Auluck PK, Bonini NM (2002) Pharmacological prevention of Parkinson disease in Drosophila. Nat Med 8:1185-1186.

Auluck PK, Chan HY, Trojanowski JQ, Lee VM, Bonini NM (2002) Chaperone suppression of alpha-synuclein toxicity in a Drosophila model for Parkinson's disease. Science 295:865-868.

Baechner D, Liehr T, Hameister H, Altenberger H, Grehl H, Suter U, Rautenstrauss B (1995) Widespread expression of the peripheral myelin protein-22 gene (PMP22) in neural and non-neural tissues during murine development. J Neurosci Res 42:733-741.

Ballinger CA, Connell P, Wu Y, Hu Z, Thompson LJ, Yin LY, Patterson C (1999) Identification of CHIP, a novel tetratricopeptide repeat-containing protein that interacts with heat shock proteins and negatively regulates chaperone functions. Mol Cell Biol 19:4535-4545.

Beal MF (2002) Oxidatively modified proteins in aging and disease. Free Radic Biol Med 32:797-803.

Beckman KB, Ames BN (1998) The free radical theory of aging matures. Physiol Rev 78:547-581.

Bence NF, Sampat RM, Kopito RR (2001) Impairment of the ubiquitin-proteasome system by protein aggregation. Science 292:1552-1555.

Benz I, Beck W, Kraas W, Stoll D, Jung G, Kohlhardt M (1997) Two types of modified cardiac Na+ channels after cytosolic interventions at the alpha-subunit capable of removing Na+ inactivation. Eur Biophys J 25:189-200.

Bergamini E, Cavallini G, Donati A, Gori Z (2003) The anti-ageing effects of caloric restriction may involve stimulation of macroautophagy and lysosomal degradation, and can be intensified pharmacologically. Biomed Pharmacother 57:203-208.

Bergamini E, Cavallini G, Donati A, Gori Z (2004) The role of macroautophagy in the ageing process, anti-ageing intervention and age-associated diseases. Int J Biochem Cell Biol 36:2392-2404.

Blair IA (2001) Lipid hydroperoxide-mediated DNA damage. Exp Gerontol 36:1473-1481.

Blommaart EF, Luiken JJ, Blommaart PJ, van Woerkom GM, Meijer AJ (1995) Phosphorylation of ribosomal protein S6 is inhibitory for autophagy in isolated rat hepatocytes. J Biol Chem 270:2320-2326.

Boerkoel CF, Takashima H, Garcia CA, Olney RK, Johnson J, Berry K, Russo P, Kennedy S, Teebi AS, Scavina M, Williams LL, Mancias P, Butler IJ, Krajewski K, Shy M, Lupski JR (2002) Charcot-Marie-Tooth disease and related neuropathies: mutation distribution and genotype-phenotype correlation. Ann Neurol 51:190-201.

Bokov A, Chaudhuri A, Richardson A (2004) The role of oxidative damage and stress in aging. Mech Ageing Dev 125:811-826.

Bolis A, Coviello S, Visigalli I, Taveggia C, Bachi A, Chishti AH, Hanada T, Quattrini A, Previtali SC, Biffi A, Bolino A (2009) Dlg1, Sec8, and Mtmr2 regulate membrane homeostasis in Schwann cell myelination. J Neurosci 29:8858-8870.

Bosse F, Brodbeck J, Muller HW (1999) Post-transcriptional regulation of the peripheral myelin protein gene PMP22/gas3. J Neurosci Res 55:164-177.

Bosse F, Zoidl G, Wilms S, Gillen CP, Kuhn HG, Muller HW (1994) Differential expression of two mRNA species indicates a dual function of peripheral myelin protein PMP22 in cell growth and myelination. J Neurosci Res 37:529-537.

Boulton M, Rozanowska M, Rozanowski B, Wess T (2004) The photoreactivity of ocular lipofuscin. Photochem Photobiol Sci 3:759-764.

Brancolini C, Edomi P, Marzinotto S, Schneider C (2000) Exposure at the cell surface is required for gas3/PMP22 To regulate both cell death and cell spreading: implication for the Charcot-Marie-Tooth type 1A and Dejerine-Sottas diseases. Mol Biol Cell 11:2901-2914.

Brancolini C, Marzinotto S, Edomi P, Agostoni E, Fiorentini C, Muller HW, Schneider C (1999) Rho-dependent regulation of cell spreading by the tetraspan membrane protein Gas3/PMP22. Mol Biol Cell 10:2441-2459.

Broadley SA, Hartl FU (2009) The role of molecular chaperones in human misfolding diseases. FEBS Lett 583:2647-2653.

Brunk UT, Terman A (2002) The mitochondrial-lysosomal axis theory of aging: accumulation of damaged mitochondria as a result of imperfect autophagocytosis. Eur J Biochem 269:1996-2002.

Bruunsgaard H (2006) The clinical impact of systemic low-level inflammation in elderly populations. With special reference to cardiovascular disease, dementia and mortality. Dan Med Bull 53:285-309.

Bunge RP, Bunge MB, Bates M (1989) Movements of the Schwann cell nucleus implicate progression of the inner (axon-related) Schwann cell process during myelination. J Cell Biol 109:273-284.

Byun Y, Chen F, Chang R, Trivedi M, Green KJ, Cryns VL (2001) Caspase cleavage of vimentin disrupts intermediate filaments and promotes apoptosis. Cell Death Differ 8:443-450.

Calabrese V, Scapagnini G, Ravagna A, Colombrita C, Spadaro F, Butterfield DA, Giuffrida Stella AM (2004) Increased expression of heat shock proteins in rat brain during aging: relationship with mitochondrial function and glutathione redox state. Mech Ageing Dev 125:325-335.

Carey DJ, Todd MS, Rafferty CM (1986) Schwann cell myelination: induction by exogenous basement membrane-like extracellular matrix. J Cell Biol 102:2254-2263.

Ceballos D, Cuadras J, Verdu E, Navarro X (1999) Morphometric and ultrastructural changes with ageing in mouse peripheral nerve. J Anat 195 (Pt 4):563-576.

Chance PF (1999) Overview of hereditary neuropathy with liability to pressure palsies. Ann N Y Acad Sci 883:14-21.

Chance PF, Alderson MK, Leppig KA, Lensch MW, Matsunami N, Smith B, Swanson PD, Odelberg SJ, Disteche CM, Bird TD (1993) DNA deletion associated with hereditary neuropathy with liability to pressure palsies. Cell 72:143-151.

Chandrasekar B, Freeman GL (1997) Induction of nuclear factor kappaB and activation protein 1 in postischemic myocardium. FEBS Lett 401:30-34.

Chies R, Nobbio L, Edomi P, Schenone A, Schneider C, Brancolini C (2003) Alterations in the Arf6-regulated plasma membrane endosomal recycling pathway in cells overexpressing the tetraspan protein Gas3/PMP22. J Cell Sci 116:987-999.

Chung HY, Cesari M, Anton S, Marzetti E, Giovannini S, Seo AY, Carter C, Yu BP, Leeuwenburgh C (2009) Molecular inflammation: underpinnings of aging and age-related diseases. Ageing Res Rev 8:18-30.

Colby J, Nicholson R, Dickson KM, Orfali W, Naef R, Suter U, Snipes GJ (2000) PMP22 carrying the trembler or trembler-J mutation is intracellularly retained in myelinating Schwann cells. Neurobiol Dis 7:561-573.

Corboy MJ, Thomas PJ, Wigley WC (2005) Aggresome formation. Methods Mol Biol 301:305-327.

Cosgaya JM, Chan JR, Shooter EM (2002) The neurotrophin receptor p75NTR as a positive modulator of myelination. Science 298:1245-1248.

Cristofalo VJ, Lorenzini A, Allen RG, Torres C, Tresini M (2004) Replicative senescence: a critical review. Mech Ageing Dev 125:827-848.

Cuervo AM, Bergamini E, Brunk UT, Droge W, Ffrench M, Terman A (2005) Autophagy and aging: the importance of maintaining "clean" cells. Autophagy 1:131-140.

D'Antonio M, Feltri ML, Wrabetz L (2009) Myelin under stress. J Neurosci Res 87:3241-3249.

D'Urso D, Ehrhardt P, Muller HW (1999) Peripheral myelin protein 22 and protein zero: a novel association in peripheral nervous system myelin. J Neurosci 19:3396-3403.

D'Urso D, Prior R, Greiner-Petter R, Gabreels-Festen AA, Muller HW (1998) Overloaded endoplasmic reticulum-Golgi compartments, a possible pathomechanism of peripheral neuropathies caused by mutations of the peripheral myelin protein PMP22. J Neurosci 18:731-740.

Davies KJ (2001) Degradation of oxidized proteins by the 20S proteasome. Biochimie 83:301-310.

Dello Russo C, Polak PE, Mercado PR, Spagnolo A, Sharp A, Murphy P, Kamal A, Burrows FJ, Fritz LC, Feinstein DL (2006) The heat-shock protein 90 inhibitor 17-allylamino-17-demethoxygeldanamycin suppresses glial inflammatory responses and ameliorates experimental autoimmune encephalomyelitis. J Neurochem 99:1351-1362.

Devaux JJ, Scherer SS (2005) Altered ion channels in an animal model of Charcot-Marie-Tooth disease type IA. J Neurosci 25:1470-1480.

Dickey CA, Eriksen J, Kamal A, Burrows F, Kasibhatla S, Eckman CB, Hutton M, Petrucelli L (2005) Development of a high throughput drug screening assay for the detection of changes in tau levels -- proof of concept with HSP90 inhibitors. Curr Alzheimer Res 2:231-238.

Dickey CA, Dunmore J, Lu B, Wang JW, Lee WC, Kamal A, Burrows F, Eckman C, Hutton M, Petrucelli L (2006) HSP induction mediates selective clearance of tau phosphorylated at proline-directed Ser/Thr sites but not KXGS (MARK) sites. Faseb J 20:753-755.

Dickey CA, Kamal A, Lundgren K, Klosak N, Bailey RM, Dunmore J, Ash P, Shoraka S, Zlatkovic J, Eckman CB, Patterson C, Dickson DW, Nahman NS, Jr., Hutton M, Burrows F, Petrucelli L (2007) The high-affinity HSP90-CHIP complex recognizes and selectively degrades phosphorylated tau client proteins. J Clin Invest 117:648-658.

Dickson KM, Bergeron JJ, Shames I, Colby J, Nguyen DT, Chevet E, Thomas DY, Snipes GJ (2002) Association of calnexin with mutant peripheral myelin protein-22 ex vivo: a basis for "gain-of-function" ER diseases. Proc Natl Acad Sci U S A 99:9852-9857.

Ding WX, Ni HM, Gao W, Yoshimori T, Stolz DB, Ron D, Yin XM (2007) Linking of autophagy to ubiquitin-proteasome system is important for the regulation of endoplasmic reticulum stress and cell viability. Am J Pathol 171:513-524.

Dreux M, Gastaminza P, Wieland SF, Chisari FV (2009) The autophagy machinery is required to initiate hepatitis C virus replication. Proc Natl Acad Sci U S A 106:14046-14051.

Dunn WA, Jr. (1990) Studies on the mechanisms of autophagy: maturation of the autophagic vacuole. J Cell Biol 110:1935-1945.

Einheber S, Milner TA, Giancotti F, Salzer JL (1993) Axonal regulation of Schwann cell integrin expression suggests a role for alpha 6 beta 4 in myelination. J Cell Biol 123:1223-1236.

Eldridge CF, Bunge MB, Bunge RP, Wood PM (1987) Differentiation of axon-related Schwann cells in vitro. I. Ascorbic acid regulates basal lamina assembly and myelin formation. J Cell Biol 105:1023-1034.

Everitt AV, Hilmer SN, Brand-Miller JC, Jamieson HA, Truswell AS, Sharma AP, Mason RS, Morris BJ, Le Couteur DG (2006) Dietary approaches that delay age-related diseases. Clin Interv Aging 1:11-31.

Fabbretti E, Edomi P, Brancolini C, Schneider C (1995) Apoptotic phenotype induced by overexpression of wild-type gas3/PMP22: its relation to the demyelinating peripheral neuropathy CMT1A. Genes Dev 9:1846-1856.

Farinha CM, Nogueira P, Mendes F, Penque D, Amaral MD (2002) The human DnaJ homologue (Hdj)-1/heat-shock protein (Hsp) 40 co-chaperone is required for the in vivo stabilization of the cystic fibrosis transmembrane conductance regulator by Hsp70. Biochem J 366:797-806.

Farout L, Friguet B (2006) Proteasome function in aging and oxidative stress: implications in protein maintenance failure. Antioxid Redox Signal 8:205-216.

Feuers RJ, Duffy PH, Leakey JA, Turturro A, Mittelstaedt RA, Hart RW (1989) Effect of chronic caloric restriction on hepatic enzymes of intermediary metabolism in the male Fischer 344 rat. Mech Ageing Dev 48:179-189.

Filbin MT, Walsh FS, Trapp BD, Pizzey JA, Tennekoon GI (1990) Role of myelin P0 protein as a homophilic adhesion molecule. Nature 344:871-872.

Fontanini A, Chies R, Snapp EL, Ferrarini M, Fabrizi GM, Brancolini C (2005) Glycan-independent role of calnexin in the intracellular retention of Charcot-Marie-tooth 1A Gas3/PMP22 mutants. J Biol Chem 280:2378-2387.

Fortun J, Dunn WA, Jr., Joy S, Li J, Notterpek L (2003) Emerging role for autophagy in the removal of aggresomes in Schwann cells. J Neurosci 23:10672-10680.

Fortun J, Li J, Go J, Fenstermaker A, Fletcher BS, Notterpek L (2005) Impaired proteasome activity and accumulation of ubiquitinated substrates in a hereditary neuropathy model. J Neurochem 92:1531-1541.

Fortun J, Go JC, Li J, Amici SA, Dunn WA, Jr., Notterpek L (2006) Alterations in degradative pathways and protein aggregation in a neuropathy model based on PMP22 overexpression. Neurobiol Dis 22:153-164.

Fortun J, Verrier JD, Go JC, Madorsky I, Dunn WA, Notterpek L (2007) The formation of peripheral myelin protein 22 aggregates is hindered by the enhancement of autophagy and expression of cytoplasmic chaperones. Neurobiol Dis 25:252-265.

Fruttiger M, Montag D, Schachner M, Martini R (1995) Crucial role for the myelin-associated glycoprotein in the maintenance of axon-myelin integrity. Eur J Neurosci 7:511-515.

Frydman J (2001) Folding of newly translated proteins in vivo: the role of molecular chaperones. Annu Rev Biochem 70:603-647.

Fusek M, Vetvicka V (2005) Dual role of cathepsin D: ligand and protease. Biomed Pap Med Fac Univ Palacky Olomouc Czech Repub 149:43-50.

Gabreels-Festen A, Wetering RV (1999) Human nerve pathology caused by different mutational mechanisms of the PMP22 gene. Ann N Y Acad Sci 883:336-343.

Gabreels-Festen AA, Bolhuis PA, Hoogendijk JE, Valentijn LJ, Eshuis EJ, Gabreels FJ (1995) Charcot-Marie-Tooth disease type 1A: morphological phenotype of the 17p duplication versus PMP22 point mutations. Acta Neuropathol 90:645-649.

Gabriel JM, Erne B, Pareyson D, Sghirlanzoni A, Taroni F, Steck AJ (1997) Gene dosage effects in hereditary peripheral neuropathy. Expression of peripheral myelin protein 22 in Charcot-Marie-Tooth disease type 1A and hereditary neuropathy with liability to pressure palsies nerve biopsies. Neurology 49:1635-1640.

Garbay B, Heape AM, Sargueil F, Cassagne C (2000) Myelin synthesis in the peripheral nervous system. Prog Neurobiol 61:267-304.

Gard AL, Solodushko VG, Waeg G, Majic T (2001) 4-Hydroxynonenal, a lipid peroxidation byproduct of spinal cord injury, is cytotoxic for oligodendrocyte progenitors and inhibits their responsiveness to PDGF. Microsc Res Tech 52:709-718.

Goldberg AL (2003) Protein degradation and protection against misfolded or damaged proteins. Nature 426:895-899.

Gregson NA, Hall SM (1973) A quantitative analysis of the effects of the intraneural injection of lysophosphatidyl choline. J Cell Sci 13:257-277.

Grover-Johnson N, Spencer PS (1981) Peripheral nerve abnormalities in aging rats. J Neuropathol Exp Neurol 40:155-165.

Grune T, Davies KJ (2003) The proteasomal system and HNE-modified proteins. Mol Aspects Med 24:195-204.

Grune T, Merker K, Sandig G, Davies KJ (2003) Selective degradation of oxidatively modified protein substrates by the proteasome. Biochem Biophys Res Commun 305:709-718.

Grune T, Jung T, Merker K, Davies KJ (2004) Decreased proteolysis caused by protein aggregates, inclusion bodies, plaques, lipofuscin, ceroid, and 'aggresomes' during oxidative stress, aging, and disease. Int J Biochem Cell Biol 36:2519-2530.

Grune T, Merker K, Jung T, Sitte N, Davies KJ (2005) Protein oxidation and degradation during postmitotic senescence. Free Radic Biol Med 39:1208-1215.

Hagedorn L, Suter U, Sommer L (1999) P0 and PMP22 mark a multipotent neural crest-derived cell type that displays community effects in response to TGF-beta family factors. Development 126:3781-3794.

Hanemann CO, D'Urso D, Gabreels-Festen AA, Muller HW (2000) Mutation-dependent alteration in cellular distribution of peripheral myelin protein 22 in nerve biopsies from Charcot-Marie-Tooth type 1A. Brain 123 (Pt 5):1001-1006.

Hanemann CO, Stoll G, D'Urso D, Fricke W, Martin JJ, Van Broeckhoven C, Mancardi GL, Bartke I, Muller HW (1994) Peripheral myelin protein-22 expression in Charcot-Marie-Tooth disease type 1a sural nerve biopsies. J Neurosci Res 37:654-659.

Haney C, Snipes GJ, Shooter EM, Suter U, Garcia C, Griffin JW, Trapp BD (1996) Ultrastructural distribution of PMP22 in Charcot-Marie-Tooth disease type 1A. J Neuropathol Exp Neurol 55:290-299.

Hara T, Nakamura K, Matsui M, Yamamoto A, Nakahara Y, Suzuki-Migishima R, Yokoyama M, Mishima K, Saito I, Okano H, Mizushima N (2006) Suppression of basal autophagy in neural cells causes neurodegenerative disease in mice. Nature 441:885-889.

Harrison DE, Strong R, Sharp ZD, Nelson JF, Astle CM, Flurkey K, Nadon NL, Wilkinson JE, Frenkel K, Carter CS, Pahor M, Javors MA, Fernandez E, Miller RA (2009) Rapamycin fed late in life extends lifespan in genetically heterogeneous mice. Nature 460:392-395.

Hartl FU (1996) Molecular chaperones in cellular protein folding. Nature 381:571-579.

Hartung HP, Jung S, Stoll G, Zielasek J, Schmidt B, Archelos JJ, Toyka KV (1992) Inflammatory mediators in demyelinating disorders of the CNS and PNS. J Neuroimmunol 40:197-210.

Hasse B, Bosse F, Hanenberg H, Muller HW (2004) Peripheral myelin protein 22 kDa and protein zero: domain specific trans-interactions. Mol Cell Neurosci 27:370-378.

Hay DG, Sathasivam K, Tobaben S, Stahl B, Marber M, Mestril R, Mahal A, Smith DL, Woodman B, Bates GP (2004) Progressive decrease in chaperone protein levels in a mouse model of Huntington's disease and induction of stress proteins as a therapeutic approach. Hum Mol Genet 13:1389-1405.

Heaton MB, Madorsky I, Paiva M, Siler-Marsiglio KI (2004) Vitamin E amelioration of ethanol neurotoxicity involves modulation of apoptotis-related protein levels in neonatal rat cerebellar granule cells. Brain Res Dev Brain Res 150:117-124.

Herbst M, Wanker EE (2007) Small molecule inducers of heat-shock response reduce polyQ-mediated huntingtin aggregation. A possible therapeutic strategy. Neurodegener Dis 4:254-260.

Heydari AR, Wu B, Takahashi R, Strong R, Richardson A (1993) Expression of heat shock protein 70 is altered by age and diet at the level of transcription. Mol Cell Biol 13:2909-2918.

Heydari AR, You S, Takahashi R, Gutsmann A, Sarge KD, Richardson A (1996) Effect of caloric restriction on the expression of heat shock protein 70 and the activation of heat shock transcription factor 1. Dev Genet 18:114-124.

Heydari AR, You S, Takahashi R, Gutsmann-Conrad A, Sarge KD, Richardson A (2000) Age-related alterations in the activation of heat shock transcription factor 1 in rat hepatocytes. Exp Cell Res 256:83-93.

Hinman JD, Peters A, Cabral H, Rosene DL, Hollander W, Rasband MN, Abraham CR (2006) Age-related molecular reorganization at the node of Ranvier. J Comp Neurol 495:351-362.

Homma S, Jin X, Wang G, Tu N, Min J, Yanasak N, Mivechi NF (2007) Demyelination, astrogliosis, and accumulation of ubiquitinated proteins, hallmarks of CNS disease in hsf1-deficient mice. J Neurosci 27:7974-7986.

Hori N, Hirotsu I, Davis PJ, Carpenter DO (1992) Long-term potentiation is lost in aged rats but preserved by calorie restriction. Neuroreport 3:1085-1088.

Huxley C, Passage E, Manson A, Putzu G, Figarella-Branger D, Pellissier JF, Fontes M (1996) Construction of a mouse model of Charcot-Marie-Tooth disease type 1A by pronuclear injection of human YAC DNA. Hum Mol Genet 5:563-569.

Huxley C, Passage E, Robertson AM, Youl B, Huston S, Manson A, Saberan-Djoniedi D, Figarella-Branger D, Pellissier JF, Thomas PK, Fontes M (1998) Correlation between varying levels of PMP22 expression and the degree of demyelination and reduction in nerve conduction velocity in transgenic mice. Hum Mol Genet 7:449-458.

Ingram DK, Young J, Mattison JA (2007) Calorie restriction in nonhuman primates: assessing effects on brain and behavioral aging. Neuroscience 145:1359-1364.

Inuzuka T, Quarles RH, Noronha AB, Dobersen MJ, Brady RO (1984) A human lymphocyte antigen is shared with a group of glycoproteins in peripheral nerve. Neurosci Lett 51:105-111.

Isaacs AM, Jeans A, Oliver PL, Vizor L, Brown SD, Hunter AJ, Davies KE (2002) Identification of a new Pmp22 mouse mutant and trafficking analysis of a Pmp22 allelic series suggesting that protein aggregates may be protective in Pmp22-associated peripheral neuropathy. Mol Cell Neurosci 21:114-125.

Iwata A, Riley BE, Johnston JA, Kopito RR (2005) HDAC6 and microtubules are required for autophagic degradation of aggregated huntingtin. J Biol Chem 280:40282-40292.

Jaeger PA, Wyss-Coray T (2009) All-you-can-eat: autophagy in neurodegeneration and neuroprotection. Mol Neurodegener 4:16.

Jessen KR, Mirsky R (2005) The origin and development of glial cells in peripheral nerves. Nat Rev Neurosci 6:671-682.

Jiang J, Ballinger CA, Wu Y, Dai Q, Cyr DM, Hohfeld J, Patterson C (2001) CHIP is a U-box-dependent E3 ubiquitin ligase: identification of Hsc70 as a target for ubiquitylation. J Biol Chem 276:42938-42944.

Johnson JB, Laub DR, John S (2006) The effect on health of alternate day calorie restriction: eating less and more than needed on alternate days prolongs life. Med Hypotheses 67:209-211.

Johnson JS, Roux KJ, Fletcher BS, Fortun J, Notterpek L (2005) Molecular alterations resulting from frameshift mutations in peripheral myelin protein 22: implications for neuropathy severity. J Neurosci Res 82:743-752.

Johnston JA, Ward CL, Kopito RR (1998) Aggresomes: a cellular response to misfolded proteins. J Cell Biol 143:1883-1898.

Jolly CA (2004) Dietary restriction and immune function. J Nutr 134:1853-1856.

Jung T, Bader N, Grune T (2007) Lipofuscin: formation, distribution, and metabolic consequences. Ann N Y Acad Sci 1119:97-111.

Kabeya Y, Mizushima N, Ueno T, Yamamoto A, Kirisako T, Noda T, Kominami E, Ohsumi Y, Yoshimori T (2000) LC3, a mammalian homologue of yeast Apg8p, is localized in autophagosome membranes after processing. Embo J 19:5720-5728.

Kahan BD (2008) Fifteen years of clinical studies and clinical practice in renal transplantation: reviewing outcomes with de novo use of sirolimus in combination with cyclosporine. Transplant Proc 40:S17-20.

Kalmar B, Greensmith L (2009) Induction of heat shock proteins for protection against oxidative stress. Adv Drug Deliv Rev 61:310-318.

Kamholz J, Awatramani R, Menichella D, Jiang H, Xu W, Shy M (1999) Regulation of myelin-specific gene expression. Relevance to CMT1. Ann N Y Acad Sci 883:91-108.

Karin M (2006) Role for IKK2 in muscle: waste not, want not. J Clin Invest 116:2866-2868.

Kazemi-Esfarjani P, Benzer S (2002) Suppression of polyglutamine toxicity by a Drosophila homolog of myeloid leukemia factor 1. Hum Mol Genet 11:2657-2672.

Keller JN, Dimayuga E, Chen Q, Thorpe J, Gee J, Ding Q (2004) Autophagy, proteasomes, lipofuscin, and oxidative stress in the aging brain. Int J Biochem Cell Biol 36:2376-2391.

Kim HJ, Yu BP, Chung HY (2002a) Molecular exploration of age-related NF-kappaB/IKK downregulation by calorie restriction in rat kidney. Free Radic Biol Med 32:991-1005.

Kim HR, Kang HS, Kim HD (1999) Geldanamycin induces heat shock protein expression through activation of HSF1 in K562 erythroleukemic cells. IUBMB Life 48:429-433.

Kim S, Nollen EA, Kitagawa K, Bindokas VP, Morimoto RI (2002b) Polyglutamine protein aggregates are dynamic. Nat Cell Biol 4:826-831.

Kincaid MM, Cooper AA (2007) ERADicate ER stress or die trying. Antioxid Redox Signal 9:2373-2387.

Klionsky DJ, Emr SD (2000) Autophagy as a regulated pathway of cellular degradation. Science 290:1717-1721.

Klionsky DJ, Meijer AJ, Codogno P (2005) Autophagy and p70S6 kinase. Autophagy 1:59-60; discussion 60-51.

Klionsky DJ, Abeliovich H, Agostinis P, Agrawal DK, Aliev G, Askew DS, Baba M, Baehrecke EH, Bahr BA, Ballabio A, Bamber BA, Bassham DC, Bergamini E, Bi X, Biard-Piechaczyk M, Blum JS, Bredesen DE, Brodsky JL, Brumell JH, Brunk UT, Bursch W, Camougrand N, Cebollero E, Cecconi F, Chen Y, Chin LS, Choi A, Chu CT, Chung J, Clarke PG, Clark RS, Clarke SG, Clave C, Cleveland JL, Codogno P, Colombo MI, Coto-Montes A, Cregg JM, Cuervo AM, Debnath J, Demarchi F, Dennis PB, Dennis PA, Deretic V, Devenish RJ, Di Sano F, Dice JF, Difiglia M, Dinesh-Kumar S, Distelhorst CW, Djavaheri-Mergny M, Dorsey FC, Droge W, Dron M, Dunn WA, Jr., Duszenko M, Eissa NT, Elazar Z, Esclatine A, Eskelinen EL, Fesus L, Finley KD, Fuentes JM, Fueyo J, Fujisaki K, Galliot B, Gao FB, Gewirtz DA, Gibson SB, Gohla A, Goldberg AL, Gonzalez R, Gonzalez-Estevez C, Gorski S, Gottlieb RA, Haussinger D, He YW, Heidenreich K, Hill JA, Hoyer-Hansen M, Hu X, Huang WP, Iwasaki A, Jaattela M, Jackson WT, Jiang X, Jin S, Johansen T, Jung JU, Kadowaki M, Kang C, Kelekar A, Kessel DH, Kiel JA, Kim HP, Kimchi A, Kinsella TJ, Kiselyov K, Kitamoto K, Knecht E, et al. (2008) Guidelines for the use and interpretation of assays for monitoring autophagy in higher eukaryotes. Autophagy 4:151-175.

Kohl B, Fischer S, Groh J, Wessig C, Martini R MCP-1/CCL2 Modifies Axon Properties in a PMP22-Overexpressing Mouse Model for Charcot-Marie-Tooth 1A Neuropathy. Am J Pathol 176:1390-1399.

Kohl B, Groh J, Wessig C, Wiendl H, Kroner A, Martini R Lack of evidence for a pathogenic role of T-lymphocytes in an animal model for Charcot-Marie-Tooth disease 1A. Neurobiol Dis 38:78-84.

Komatsu M, Waguri S, Chiba T, Murata S, Iwata J, Tanida I, Ueno T, Koike M, Uchiyama Y, Kominami E, Tanaka K (2006) Loss of autophagy in the central nervous system causes neurodegeneration in mice. Nature 441:880-884.

Komatsu M, Waguri S, Ueno T, Iwata J, Murata S, Tanida I, Ezaki J, Mizushima N, Ohsumi Y, Uchiyama Y, Kominami E, Tanaka K, Chiba T (2005) Impairment of starvation-induced and constitutive autophagy in Atg7-deficient mice. J Cell Biol 169:425-434.

Kopito RR (2000) Aggresomes, inclusion bodies and protein aggregation. Trends Cell Biol 10:524-530.

Kruse J, Keilhauer G, Faissner A, Timpl R, Schachner M (1985) The J1 glycoprotein--a novel nervous system cell adhesion molecule of the L2/HNK-1 family. Nature 316:146-148.

Kuhlenbaumer G, Young P, Hunermund G, Ringelstein B, Stogbauer F (2002) Clinical features and molecular genetics of hereditary peripheral neuropathies. J Neurol 249:1629-1650.

Kuhn G, Lie A, Wilms S, Muller HW (1993) Coexpression of PMP22 gene with MBP and P0 during de novo myelination and nerve repair. Glia 8:256-264.

Lambert AJ, Portero-Otin M, Pamplona R, Merry BJ (2004) Effect of ageing and caloric restriction on specific markers of protein oxidative damage and membrane peroxidizability in rat liver mitochondria. Mech Ageing Dev 125:529-538.

Levine RL, Stadtman ER (2001) Oxidative modification of proteins during aging. Exp Gerontol 36:1495-1502.

Li Y, Tennekoon GI, Birnbaum M, Marchionni MA, Rutkowski JL (2001) Neuregulin signaling through a PI3K/Akt/Bad pathway in Schwann cell survival. Mol Cell Neurosci 17:761-767.

Luders J, Demand J, Hohfeld J (2000) The ubiquitin-related BAG-1 provides a link between the molecular chaperones Hsc70/Hsp70 and the proteasome. J Biol Chem 275:4613-4617.

Lund BT, Chakryan Y, Ashikian N, Mnatsakanyan L, Bevan CJ, Aguilera R, Gallaher T, Jakowec MW (2006) Association of MBP peptides with Hsp70 in normal appearing human white matter. J Neurol Sci 249:122-134.

Lupski JR, de Oca-Luna RM, Slaugenhaupt S, Pentao L, Guzzetta V, Trask BJ, Saucedo-Cardenas O, Barker DF, Killian JM, Garcia CA, Chakravarti A, Patel PI (1991) DNA duplication associated with Charcot-Marie-Tooth disease type 1A. Cell 66:219-232.

Macario AJ, Conway de Macario E (2002) Sick chaperones and ageing: a perspective. Ageing Res Rev 1:295-311.

Madorsky I, Opalach K, Waber A, Verrier JD, Solmo C, Foster T, Dunn WA, Jr., Notterpek L (2009) Intermittent fasting alleviates the neuropathic phenotype in a mouse model of Charcot-Marie-Tooth disease. Neurobiol Dis 34:146-154.

Magyar JP, Martini R, Ruelicke T, Aguzzi A, Adlkofer K, Dembic Z, Zielasek J, Toyka KV, Suter U (1996) Impaired differentiation of Schwann cells in transgenic mice with increased PMP22 gene dosage. J Neurosci 16:5351-5360.

Maier M, Berger P, Suter U (2002) Understanding Schwann cell-neurone interactions: the key to Charcot-Marie-Tooth disease? J Anat 200:357-366.

Maiuri MC, Zalckvar E, Kimchi A, Kroemer G (2007) Self-eating and self-killing: crosstalk between autophagy and apoptosis. Nat Rev Mol Cell Biol 8:741-752.

Malagelada C, Jin ZH, Jackson-Lewis V, Przedborski S, Greene LA Rapamycin protects against neuron death in in vitro and in vivo models of Parkinson's disease. J Neurosci 30:1166-1175.

Martin B, Mattson MP, Maudsley S (2006) Caloric restriction and intermittent fasting: two potential diets for successful brain aging. Ageing Res Rev 5:332-353.

Martinez A, Portero-Otin M, Pamplona R, Ferrer I (2009) Protein Targets of Oxidative Damage in Human Neurodegenerative Diseases with Abnormal Protein Aggregates. Brain Pathol.

Martini R, Schachner M (1986) Immunoelectron microscopic localization of neural cell adhesion molecules (L1, N-CAM, and MAG) and their shared carbohydrate epitope and myelin basic protein in developing sciatic nerve. J Cell Biol 103:2439-2448.

Martini R, Fischer S, Lopez-Vales R, David S (2008) Interactions between Schwann cells and macrophages in injury and inherited demyelinating disease. Glia 56:1566-1577.

Martini R, Mohajeri MH, Kasper S, Giese KP, Schachner M (1995) Mice doubly deficient in the genes for P0 and myelin basic protein show that both proteins contribute to the formation of the major dense line in peripheral nerve myelin. J Neurosci 15:4488-4495.

Marzetti E, Lawler JM, Hiona A, Manini T, Seo AY, Leeuwenburgh C (2008) Modulation of age-induced apoptotic signaling and cellular remodeling by exercise and calorie restriction in skeletal muscle. Free Radic Biol Med 44:160-168.

Mattson MP, Magnus T (2006) Ageing and neuronal vulnerability. Nat Rev Neurosci 7:278-294.

Mattson MP, Duan W, Lee J, Guo Z (2001) Suppression of brain aging and neurodegenerative disorders by dietary restriction and environmental enrichment: molecular mechanisms. Mech Ageing Dev 122:757-778.

Maycox PR, Ortuno D, Burrola P, Kuhn R, Bieri PL, Arrezo JC, Lemke G (1997) A transgenic mouse model for human hereditary neuropathy with liability to pressure palsies. Mol Cell Neurosci 8:405-416.

McDonough H, Patterson C (2003) CHIP: a link between the chaperone and proteasome systems. Cell Stress Chaperones 8:303-308.

McGarry RC, Helfand SL, Quarles RH, Roder JC (1983) Recognition of myelin-associated glycoprotein by the monoclonal antibody HNK-1. Nature 306:376-378.

McKerracher L, David S, Jackson DL, Kottis V, Dunn RJ, Braun PE (1994) Identification of myelin-associated glycoprotein as a major myelin-derived inhibitor of neurite growth. Neuron 13:805-811.

McLean PJ, Klucken J, Shin Y, Hyman BT (2004) Geldanamycin induces Hsp70 and prevents alpha-synuclein aggregation and toxicity in vitro. Biochem Biophys Res Commun 321:665-669.

Meikle L, Pollizzi K, Egnor A, Kramvis I, Lane H, Sahin M, Kwiatkowski DJ (2008) Response of a neuronal model of tuberous sclerosis to mammalian target of rapamycin (mTOR) inhibitors: effects on mTORC1 and Akt signaling lead to improved survival and function. J Neurosci 28:5422-5432.

Melcangi RC, Magnaghi V, Martini L (2000) Aging in peripheral nerves: regulation of myelin protein genes by steroid hormones. Prog Neurobiol 60:291-308.

Melcangi RC, Magnaghi V, Cavarretta I, Zucchi I, Bovolin P, D'Urso D, Martini L (1999) Progesterone derivatives are able to influence peripheral myelin protein 22 and P0 gene expression: possible mechanisms of action. J Neurosci Res 56:349-357.

Menzies FM, Huebener J, Renna M, Bonin M, Riess O, Rubinsztein DC Autophagy induction reduces mutant ataxin-3 levels and toxicity in a mouse model of spinocerebellar ataxia type 3. Brain 133:93-104.

Merker K, Stolzing A, Grune T (2001) Proteolysis, caloric restriction and aging. Mech Ageing Dev 122:595-615.

Meyer zu Horste G, Prukop T, Liebetanz D, Mobius W, Nave KA, Sereda MW (2007) Antiprogesterone therapy uncouples axonal loss from demyelination in a transgenic rat model of CMT1A neuropathy. Ann Neurol 61:61-72.

Micallef J, Attarian S, Dubourg O, Gonnaud PM, Hogrel JY, Stojkovic T, Bernard R, Jouve E, Pitel S, Vacherot F, Remec JF, Jomir L, Azabou E, Al-Moussawi M, Lefebvre MN, Attolini L, Yaici S, Tanesse D, Fontes M, Pouget J, Blin O (2009) Effect of ascorbic acid in patients with Charcot-Marie-Tooth disease type 1A: a multicentre, randomised, double-blind, placebo-controlled trial. Lancet Neurol.

Misko A, Ferguson T, Notterpek L (2002) Matrix metalloproteinase mediated degradation of basement membrane proteins in Trembler J neuropathy nerves. J Neurochem 83:885-894.

Miyata Y (2005) Hsp90 inhibitor geldanamycin and its derivatives as novel cancer chemotherapeutic agents. Curr Pharm Des 11:1131-1138.

Mizushima N, Hara T (2006) Intracellular quality control by autophagy: how does autophagy prevent neurodegeneration? Autophagy 2:302-304.

Mizushima N, Yoshimori T (2007) How to interpret LC3 immunoblotting. Autophagy 3:542-545.

Mosmann T (1983) Rapid colorimetric assay for cellular growth and survival: application to proliferation and cytotoxicity assays. J Immunol Methods 65:55-63.

Muchowski PJ, Wacker JL (2005) Modulation of neurodegeneration by molecular chaperones. Nat Rev Neurosci 6:11-22.

Mukhopadhyay G, Doherty P, Walsh FS, Crocker PR, Filbin MT (1994) A novel role for myelin-associated glycoprotein as an inhibitor of axonal regeneration. Neuron 13:757-767.

Naef R, Suter U (1998) Many facets of the peripheral myelin protein PMP22 in myelination and disease. Microsc Res Tech 41:359-371.

Naef R, Suter U (1999) Impaired intracellular trafficking is a common disease mechanism of PMP22 point mutations in peripheral neuropathies. Neurobiol Dis 6:1-14.

Narayanan SP, Flores AI, Wang F, Macklin WB (2009) Akt signals through the mammalian target of rapamycin pathway to regulate CNS myelination. J Neurosci 29:6860-6870.

Nave KA, Trapp BD (2008) Axon-glial signaling and the glial support of axon function. Annu Rev Neurosci 31:535-561.

Nicholson SM, Gomes D, de Nechaud B, Bruzzone R (2001) Altered gene expression in Schwann cells of connexin32 knockout animals. J Neurosci Res 66:23-36.

Niemann S, Sereda MW, Suter U, Griffiths IR, Nave KA (2000) Uncoupling of myelin assembly and schwann cell differentiation by transgenic overexpression of peripheral myelin protein 22. J Neurosci 20:4120-4128.

Niemann S, Sereda MW, Rossner M, Stewart H, Suter U, Meinck HM, Griffiths IR, Nave KA (1999) The "CMT rat": peripheral neuropathy and dysmyelination caused by transgenic overexpression of PMP22. Ann N Y Acad Sci 883:254-261.

Nishimura T, Yoshikawa H, Fujimura H, Sakoda S, Yanagihara T (1996) Accumulation of peripheral myelin protein 22 in onion bulbs and Schwann cells of biopsied nerves from patients with Charcot-Marie-Tooth disease type 1A. Acta Neuropathol 92:454-460.

Nixon RA, Paskevich PA, Sihag RK, Thayer CY (1994) Phosphorylation on carboxyl terminus domains of neurofilament proteins in retinal ganglion cell neurons in vivo: influences on regional neurofilament accumulation, interneurofilament spacing, and axon caliber. J Cell Biol 126:1031-1046.

Nobbio L, Vigo T, Abbruzzese M, Levi G, Brancolini C, Mantero S, Grandis M, Benedetti L, Mancardi G, Schenone A (2004) Impairment of PMP22 transgenic Schwann cells differentiation in culture: implications for Charcot-Marie-Tooth type 1A disease. Neurobiol Dis 16:263-273.

Noebels JL, Marcom PK, Jalilian-Tehrani MH (1991) Sodium channel density in hypomyelinated brain increased by myelin basic protein gene deletion. Nature 352:431-434.

Norris CM, Korol DL, Foster TC (1996) Increased susceptibility to induction of long-term depression and long-term potentiation reversal during aging. J Neurosci 16:5382-5392.

Notterpek L, Tolwani RJ (1999) Experimental models of peripheral neuropathies. Lab Anim Sci 49:588-599.

Notterpek L, Shooter EM, Snipes GJ (1997) Upregulation of the endosomal-lysosomal pathway in the trembler-J neuropathy. J Neurosci 17:4190-4200.

Notterpek L, Snipes GJ, Shooter EM (1999a) Temporal expression pattern of peripheral myelin protein 22 during in vivo and in vitro myelination. Glia 25:358-369.

Notterpek L, Ryan MC, Tobler AR, Shooter EM (1999b) PMP22 accumulation in aggresomes: implications for CMT1A pathology. Neurobiol Dis 6:450-460.

Notterpek L, Roux KJ, Amici SA, Yazdanpour A, Rahner C, Fletcher BS (2001) Peripheral myelin protein 22 is a constituent of intercellular junctions in epithelia. Proc Natl Acad Sci U S A 98:14404-14409.

Novakovic SD, Eglen RM, Hunter JC (2001) Regulation of Na+ channel distribution in the nervous system. Trends Neurosci 24:473-478.

Ohtsuka K, Suzuki T (2000) Roles of molecular chaperones in the nervous system. Brain Res Bull 53:141-146.

Omlin FX, Webster HD, Palkovits CG, Cohen SR (1982) Immunocytochemical localization of basic protein in major dense line regions of central and peripheral myelin. J Cell Biol 95:242-248.

Pamplona R, Portero-Otin M, Riba D, Requena JR, Thorpe SR, Lopez-Torres M, Barja G (2000) Low fatty acid unsaturation: a mechanism for lowered lipoperoxidative modification of tissue proteins in mammalian species with long life spans. J Gerontol A Biol Sci Med Sci 55:B286-291.

Pareek S, Suter U, Snipes GJ, Welcher AA, Shooter EM, Murphy RA (1993) Detection and processing of peripheral myelin protein PMP22 in cultured Schwann cells. J Biol Chem 268:10372-10379.

Pareek S, Notterpek L, Snipes GJ, Naef R, Sossin W, Laliberte J, Iacampo S, Suter U, Shooter EM, Murphy RA (1997) Neurons promote the translocation of peripheral myelin protein 22 into myelin. J Neurosci 17:7754-7762.

Pareyson D, Marchesi C (2009) Diagnosis, natural history, and management of Charcot-Marie-Tooth disease. Lancet Neurol 8:654-667.

Pareyson D, Scaioli V, Taroni F, Botti S, Lorenzetti D, Solari A, Ciano C, Sghirlanzoni A (1996) Phenotypic heterogeneity in hereditary neuropathy with liability to pressure palsies associated with chromosome 17p11.2-12 deletion. Neurology 46:1133-1137.

Pareyson D, Schenone A, Fabrizi GM, Santoro L, Padua L, Quattrone A, Vita G, Gemignani F, Visioli F, Solari A (2006) A multicenter, randomized, double-blind, placebo-controlled trial of long-term ascorbic acid treatment in Charcot-Marie-Tooth disease type 1A (CMT-TRIAAL): the study protocol [EudraCT no.: 2006-000032-27]. Pharmacol Res 54:436-441.

Parhad IM, Scott JN, Cellars LA, Bains JS, Krekoski CA, Clark AW (1995) Axonal atrophy in aging is associated with a decline in neurofilament gene expression. J Neurosci Res 41:355-366.

Parmantier E, Cabon F, Braun C, D'Urso D, Muller HW, Zalc B (1995) Peripheral myelin protein-22 is expressed in rat and mouse brain and spinal cord motoneurons. Eur J Neurosci 7:1080-1088.

Passage E, Norreel JC, Noack-Fraissignes P, Sanguedolce V, Pizant J, Thirion X, Robaglia-Schlupp A, Pellissier JF, Fontes M (2004) Ascorbic acid treatment corrects the phenotype of a mouse model of Charcot-Marie-Tooth disease. Nat Med 10:396-401.

Patel PI, Roa BB, Welcher AA, Schoener-Scott R, Trask BJ, Pentao L, Snipes GJ, Garcia CA, Francke U, Shooter EM, Lupski JR, Suter U (1992) The gene for the peripheral myelin protein PMP-22 is a candidate for Charcot-Marie-Tooth disease type 1A. Nat Genet 1:159-165.

Perea J, Robertson A, Tolmachova T, Muddle J, King RH, Ponsford S, Thomas PK, Huxley C (2001) Induced myelination and demyelination in a conditional mouse model of Charcot-Marie-Tooth disease type 1A. Hum Mol Genet 10:1007-1018.

Petrucelli L, Dickson D, Kehoe K, Taylor J, Snyder H, Grover A, De Lucia M, McGowan E, Lewis J, Prihar G, Kim J, Dillmann WH, Browne SE, Hall A, Voellmy R, Tsuboi Y, Dawson TM, Wolozin B, Hardy J, Hutton M (2004) CHIP and Hsp70 regulate tau ubiquitination, degradation and aggregation. Hum Mol Genet 13:703-714.

Phillips T, Leeuwenburgh C (2005) Muscle fiber specific apoptosis and TNF-alpha signaling in sarcopenia are attenuated by life-long calorie restriction. Faseb J 19:668-670.

Pirkkala L, Nykanen P, Sistonen L (2001) Roles of the heat shock transcription factors in regulation of the heat shock response and beyond. Faseb J 15:1118-1131.

Pitsikas N, Algeri S (1992) Deterioration of spatial and nonspatial reference and working memory in aged rats: protective effect of life-long calorie restriction. Neurobiol Aging 13:369-373.

Plakidou-Dymock S, McGivan JD (1994) Amino acid deprivation-induced stress response in the bovine renal epithelial cell line NBL-1: induction of HSP 70 by phenylalanine. Biochim Biophys Acta 1224:189-197.

Prodromou C, Roe SM, O'Brien R, Ladbury JE, Piper PW, Pearl LH (1997) Identification and structural characterization of the ATP/ADP-binding site in the Hsp90 molecular chaperone. Cell 90:65-75.

Rangaraju S, Madorsky I, Pileggi JG, Kamal A, Notterpek L (2008) Pharmacological induction of the heat shock response improves myelination in a neuropathic model. Neurobiol Dis 32:105-115.

Rangaraju S, Hankins D, Madorsky I, Madorsky E, Lee WH, Carter CS, Leeuwenburgh C, Notterpek L (2009) Molecular architecture of myelinated peripheral nerves is supported by calorie restriction with aging. Aging Cell 8:178-191.

Rattan SI (2004) Hormetic mechanisms of anti-aging and rejuvenating effects of repeated mild heat stress on human fibroblasts in vitro. Rejuvenation Res 7:40-48.

Ravikumar B, Duden R, Rubinsztein DC (2002) Aggregate-prone proteins with polyglutamine and polyalanine expansions are degraded by autophagy. Hum Mol Genet 11:1107-1117.

Ribalta T, McCutcheon IE, Aldape KD, Bruner JM, Fuller GN (2004) The mitosis-specific antibody anti-phosphohistone-H3 (PHH3) facilitates rapid reliable grading of meningiomas according to WHO 2000 criteria. Am J Surg Pathol 28:1532-1536.

Roa BB, Dyck PJ, Marks HG, Chance PF, Lupski JR (1993) Dejerine-Sottas syndrome associated with point mutation in the peripheral myelin protein 22 (PMP22) gene. Nat Genet 5:269-273.

Robertson A, Perea J, Tolmachova T, Thomas PK, Huxley C (2002a) Effects of mouse strain, position of integration and tetracycline analogue on the tetracycline conditional system in transgenic mice. Gene 282:65-74.

Robertson AM, Huxley C, King RH, Thomas PK (1999) Development of early postnatal peripheral nerve abnormalities in Trembler-J and PMP22 transgenic mice. J Anat 195 (Pt 3):331-339.

Robertson AM, Perea J, McGuigan A, King RH, Muddle JR, Gabreels-Festen AA, Thomas PK, Huxley C (2002b) Comparison of a new pmp22 transgenic mouse line with other mouse models and human patients with CMT1A. J Anat 200:377-390.

Rocca A, Lamaze C, Subtil A, Dautry-Varsat A (2001) Involvement of the ubiquitin/proteasome system in sorting of the interleukin 2 receptor beta chain to late endocytic compartments. Mol Biol Cell 12:1293-1301.

Roux KJ, Amici SA, Notterpek L (2004) The temporospatial expression of peripheral myelin protein 22 at the developing blood-nerve and blood-brain barriers. J Comp Neurol 474:578-588.

Roux KJ, Amici SA, Fletcher BS, Notterpek L (2005) Modulation of epithelial morphology, monolayer permeability, and cell migration by growth arrest specific 3/peripheral myelin protein 22. Mol Biol Cell 16:1142-1151.

Ryan MC, Shooter EM, Notterpek L (2002) Aggresome formation in neuropathy models based on peripheral myelin protein 22 mutations. Neurobiol Dis 10:109-118.

Ryhanen T, Hyttinen JM, Kopitz J, Rilla K, Kuusisto E, Mannermaa E, Viiri J, Holmberg CI, Immonen I, Meri S, Parkkinen J, Eskelinen EL, Uusitalo H, Salminen A, Kaarniranta K (2009) Crosstalk between Hsp70 molecular chaperone, lysosomes and proteasomes in autophagy-mediated proteolysis in human retinal pigment epithelial cells. J Cell Mol Med 13:3616-3631.

Ryu EJ, Yang M, Gustin JA, Chang LW, Freimuth RR, Nagarajan R, Milbrandt J (2008) Analysis of peripheral nerve expression profiles identifies a novel myelin glycoprotein, MP11. J Neurosci 28:7563-7573.

Sabers CJ, Martin MM, Brunn GJ, Williams JM, Dumont FJ, Wiederrecht G, Abraham RT (1995) Isolation of a protein target of the FKBP12-rapamycin complex in mammalian cells. J Biol Chem 270:815-822.

Saito H, Kobayashi K, Mochizuki H, Ishii T (1990) Axonal degeneration of the peripheral nerves and postganglionic anhidrosis in a patient with multiple sclerosis. Tohoku J Exp Med 162:279-291.

Saito K, Araki Y, Kontani K, Nishina H, Katada T (2005) Novel role of the small GTPase Rheb: its implication in endocytic pathway independent of the activation of mammalian target of rapamycin. J Biochem 137:423-430.

Salminen A, Ojala J, Huuskonen J, Kauppinen A, Suuronen T, Kaarniranta K (2008) Interaction of aging-associated signaling cascades: inhibition of NF-kappaB signaling by longevity factors FoxOs and SIRT1. Cell Mol Life Sci 65:1049-1058.

Salzer JL (1997) Clustering sodium channels at the node of Ranvier: close encounters of the axon-glia kind. Neuron 18:843-846.

Samarel AM, Ferguson AG, Decker RS, Lesch M (1989) Effects of cysteine protease inhibitors on rabbit cathepsin D maturation. Am J Physiol 257:C1069-1079.

Samson FE, Nelson SR (2000) The aging brain, metals and oxygen free radicals. Cell Mol Biol (Noisy-le-grand) 46:699-707.

Sancho S, Young P, Suter U (2001) Regulation of Schwann cell proliferation and apoptosis in PMP22-deficient mice and mouse models of Charcot-Marie-Tooth disease type 1A. Brain 124:2177-2187.

Sanders CR, Ismail-Beigi F, McEnery MW (2001) Mutations of peripheral myelin protein 22 result in defective trafficking through mechanisms which may be common to diseases involving tetraspan membrane proteins. Biochemistry 40:9453-9459.

Sarbassov DD, Ali SM, Sengupta S, Sheen JH, Hsu PP, Bagley AF, Markhard AL, Sabatini DM (2006) Prolonged rapamycin treatment inhibits mTORC2 assembly and Akt/PKB. Mol Cell 22:159-168.

Sarkar S, Rubinsztein DC (2008) Small molecule enhancers of autophagy for neurodegenerative diseases. Mol Biosyst 4:895-901.

Sarkar S, Ravikumar B, Floto RA, Rubinsztein DC (2009) Rapamycin and mTOR-independent autophagy inducers ameliorate toxicity of polyglutamine-expanded huntingtin and related proteinopathies. Cell Death Differ 16:46-56.

Scherer SS, Wrabetz L (2008) Molecular mechanisms of inherited demyelinating neuropathies. Glia 56:1578-1589.

Scherer SS, Bone LJ, Deschenes SM, Abel A, Balice-Gordon RJ, Fischbeck KH (1999) The role of the gap junction protein connexin32 in the pathogenesis of X-linked Charcot-Marie-Tooth disease. Novartis Found Symp 219:175-185; discussion 185-177.

Selsby JT, Judge AR, Yimlamai T, Leeuwenburgh C, Dodd SL (2005) Life long calorie restriction increases heat shock proteins and proteasome activity in soleus muscles of Fisher 344 rats. Exp Gerontol 40:37-42.

Seo AY, Hofer T, Sung B, Judge S, Chung HY, Leeuwenburgh C (2006) Hepatic oxidative stress during aging: effects of 8% long-term calorie restriction and lifelong exercise. Antioxid Redox Signal 8:529-538.

Sereda M, Griffiths I, Puhlhofer A, Stewart H, Rossner MJ, Zimmerman F, Magyar JP, Schneider A, Hund E, Meinck HM, Suter U, Nave KA (1996) A transgenic rat model of Charcot-Marie-Tooth disease. Neuron 16:1049-1060.

Sereda MW, Meyer zu Horste G, Suter U, Uzma N, Nave KA (2003) Therapeutic administration of progesterone antagonist in a model of Charcot-Marie-Tooth disease (CMT-1A). Nat Med 9:1533-1537.

Sharma AK, Bajada S, Thomas PK (1980) Age changes in the tibial and plantar nerves of the rat. J Anat 130:417-428.

Sherman MY, Goldberg AL (2001) Cellular defenses against unfolded proteins: a cell biologist thinks about neurodegenerative diseases. Neuron 29:15-32.

Shy ME, Balsamo J, Lilien J, Kamholz J (2001) A molecular basis for hereditary motor and sensory neuropathy disorders. Curr Neurol Neurosci Rep 1:77-88.

Shy ME, Chen L, Swan ER, Taube R, Krajewski KM, Herrmann D, Lewis RA, McDermott MP (2008) Neuropathy progression in Charcot-Marie-Tooth disease type 1A. Neurology 70:378-383.

Sitte N, Merker K, Von Zglinicki T, Davies KJ, Grune T (2000) Protein oxidation and degradation during cellular senescence of human BJ fibroblasts: part II--aging of nondividing cells. Faseb J 14:2503-2510.

Sittler A, Lurz R, Lueder G, Priller J, Lehrach H, Hayer-Hartl MK, Hartl FU, Wanker EE (2001) Geldanamycin activates a heat shock response and inhibits huntingtin aggregation in a cell culture model of Huntington's disease. Hum Mol Genet 10:1307-1315.

Smith KJ, Kapoor R, Felts PA (1999) Demyelination: the role of reactive oxygen and nitrogen species. Brain Pathol 9:69-92.

Snipes GJ, Suter U, Shooter EM (1993) Human peripheral myelin protein-22 carries the L2/HNK-1 carbohydrate adhesion epitope. J Neurochem 61:1961-1964.

Snipes GJ, Suter U, Welcher AA, Shooter EM (1992) Characterization of a novel peripheral nervous system myelin protein (PMP-22/SR13). J Cell Biol 117:225-238.

Sohal RS, Weindruch R (1996) Oxidative stress, caloric restriction, and aging. Science 273:59-63.

Sohal RS, Agarwal S, Candas M, Forster MJ, Lal H (1994) Effect of age and caloric restriction on DNA oxidative damage in different tissues of C57BL/6 mice. Mech Ageing Dev 76:215-224.

Spaulding CC, Walford RL, Effros RB (1997) Calorie restriction inhibits the age-related dysregulation of the cytokines TNF-alpha and IL-6 in C3B10RF1 mice. Mech Ageing Dev 93:87-94.

Squier TC (2001) Oxidative stress and protein aggregation during biological aging. Exp Gerontol 36:1539-1550.

Stadtman ER (2001) Protein oxidation in aging and age-related diseases. Ann N Y Acad Sci 928:22-38.

Stefani M, Dobson CM (2003) Protein aggregation and aggregate toxicity: new insights into protein folding, misfolding diseases and biological evolution. J Mol Med 81:678-699.

Sugiyama I, Tanaka K, Akita M, Yoshida K, Kawase T, Asou H (2002) Ultrastructural analysis of the paranodal junction of myelinated fibers in 31-month-old-rats. J Neurosci Res 70:309-317.

Suter U, Snipes GJ (1995) Biology and genetics of hereditary motor and sensory neuropathies. Annu Rev Neurosci 18:45-75.

Suter U, Moskow JJ, Welcher AA, Snipes GJ, Kosaras B, Sidman RL, Buchberg AM, Shooter EM (1992) A leucine-to-proline mutation in the putative first transmembrane domain of the 22-kDa peripheral myelin protein in the trembler-J mouse. Proc Natl Acad Sci U S A 89:4382-4386.

Suter U, Snipes GJ, Schoener-Scott R, Welcher AA, Pareek S, Lupski JR, Murphy RA, Shooter EM, Patel PI (1994) Regulation of tissue-specific expression of alternative peripheral myelin protein-22 (PMP22) gene transcripts by two promoters. J Biol Chem 269:25795-25808.

Tai HC, Schuman EM (2008) Ubiquitin, the proteasome and protein degradation in neuronal function and dysfunction. Nat Rev Neurosci 9:826-838.

Tobler AR, Liu N, Mueller L, Shooter EM (2002) Differential aggregation of the Trembler and Trembler J mutants of peripheral myelin protein 22. Proc Natl Acad Sci U S A 99:483-488.

Tobler AR, Notterpek L, Naef R, Taylor V, Suter U, Shooter EM (1999) Transport of Trembler-J mutant peripheral myelin protein 22 is blocked in the intermediate compartment and affects the transport of the wild-type protein by direct interaction. J Neurosci 19:2027-2036.

Toth C, Shim SY, Wang J, Jiang Y, Neumayer G, Belzil C, Liu WQ, Martinez J, Zochodne D, Nguyen MD (2008) Ndel1 promotes axon regeneration via intermediate filaments. PLoS ONE 3:e2014.

Trapp BD (1990) Myelin-associated glycoprotein. Location and potential functions. Ann N Y Acad Sci 605:29-43.

Turturro A, Witt WW, Lewis S, Hass BS, Lipman RD, Hart RW (1999) Growth curves and survival characteristics of the animals used in the Biomarkers of Aging Program. J Gerontol A Biol Sci Med Sci 54:B492-501.

Tyson J, Ellis D, Fairbrother U, King RH, Muntoni F, Jacobs J, Malcolm S, Harding AE, Thomas PK (1997) Hereditary demyelinating neuropathy of infancy. A genetically complex syndrome. Brain 120 (Pt 1):47-63.

Uchida A, Brown A (2004) Arrival, reversal, and departure of neurofilaments at the tips of growing axons. Mol Biol Cell 15:4215-4225.

Uchida A, Tashiro T, Komiya Y, Yorifuji H, Kishimoto T, Hisanaga S (2004) Morphological and biochemical changes of neurofilaments in aged rat sciatic nerve axons. J Neurochem 88:735-745.

Uyemura K, Kitamura K (1991) Comparative studies on myelin proteins in mammalian peripheral nerve. Comp Biochem Physiol C 98:63-72.

Vabnick I, Messing A, Chiu SY, Levinson SR, Schachner M, Roder J, Li C, Novakovic S, Shrager P (1997) Sodium channel distribution in axons of hypomyelinated and MAG null mutant mice. J Neurosci Res 50:321-336.

Valentijn LJ, Baas F, Wolterman RA, Hoogendijk JE, van den Bosch NH, Zorn I, Gabreels-Festen AW, de Visser M, Bolhuis PA (1992) Identical point mutations of PMP-22 in Trembler-J mouse and Charcot-Marie-Tooth disease type 1A. Nat Genet 2:288-291.

Van Itallie CM, Anderson JM (2006) Claudins and epithelial paracellular transport. Annu Rev Physiol 68:403-429.

Verdu E, Ceballos D, Vilches JJ, Navarro X (2000) Influence of aging on peripheral nerve function and regeneration. J Peripher Nerv Syst 5:191-208.

Verhamme C, van Schaik IN, Koelman JH, de Haan RJ, de Visser M (2009a) The natural history of Charcot-Marie-Tooth type 1A in adults: a 5-year follow-up study. Brain 132:3252-3262.

Verhamme C, de Haan RJ, Vermeulen M, Baas F, de Visser M, van Schaik IN (2009b) Oral high dose ascorbic acid treatment for one year in young CMT1A patients: a randomised, double-blind, placebo-controlled phase II trial. BMC Med 7:70.

Verrier JD, Lau P, Hudson L, Murashov AK, Renne R, Notterpek L (2009) Peripheral myelin protein 22 is regulated post-transcriptionally by miRNA-29a. Glia 57:1265-1279.

Voellmy R, Boellmann F (2007) Chaperone regulation of the heat shock protein response. Adv Exp Med Biol 594:89-99.

Wang Y, Kawamura N, Schmelzer JD, Schmeichel AM, Low PA (2008) Decreased peripheral nerve damage after ischemia-reperfusion injury in mice lacking TNF-alpha. J Neurol Sci 267:107-111.

Warrick JM, Chan HY, Gray-Board GL, Chai Y, Paulson HL, Bonini NM (1999) Suppression of polyglutamine-mediated neurodegeneration in Drosophila by the molecular chaperone HSP70. Nat Genet 23:425-428.

Weissman L, de Souza-Pinto NC, Stevnsner T, Bohr VA (2007) DNA repair, mitochondria, and neurodegeneration. Neuroscience 145:1318-1329.

Westenbroek RE, Noebels JL, Catterall WA (1992) Elevated expression of type II Na+ channels in hypomyelinated axons of shiverer mouse brain. J Neurosci 12:2259-2267.

Westerheide SD, Morimoto RI (2005) Heat shock response modulators as therapeutic tools for diseases of protein conformation. J Biol Chem 280:33097-33100.

Winklhofer KF, Tatzelt J, Haass C (2008) The two faces of protein misfolding: gain- and loss-of-function in neurodegenerative diseases. Embo J 27:336-349.

Winterstein C, Trotter J, Kramer-Albers EM (2008) Distinct endocytic recycling of myelin proteins promotes oligodendroglial membrane remodeling. J Cell Sci 121:834-842.

Wohlgemuth SE, Julian D, Akin DE, Fried J, Toscano K, Leeuwenburgh C, Dunn WA, Jr. (2007) Autophagy in the heart and liver during normal aging and calorie restriction. Rejuvenation Res 10:281-292.

Wood PM, Bunge RP (1975) Evidence that sensory axons are mitogenic for Schwann cells. Nature 256:662-664.

Xu J, Knutson MD, Carter CS, Leeuwenburgh C (2008) Iron accumulation with age, oxidative stress and functional decline. PLoS ONE 3:e2865.

Yamada K, Sato J, Oku H, Katakai R (2003) Conformation of the transmembrane domains in peripheral myelin protein 22. Part 1. Solution-phase synthesis and circular dichroism study of protected 17-residue partial peptides in the first putative transmembrane domain. J Pept Res 62:78-87.

Yin X, Kidd GJ, Wrabetz L, Feltri ML, Messing A, Trapp BD (2000) Schwann cell myelination requires timely and precise targeting of P(0) protein. J Cell Biol 148:1009-1020.

Zanazzi G, Einheber S, Westreich R, Hannocks MJ, Bedell-Hogan D, Marchionni MA, Salzer JL (2001) Glial growth factor/neuregulin inhibits Schwann cell myelination and induces demyelination. J Cell Biol 152:1289-1299.

Zandi E, Rothwarf DM, Delhase M, Hayakawa M, Karin M (1997) The IkappaB kinase complex (IKK) contains two kinase subunits, IKKalpha and IKKbeta, necessary for IkappaB phosphorylation and NF-kappaB activation. Cell 91:243-252.

Zoidl G, Blass-Kampmann S, D'Urso D, Schmalenbach C, Muller HW (1995) Retroviral-mediated gene transfer of the peripheral myelin protein PMP22 in Schwann cells: modulation of cell growth. Embo J 14:1122-1128.

Zoidl G, D'Urso D, Blass-Kampmann S, Schmalenbach C, Kuhn R, Muller HW (1997) Influence of elevated expression of rat wild-type PMP22 and its mutant PMP22Trembler on cell growth of NIH3T3 fibroblasts. Cell Tissue Res 287:459-470.

Zou J, Guo Y, Guettouche T, Smith DF, Voellmy R (1998) Repression of heat shock transcription factor HSF1 activation by HSP90 (HSP90 complex) that forms a stress-sensitive complex with HSF1. Cell 94:471-480.

Zwerling SJ, Cohen SA, Barchi RL (1991) Analysis of protease-sensitive regions in the skeletal muscle sodium channel in vitro and implications for channel tertiary structure. J Biol Chem 266:4574-4580.

BIOGRAPHICAL SKETCH

Sunitha Rangaraju was born in the year 1984, in the Union Territory of Pondicherry, a former French colony in India and was raised in the coastal city of Chennai in the southern part of India. She is the eldest daughter of Mr. Venga Kandar Rangaraju who is a retired government officer and Mrs. Bala Sarassa Manicassamy who is a retired Professor of Botany. She has a younger sister, Vidhya Rangaraju and a younger brother, Vengada Karthik Rangaraju. After completing high school in 2001, she pursued her undergraduate studies at Anna University, Chennai. In 2004, during her undergraduate studies, she gained research experience as a scholarship student under the guidance of Dr.K.S.Krishnan at the Tata Institute of Fundamental Research (TIFR), in Mumbai, the financial capital of India. In 2005, she carried out her undergraduate research thesis in the laboratory of Dr.Vinay Kumar Nandicoori at the National Institute of Immunology (NII), in New Delhi, the capital of India. She graduated with a Bachelors degree in Industrial Biotechnology in 2005. She came to the U.S. to join the Interdisciplinary Program in Biomedical Sciences at University of Florida in 2005 and a year later in 2006, became a member in the laboratory of Dr.Lucia Notterpek.